Characterizing the effects of Robinow Syndrome-associated *Dishevelled1* variants in cell signalling and development in fruit fly model

by

Gamze Akarsu

B.Sc., Boğaziçi University, 2022

Thesis Submitted in Partial Fulfillment of the
Requirements for the Degree of
Master of Science

in the
Department of Molecular Biology and Biochemistry
Faculty of Science

SIMON FRASER UNIVERSITY
Fall 2024

Declaration of Committee

Name:	**Gamze Akarsu**
Degree:	**Master of Science**
Title:	**Characterizing the effects of Robinow Syndrome-associated *Dishevelled1* variants in cell signalling and development in fruit fly model**
Committee:	**Chair: Lynne Quarmby** Professor, Molecular Biology and Biochemistry
	Esther Verheyen Supervisor Professor, Molecular Biology and Biochemistry
	Sharon Gorski Committee Member Professor, Molecular Biology and Biochemistry
	Nancy Hawkins Committee Member Associate Professor, Molecular Biology and Biochemistry
	Stephanie Vlachos Examiner Senior Lecturer, Molecular Biology and Biochemistry

Abstract

Studying developmental disorders sheds light on how signalling networks regulate development. Our research focuses on the *Dishevelled 1* (*DVL1*) variant *DVL1*$^{1519\Delta T}$, found in Autosomal Dominant Robinow Syndrome (RS) patients. RS is a rare disorder linked to mutations in genes involved in the noncanonical/Planar Cell Polarity pathway of Wnt signalling, essential for tissue homeostasis and development. DVL1 acts in both canonical and noncanonical Wnt pathways. The variant *DVL1*$^{1519\Delta T}$ has a frameshift mutation replacing the C-terminus with a novel peptide. We used the Gal4-UAS system to study its effects in fruit flies, comparing wildtype and variant DVL1. Our results show that the variant alters tissue morphology, induces apoptosis, and disrupts wing development. RNA-seq revealed differential gene expression related to developmental processes. Our investigation with C-terminal truncated DVL1 constructs found that the novel peptide, rather than the loss of the C-terminus, drives these changes. This research advances our understanding of RS and DVL1 function.

Keywords: Robinow Syndrome; Dishevelled; Wnt signalling; *Drosophila melanogaster*; disease modelling

Dedication

This thesis is dedicated to the Akarsu family and to all the flies sacrificed for science.

Acknowledgements

I am deeply grateful to everyone who has played a role in supporting me throughout the completion of this degree.

First, I would like to express my sincere appreciation and deepest gratitude to my supervisor, Dr. Esther Verheyen, for your endless support and mentorship since the first day I set foot in Canada. Your insightful feedback and constructive criticism have been invaluable in guiding me through this research process. I am especially thankful for the patience you showed as I went through various challenges.

A special thank you goes to my thesis committee members, Dr. Sharon Gorski, and Dr. Nancy Hawkins, whose expertise and insightful suggestions have significantly enriched my work over the past two years. Thank you to my internal examiner, Dr. Stephanie Vlachos, and to the chair at my defence, Dr. Lynne Quarmby.

I would also like to acknowledge my first trainer in the Verheyen Lab, Katja MacCharles. I am thankful for all the members of the Verheyen Lab; Dr. Gritta Tettweiler, Dr. Kenneth Kim Lam Wong, Jenny Liao, Kewei Yu, Claire Shih, Landiso Madonsela Karampal Grewal, Gurpreet Moroak and my lab-sister Ece Yücel. Your friendship and the many discussions we have shared have provided me with new insights and the motivation to persevere through difficult times. Thank you as well to the hardworking undergraduate students who worked in the lab, Sage Lougheed, Katie Sew, Andrew Huang and Chris Tam.

I would like to thank our collaborators in Dr. Joy Richman's Lab at UBC for all their work on the project.

Many thanks to the MBB department staff at SFU, Jamie Chen, Christine Beauchamp, Deidre de Jong-Wong, Ziwei Ding and Tim Heslip.

I also would like to thank Dr. Arzu Çelik for introducing me to the world of *Drosophila* and my friends Eren Can Ekşi, Ayça Küpeli and Ayşe Kahraman for their camaraderie on this path.

My deepest thanks go to my family, my parents Fatma and Metin Akarsu, my sister Gizem Akarsu Sesli and my brother Bahadır Sesli, whose love and encouragement have been a constant source of strength. Thank you for everything. To my best friend Alperen Bahar, who always have been with me while 10000 kilometers apart. Mon gâté, Jérémy Cêtre, who has been the most patient with me whenever I wanted to go to 3 concerts in one week but also worked late on my experiments—thank you for your support and understanding.

Lastly, I would like to extend my gratitude to all those whose names may not appear here but whose contributions, in various forms, have made this thesis possible. Your support has meant more than words can express.

Hepinize çok teşekkür ederim.

Table of Contents

List of Tables

List of Figures

List of Acronyms

ACV	Anterior cross vein
ANOVA	Analysis of variance
AP	Anterior-posterior
Ap	Apterous
Arm	Armadillo
BMP	Bone morphogenic protein
BM	Basement membrane
cDNA	Complementary DNA
DAPI	4′,6-diamidino-2-phenylindole
DEP	DVL, EGL-10, Pleckstrin
DIX	DVL/Axin
Dpp	Decapentaplegic
Dsh	*Drosophila* dishevelled
DV	Dorsal-ventral
DVL	Vertebrate Dishevelled
ECL	Enhanced chemiluminescence
ECM	Extracellular matrix
FZ	Frizzled
GFP	Green fluorescent protein
GO	Gene Ontology
Hh	hedgehog
HRP	Horseradish peroxidase
Jak-Stat	Janus kinases (JAKs), signal transducer and activator of transcription proteins (STATs)
JNK	Jun N-terminal kinase
L3	Longitudinal vein 3
L4	Longitudinal vein 4
LRP	Low-density lipoprotein receptor-related protein

MIM	Mendelian Inheritance in Man
Mmp1	Matric metalloproteinase 1
Mmp2	Matric metalloproteinase 2
mRNA	Messenger ribonucleic acid
n	Sample size
Ndg	Nidogen
NXN	Nucleoredoxin
Oseg5	Outer segment 5
p	Probability, p-value
PBS	Phosphate buffered saline
PBS-T	Phosphate buffered saline with 0.1% Triton X-100
PCD	Programmed cell death
PCP	Planar cell polarity
PD	Proximal-distal
PDZ	Post synaptic density protein (PSD95), *Drosophila* disc large tumor suppressor (Dlg1), zonula occludens-1 protein (zo-1)
PFA	Paraformaldehyde
puc	Puckered
qRT-PCR	Quantitative reverse transcription polymerase chain reaction
ROR	Receptor tyrosine kinase-like orphan receptor
RS	Robinow Syndrome
SD	Standard deviation
UAS	Upstream activation sequence
Vkg	Viking
WB	Western Blot
Wg	Wingless
Wnt	Wingless and Int-1
Wt	Wild type

Chapter 1. Introduction

1.1. Cell signalling pathways

Complex organisms such as children use their sensory system to adapt to their environment, overcome obstacles, establish their own nature and grow in harmony. These all happen for everyone in the society quite intricately and the harmony is established thanks to our ability to sense and response. We all receive information about our surroundings through our sensory organs, transmit the information neuron by neuron up to the brain where it is processed in order to produce a unique response. A similar system applies to all kinds of living beings for their survival.

As the most basic unit of life, cells use signalling pathways similarly to our sensory system to communicate, process information and respond to their environment (Cooper, 2000). In this context, an external ligand molecule or the internal stimulus within a cell is the sensory information, which is received by the cell's sensory organs called receptors on the membrane or other effector molecules inside the cell, the relay molecules act like the neuronal transport for carrying the message from the reception to the cell's brain, the nucleus and finally the nucleus produces a biochemical response. Proper operation and regulation of these signalling pathways are crucial for the regular growth and survival of the cell itself, the cells surrounding it, hence the tissue, the organ and the systems they form and ultimately the whole organism. It should be noted that not all signalling pathways have the same workflow.

Cell signalling simply involves three steps: Signal reception, signal transduction and cellular response generation. First the cell detects the external signal via its ligand-specific receptors embedded in the cell surface. This leads to the activation of chemical messengers present in the cytoplasm, commonly in the form of enzyme activation or phosphorylation that amplifies the signal and paves the way for a more specific cellular response. Some of these responses can occur fast within the cytoplasm as enzyme activation in the metabolic level or the signal can reach to the nucleus and cause differential gene expression (Lodish, 2000) (Fig. 1.1.).

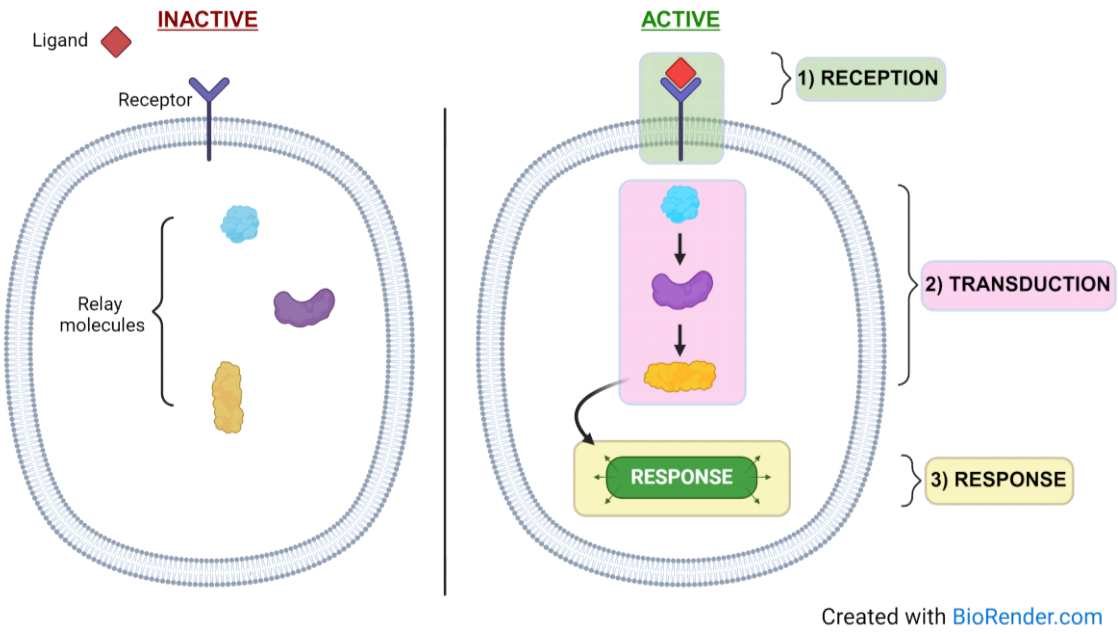

Figure 1.1. Cell signalling pathway steps
Schematic of the basic of a signalling pathway. **Reception** occurs when the ligand binds to its receptor. After the signal is received, messengers within the cell **transduce** it to other proteins e.g. enzymes. As a result of this information transfer, the cell produces a **response** in the form of gene transcription, altered metabolic activity or shape.

1.1.1. Cell signalling defects and diseases

For all cellular signalling events to work correctly, the harmony within and between the signalling pathways is fundamental. The wide and complex network between signalling pathways involves crosstalk and sharing of proteins to transduce similar or different messages. This provides a fine-tuned management for the regulation, but it also makes the whole system prone to malfunction through mutations. For example, a mutation in one protein that has functions in multiple pathways might disrupt all those pathways. In other situations, the mutations in different proteins that cause the responses through different pathways might lead to similar altered consequences. Due to this intricate nature of the cell signalling network, such dysregulations in components of cell signalling pathways can cause a multitude of diseases (Gautam, 1999; van de Stolpe et al., 2019).

Understanding the molecular mechanisms underlying diseases is important to develop precise medical solutions, hence, the study of signalling pathways is of high interest (Sebastian-Leon et al., 2014; Dugger et al., 2018). Through research that targets

identifying the genes or signalling pathways that underlie the disease progression, researchers can provide specific therapeutic approaches for a wide range of diseases, from rare conditions to the most common ones such as cancer (Tabor & Goldenberg, 2018; Might & Crouse, 2022). Thanks to an array of genomic studies, we have access to tools for the characterization and analysis of signalling molecules associated with disease causing mutations and disease phenotypes (Mirnezami et al., 2012; Nussinov et al., 2021). Science can also benefit from such studies by focusing on rare diseases and the molecular mechanisms causing the disease phenotypes on the cellular and organismal level since it provides a deeper understanding of basic molecular biology (Dugger et al., 2018). A great example of this is the 1984 study by Dr. Michael S. Brown, and Dr. Joseph L. Goldstein, in which they discovered the regulation of cholesterol metabolism and LDL receptors via their research on familial hypercholesterolemia, a rare disease, that also brought them the Nobel Prize in Physiology or Medicine in 1985. This study also increased the possibilities to prevent and treat thickening of arteries and heart attacks. (Brown & Goldstein, 1984; *The Nobel Prize in Physiology or Medicine 1985*, n.d.).

To understand the alterations in the activity of a signalling pathway caused by mutations in one of its components, the activity of the pathway can be measured. One common method to study signalling pathway activity has been the use of transcriptional reporters. These reporters are genes whose expression is directly tied to the activation of a particular signalling pathway. These reporter genes can be engineered to produce detectable signals, such as the green fluorescent protein (GFP), which emits fluorescence, or the *lacZ* gene, which encodes the enzyme β-galactosidase that can be easily identified through colorimetric assays (Honeyman et al., 2002). When the signalling pathway is activated, the transcriptional reporter gene is expressed, producing the detectable signal. By quantifying the intensity of this signal, we can determine the degree of pathway activation. This quantification provides a measurable readout of the pathway's activity, allowing scientists to dissect the dynamics and regulatory mechanisms of the pathway under various experimental conditions (Fig 1.2.). This approach offers valuable insights into how specific signalling pathways operate and respond to different stimuli, thereby enhancing our understanding of cellular communication and function.

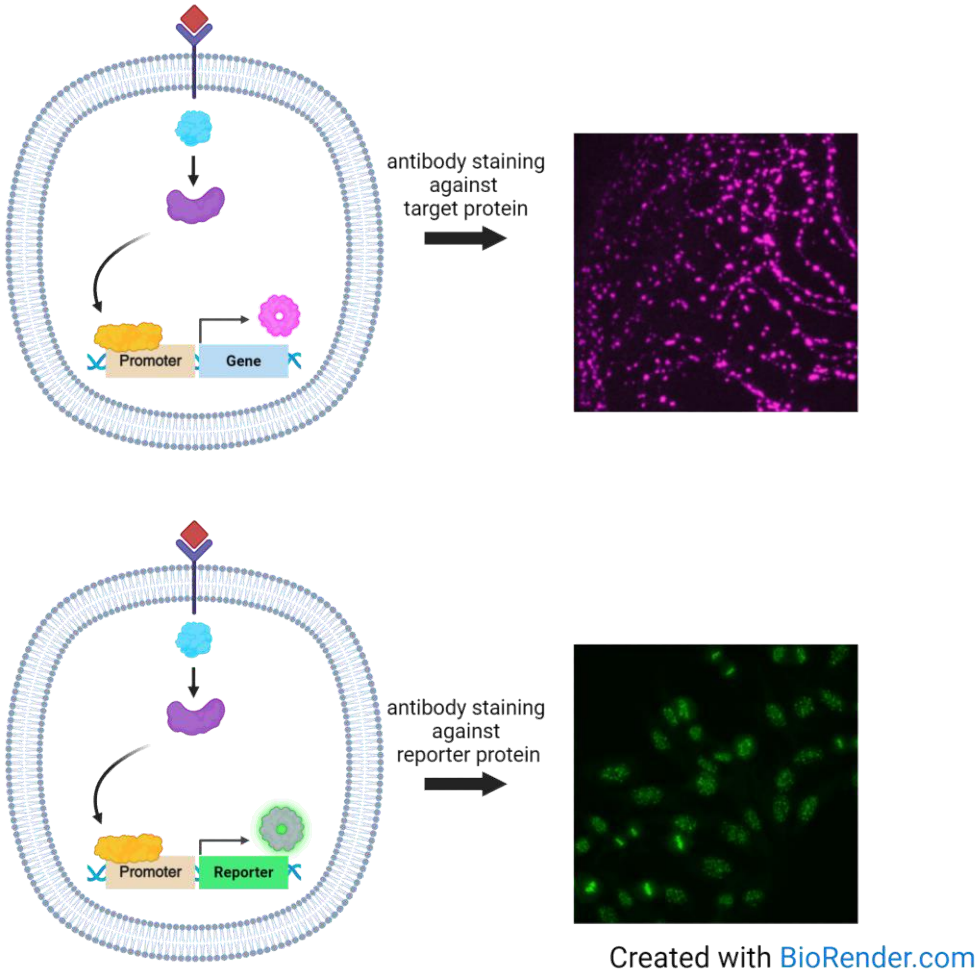

Figure 1.2. Measuring signalling pathway activity with reporters
Basic schematic of how to visualise and measure signalling pathway radouts and reporters. Above, the activity of a simple signalling pathway that leads to the transcription of a gene is depicted. This transcript and the protein product can be used as a readout of the signalling pathway activity. Below, a transcriptional reporter, in this case a GFP tag inserted under the promoter that the signalling pathway controls. The fluorescence from the GFP tag can be visualised and measured in order to observe the signalling pathway's activity.

1.2. *Drosophila melanogaster* as a model organism

Cell signalling is the basis of cellular behaviours which would ultimately lead to changes at the organismal level (van de Stolpe et al., 2019). Considering how convoluted the network of signalling pathways intra and intercellularly, studying the human diseases caused by signalling altering mutations can be extremely time consuming and challenging. Model organisms are our best helpers in order to overcome most of these challenges. Given all these factors, the fruit fly *Drosophila melanogaster* is

a highly attractive model organism with its whole genome being available (Adams et al., 2000), short lifespan, ease and low cost of husbandry and the wide selection of available genetic tools (Bier, 2005; Venken & Bellen, 2007; Ugur et al., 2016; Tolwinski, 2017).

Drosophila have been one of the most common model organisms for over a hundred years since Thomas Hunt Morgan's genetic studies (Bellen et al., 2010; Morgan, 1910). It has been established as a great model for studying many biological processes such as genetics, inheritance, developmental patterning and embryogenesis (Tolwinski, 2017; Yamamoto et al., 2014, 2024)

1.2.1. Developmental genetic disease modelling in *Drosophila*

By the look of it, a fly does not appear similar to a human. However, genomic studies in the last two decades have proved that 60% of the *Drosophila* genome is homologous to that of humans and almost 75% of the disease causing genes have homologs in the fly genome (Chien et al., 2002; Ugur et al., 2016; Mirzoyan et al., 2019). This high conservation and the genetic redundancy together with all the advances in the genetic tools make fruit flies an inexpensive and optimal model for studying genetic diseases and mutations (Yamamoto et al., 2014) (Fig. 1.3). The identification and characterization of possible pathogenic variants for rare diseases is also possible thanks to this genetic resemblance (Yamamoto et al., 2024) (Fig. 1.3).

One other important quality of the fruit fly is that many fundamental genetic pathways involved in human development and disease are also conserved in *Drosophila*. Key signalling pathways, such as Notch, Wnt, Hedgehog, and JAK/STAT, are well-characterized in fruit flies and play crucial roles in development. Mutations in these pathways can lead to developmental disorders in both *Drosophila* and humans, making the fruit fly an excellent model for the in-depth mechanical and translational study of developmental diseases (Pandey & Nichols, 2011) (Fig 1.3.). Since the Wnt and PCP signalling pathways were deciphered in large part in flies and very well established in wing tissue development, there are many available pathway reporters and robust assays together with the available genetic tools, which all make *Drosophila* a great tool for my study that aims to investigate the mechanistic of a rare genetic developmental disease (Wodarz & Nusse, 1998; Simons & Mlodzik, 2008) (Fig 1.3.).

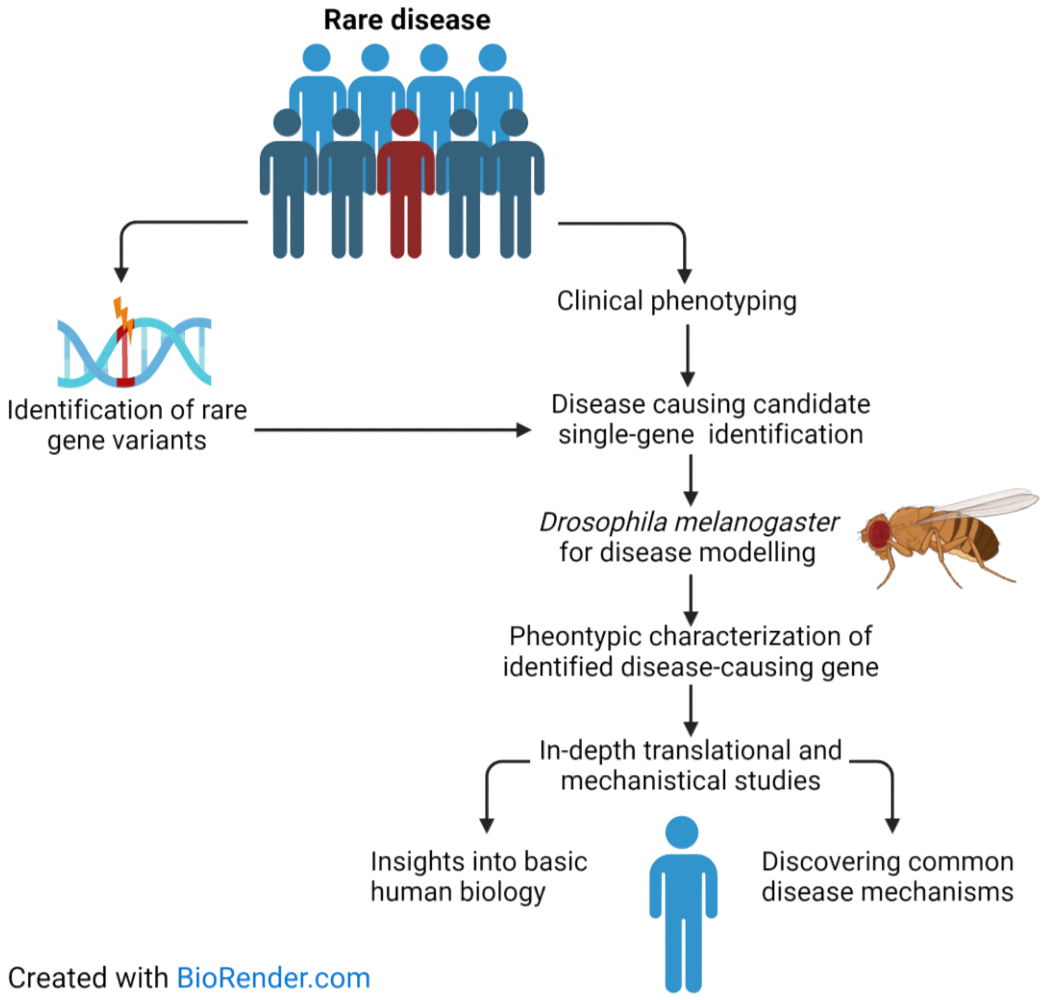

Figure 1.3. *Drosophila* as a rare genetic disease model
Individuals with rare diseases often have unique genetic variants not previously associated with disease phenotypes. Diagnosing these conditions involves clinical phenotyping, DNA sequencing, and identifying rare variants. By connecting individuals with similar genetic profiles, researchers can find common links. Studies using model organisms like fruit flies (*Drosophila melanogaster*) can help discover new disease-causing genes and enhance the understanding of known genes, aiding in mechanistic studies.

1.3. Robinow Syndrome

The disease we model in this study, Robinow Syndrome (RS), is a rare genetic disorder characterized by distinctive facial features, short stature, and skeletal abnormalities. First described by Dr. Meinhard Robinow in 1969, the syndrome manifests in two forms: autosomal dominant and autosomal recessive, each associated with different genetic mutations and varying severity of symptoms (Robinow et al., 1969;

Orphanet: Robinow Syndrome, n.d.). The first described case was an autosomal dominant RS case in a family from Ohio and a few years later autosomal recessive cases were reported in Tennessee and Kansas (Robinow et al., 1969; Wadlington et al., 1973). Since the description of the syndrome, there have been less than 250 cases reported all around the world with variable frequency of clinical symptoms in both females and males equally (*Orphanet: Robinow Syndrome*, n.d.; Schwartz et al., 2021).

Robinow Syndrome is linked to mutations in seven genes associated with the Wnt signalling pathway which is explained in section 1.4 below (Table 1). Two of those, receptor tyrosine kinase-like orphan receptor 2 (*ROR2*) and nucleoredoxin (*NXN*) are linked to the autosomal recessive RS (White et al., 2018; C. Zhang et al., 2022) while the other five, Dishevelled genes *DVL1*, *DVL2*, *DVL3*, along with *WNT5A* and *Frizzled2* (*FZD2*) were found to be causative variants in autosomal dominant cases (Nagasaki et al., 2018; Person et al., 2010; Saal et al., 2015; White et al., 2015; White et al., 2016, 2018; Zhang et al., 2022). The recessive and dominant types of RS can be distinguished with the inheritance patterns or severity of the phenotypes since the recessive form shows more severe clinical phenotypes, however, the clinical presentations of patients are quite similar (Mazzeu et al., 2007). The primary RS phenotypes are facial abnormalities called “fetal facies” such as wide-spaced eyes, broad forehead and flat nasal bridge shortened distal limbs and underdeveloped genital parts (Beiraghi et al., 2011; Kaissi et al., 2020; Conlon et al., 2021; Sakamoto et al., 2021; Zhang et al., 2022; Abu-Ghname et al., 2021). It should be noted that autosomal recessive RS patients show average neurocognitive function while some autosomal dominant RS patients, especially the ones carrying pathogenic DVL1 variants, showed learning disabilities and problems with peers (Schwartz et al., 2021). The treatments and therapies for RS patients available are limited to corrective surgeries, braces and hormone therapy (*Orphanet: Robinow Syndrome*, n.d.).

Table 1.1. Robinow Syndrome-associated genes in Wnt signalling pathway

Gene/OMIM ID	Function	Inheritance	Mutation Type	OMIM Entry
WNT5A 164975	Wnt Ligand	Autosomal dominant	Missense	180700
DVL1 601365	Wnt - Cytoplasmic adaptor protein	Autosomal dominant	-1 frameshift	616331
DVL2 602151	Wnt - Cytoplasmic adaptor protein	Autosomal dominant	+1 frameshift	602151
DVL3 601368	Cytoplasmic adaptor protein	Autosomal dominant	-1 frameshift	616894
FZD2 600667	Wnt – receptor	Autosomal dominant	Missense, nonsense	618529
ROR2 602337	PCP Wnt co-receoptor	Autosomal recessive	Missense, nonsense	268310
NXN 612895	Stabilizer of DVL	Autosomal recessive	Deletion, missense	618529

The similar phenotypes of the different types of the syndrome suggest that the genes associated with RS might share a common, indirect, downstream Wnt mediator that would be affected by the mutations. The human genetics studies predict that the autosomal dominant cases with the mutations in *WNT5A*, *FZD2* and the Dishevelled genes are not due to a loss-of-function (White et al., 2018). The mouse models with heterozygous null mutations of these genes were shown to be normal and viable (Wynshaw-Boris, 2012; Yamaguchi et al., 1999; H. Yu et al., 2010) supporting the findings in the previously mentioned genetic studies. It was also shown that the mice lacking these genes did not have skeletal abnormalities, suggesting that the phenotypes are not caused by haploinsufficiency (Lijam et al., 1997; Etheridge et al., 2008; Wynshaw-Boris, 2012).

Four of the pathogenic mutations in genes linked to RS are genes involved in both canonical and non-canonical/PCP Wnt signalling: *FZD2*, *DVL1*, *DVL2* and *DVL3*. Since the effects of these mutations on a major signalling pathway cannot only be predicted by genetic studies and cell culture studies, *in vivo* studies were a necessity. Studies from our lab and our collaborators modelling *DVL1* associated autosomal dominant RS in model organisms, fruit flies and chick embryos respectively, have shown that the RS *DVL1* variants causes a loss of canonical and gain of non-canonical/PCP Wnt signalling with several readouts and reporters used in our assays. While dominant-negative effects were shown in canonical Wnt signalling, an induction in the non-canonical pathway were reported via multiple readouts. Further neomorphic phenotypes were also reported in both models (Gignac, et al., 2023). Details of the assays and reporters used in this study are described in section 1.9 below. A later study from our collaborators aiming to model FZD2 associated RS in chick embryos showed that different variants induced RS phenotypes through different mechanisms one that is similar to the DVL1 variants and the other by causing dominant-negative effects on canonical Wnt signalling by also causing a loss-of-function in non-canonical/PCP pathway (Tophkhane, Fu, et al., 2024).

The neomorphic phenotypes in *DVL1* associated RS model in fruit flies still requires further investigation in terms of *in vivo* tissue morphology and development. This thesis aims to decipher how the DVL1 variants affect the signalling network and cellular mechanisms transcriptionally and on the protein level in fruit flies.

1.4. Wnt Signalling Pathways

Wnt signalling is an evolutionarily conserved set of cell coordination and communication pathways that play a vital role in numerous physiological processes, such as stem cell regeneration, proliferation, division, migration, cell polarity, cell fate determination, and neural crest specification, as well as neural symmetry and morphogenesis (Komiya & Habas, 2008; Simons & Mlodzik, 2008; Swarup & Verheyen, 2012; Hayat et al., 2022). This signalling pathway is divided into two main categories: the β-catenin-dependent pathway, also known as the canonical or Wnt/β-catenin pathway, and the β-catenin-independent pathway, referred to as the non-canonical (planar cell polarity, PCP) pathway. The Wnt/β-catenin-dependent signalling primarily regulates cell proliferation, while the β-catenin-independent pathway governs cell polarity and motility (Komiya & Habas, 2008; Grumolato et al., 2010; Amin & Vincan, 2012; Gajos-Michniewicz & Czyz, 2020). *Drosophila* genetic screens and functional studies were highly influential in the identification of a lot of the components of these signalling pathways and their signalling hierarchies (Baker, 1987; Chae et al., 1999; Eaton et al., 1996; Feiguin et al., 2001; Jenny et al., 2003, 2005; Jursnich et al., 1990; Nüsslein-Volhard et al., 1984; Nüsslein-Volhard & Wieschaus, 1980; Peifer et al., 1994; Peifer & Wieschaus, 1990; Perrimon et al., 1989; R. P. Sharma & Chopra, 1976; Siegfried et al., 1990; Taylor et al., 1998; Tree et al., 2002; Treisman et al., 1997; Usui et al., 1999; Vinson & Adler, 1987; Wolff & Rubin, 1998; Yanagawa et al., 2002; Zilian et al., 1999) (Fig. 1.4).

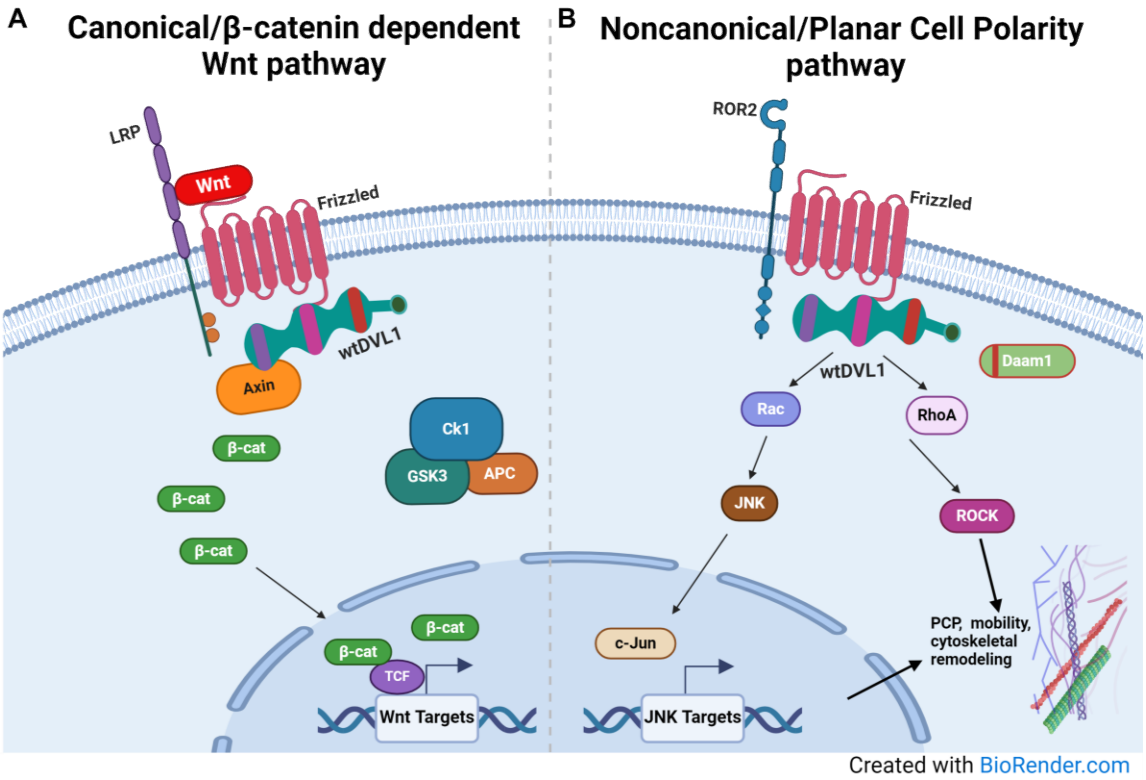

Figure 1.4. Schematic of canonical and Non-canonical Wnt signalling
A) Canonical/β-catenin dependent Wnt signalling. With the activation of Wnt, Dishevelled is recruited to the membrane and interacts with components of the destruction complex and inactivates it. This allows β-catenin to be stabilized in the cytoplasm which can enter the nucleus and help activate the expression of Wnt target genes. **B**) Noncanonical/Planar Cell Polarity Wnt signalling. Dishevelled interacts with downstream effector molecules such as Rac and RhoA to activate PCP-JNK signalling to induce target gene expression, cell polarity, cell mobility and cytoskeletal remodelling.

1.4.1. Canonical Wnt Signalling

The canonical or β-catenin-dependent Wnt signalling pathway plays a crucial role in regulating patterning, cell proliferation, cell differentiation, and stem cell maintenance (Swarup & Verheyen, 2012). Dysregulation of this pathway has long been linked to carcinogenesis in humans (Cadigan & Nusse, 1997; Clevers & Nusse, 2012; Komiya & Habas, 2008) and, more recently, to bone development defects (Monroe et al., 2012). The pathway is activated when a Wnt ligand binds to the Low-density lipoprotein receptor-related protein (LRP)-Frizzled co-receptor complex, which then recruits Dishevelled to the membrane (MacDonald & He, 2012). Once at the membrane, DVL acts as a platform for Axin and GSK3β to bind and phosphorylate LRP, which prevents the continuous degradation of β-catenin in the cytoplasm. By inhibiting the degradation

of β-catenin, DVL allows β-catenin to accumulate in the nucleus where it works as a coactivator for TCF (T cell factor) to activate Wnt-responsive genes (Behrens et al., 1996; Huber et al., 1996; van de Wetering et al., 1997; Bienz, 2014) (Fig. 1.4).

1.4.2. Noncanonical/Planar Cell Polarity Pathway

The Noncanonical/Planar Cell Polarity (PCP) pathway was discovered when mutations in *Frizzled* and *dishevelled* caused randomization of the polarity of cuticle actin hairs and sensory bristles on fly wings (Fahmy & Fahmy, 1959a; Gubb & García-Bellido, 1982). PCP is mainly known for orienting the actin-rich hair structures and sensory bristles on the abdomen, thorax, and wings of adult flies (Adler, 2002). In vertebrates, PCP signalling regulates cell intercalation, convergent extension, gastrulation, neural tube closure, inner ear sensory hairs, and ciliogenesis (Komiya & Habas, 2008; Seifert & Mlodzik, 2007; Y. Wang & Nathans, 2007). Disrupted PCP signalling has been linked to disorders like open neural tubes, cystic kidneys, and severe developmental defects (Maung & Jenny, 2011).

In *Drosophila*, activation of the Frizzled-Ror2 heterodimers recruits Dishevelled to the membrane (Teufel & Hartmann, 2019). Dishevelled activates PCP signalling via its DEP domain, affecting various cellular responses such as cell death, shape changes, mobility, adhesion, and migration (Axelrod et al., 1998; Boutros et al., 1998; Seifert & Mlodzik, 2007; Nishita et al., 2010) (Fig. 1.4).

1.5. Dishevelled protein structure and function

The *Dishevelled* gene was first discovered in *Drosophila* mutants displaying disoriented hair and bristle polarity (Fahmy & Fahmy, 1959a, 1959b; Wallingford & Habas, 2005). Known as *Dsh* in *Drosophila* and *Dvl* in vertebrates, the gene gained prominence for its crucial role in segment polarity during early embryonic development in *Drosophila* (Perrimon & Mahowald, 1987). Other homologs of the *Dishevelled* gene were later identified in *C. elegans* (*Dsh-1, Dsh-2, Mig-5*), *Xenopus* (*Xdsh*), mice (*Dvl1, Dvl2, Dvl3*), and humans (*DVL1, DVL2, DVL3*) (Sussman et al., 1994; Sokol et al., 1995; Klingensmith et al., 1996; Pizzuti et al., 1996; Semënov & Snyder, 1997; Lee et al., 2006; Tsang et al., 1996).

DVL genes and the protein structure is highly conserved across orthologs within each species as well as across different species. Ranging from *Drosophila* to humans, all DVL proteins are 600-750 amino acids long and possess three highly conserved domains. Dishevelled-Axin (DIX), PSD-95, DLG, ZO1 (PDZ) and Dishevelled-EgL10-Plekstrin (DEP) as well as a few other highly conserved sequences such as a basic region and a PDZ-binding motif (PBM) found in the highly conserved C-terminus (Fig 1.5) (Wallingford & Habas, 2005; Qi et al., 2017).

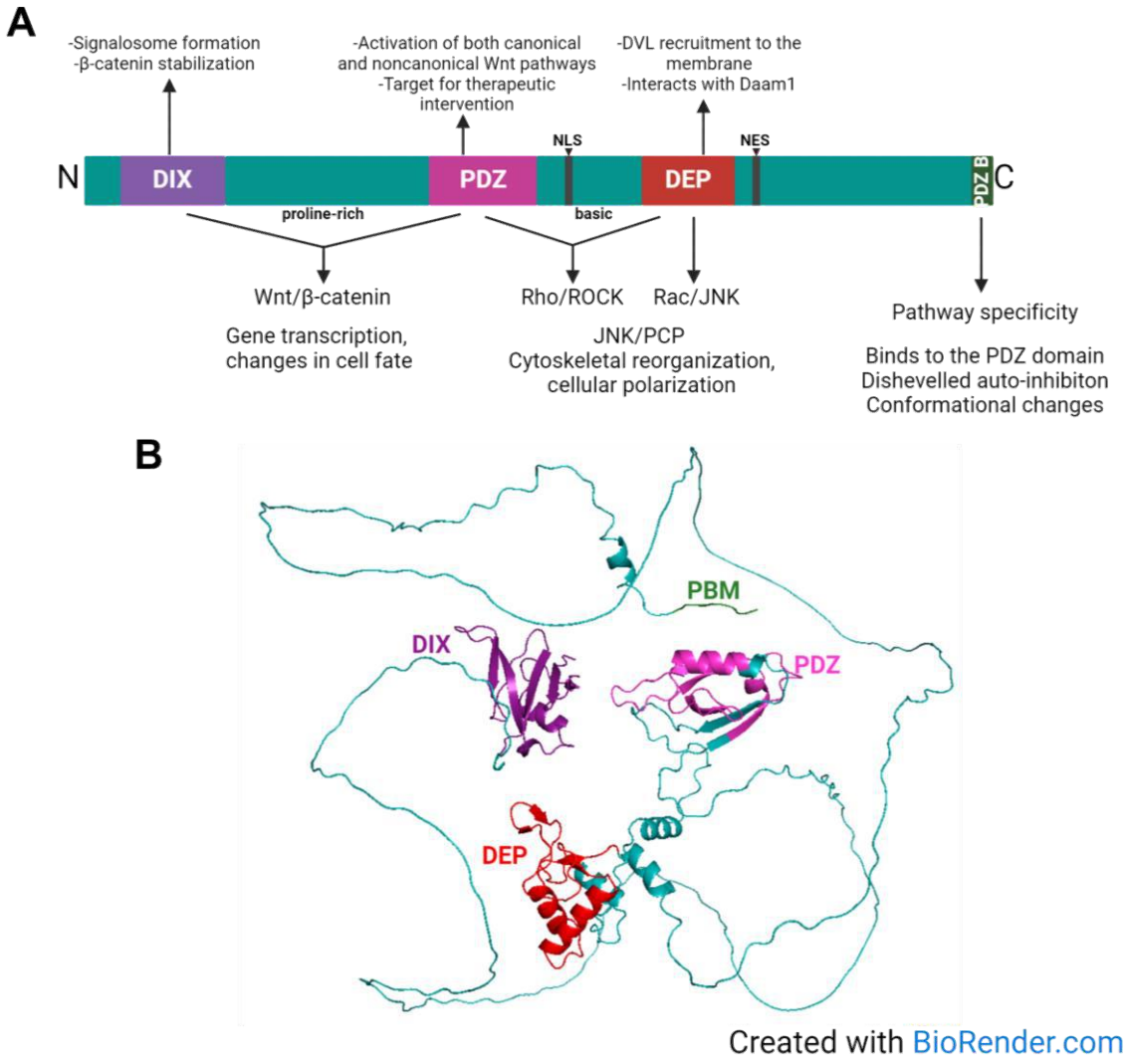

Figure 1.5. Schematic of Dishevelled protein structure and predicted model
(**A**) Cartoon depiction of the protein structure of Dishevelled showing the 3 functional domains, important motifs and regions. (**B**) 3D predicted model of human DVL1 isoform 2, used in our studies. Model generated by ColabFold2. Mirdita, M., Schütze, K., Moriwaki, Y., Heo, L., Ovchinnikov, S., & Steinegger, M. (2022). ColabFold: making protein folding accessible to all. *Nature methods*, *19*(6), 679–682. https://doi.org/10.1038/s41592-022-01488-1

The DIX (Dishevelled-Axin) domain, located in the N-terminus, contains ~82–85 amino acids. It is also present in other proteins such as Axin, as its name suggests (Shiomi et al., 2003). The DIX domain enables DVL proteins to polymerize and form cytoplasmic puncta at both normal and overexpressed levels (Gao & Chen, 2010). It facilitates the DVL dependent activation of the Wnt/β-catenin pathway by forming these puncta (Schwarz-Romond et al., 2007). It also assists in assembling signalosomes, sites of active Wnt signalling, near the plasma membrane and mediates interactions between proteins. DVL interacts with Axin through the DIX domain, preventing Axin from forming the destruction complex which targets β-catenin for proteasomal degradation, thus stabilizing β-catenin and promoting Wnt target gene activation (Kishida et al., 1999). Mutations in key residues within the DIX domain can block Wnt pathway activity (Capelluto et al., 2002; Capelluto & Overduin, 2005; Schwarz-Romond et al., 2007; Ehebauer & Arias, 2009).

The second domain which is about 73 amino acids long in humans is the PDZ domain, named after the proteins Post synaptic density-95/Discs large/Zonula-occludens-1 where it was first discovered (Kennedy, 1995). The PDZ domain facilitates essential protein-protein interactions and regulates various biological processes. It interacts directly with a conserved region of Frizzled which is crucial for activating Wnt signalling and localizing DVL proteins to the membrane (H.-C. Wong et al., 2003). The PDZ domain is shown to be important in both canonical and non-canonical Wnt pathways (Moon & Shah, 2002), and it is thought to help differentiate between the two pathways (Boutros & Mlodzik, 1999; Weston & Davis, 2001). This domain has gained significant attention, and using NMR spectroscopy, various compounds and peptides have been developed to selectively inhibit PDZ-domain interactions which led to a down-regulation in the Wnt signalling pathway activity (Gao & Chen, 2010; Grandy et al., 2009; Mahindroo et al., 2008; Tran & Zheng, 2017; Zhang et al., 2009). The crystal structure of the PDZ domain revealed a dynamic binding pocket which becomes rigid when bound by a peptide (Lee et al., 2017).

The Dishevelled, Egl-10, Pleckstrin (DEP) domain, located at the C-terminal of DVL proteins, consists of ~75 amino acids. This domain allows DVL to interact with several proteins and facilitates activating the non-canonical/PCP Wnt signalling pathway. Studies show that the DEP domain targets DVL proteins to the membrane when the Wnt signal is received (Pan et al., 2004). It is crucial for assembling functional signalosomes

and transmitting Wnt signals to the nucleus (Gammons et al., 2016). During planar epithelial polarization, DVL is located to the membrane by some basic residues within the DEP domain (Wong et al., 2000). Mutations in these residues were shown to prevent DVL's targeting to the membrane and disrupt crucial developmental processes (H. C. Wong et al., 2000; Park et al., 2005).

Other than these three conserved domains, DVL has a nuclear localization signal (NLS) and a nuclear export signal (NES) that control its movement in and out of the nucleus. The NLS, with the consensus sequence IxLT (where x is any amino acid), is located between the PDZ and DEP domains. The NES, with the consensus sequence M/LxxLxL, is found between the DEP domain and the C-terminus of the DVL protein. Recent studies indicate that DVL's nuclear localization is crucial for its role in the canonical Wnt pathway (Gan et al., 2008; Itoh et al., 2005).

The terminal seven amino acids in the C-terminus of vertebrate DVL proteins are called the PDZ-binding motif (PBM) and this motif was shown to bind competitively to the PDZ domain (Lee et al., 2015; Harnoš et al., 2019). Binding of PBM to the PDZ domain causes the autoinhibition of DVL (Fig. 1.6). Forced binding of PBM to the PDZ domain was shown to reduce noncanonical Wnt signalling while blocking the interaction freed the DVL autoinhibition, disrupting its functional interaction with LRP6 in canonical Wnt signalling and increasing the specificity towards noncanonical Wnt signalling. This showed that the PBM binding to the PDZ domain is crucial to keep the balance between the canonical and noncanonical Wnt signalling since it keeps DVL in an autoinhibited form which helps the protein to be regulated by other interaction partners (Qi et al., 2017).

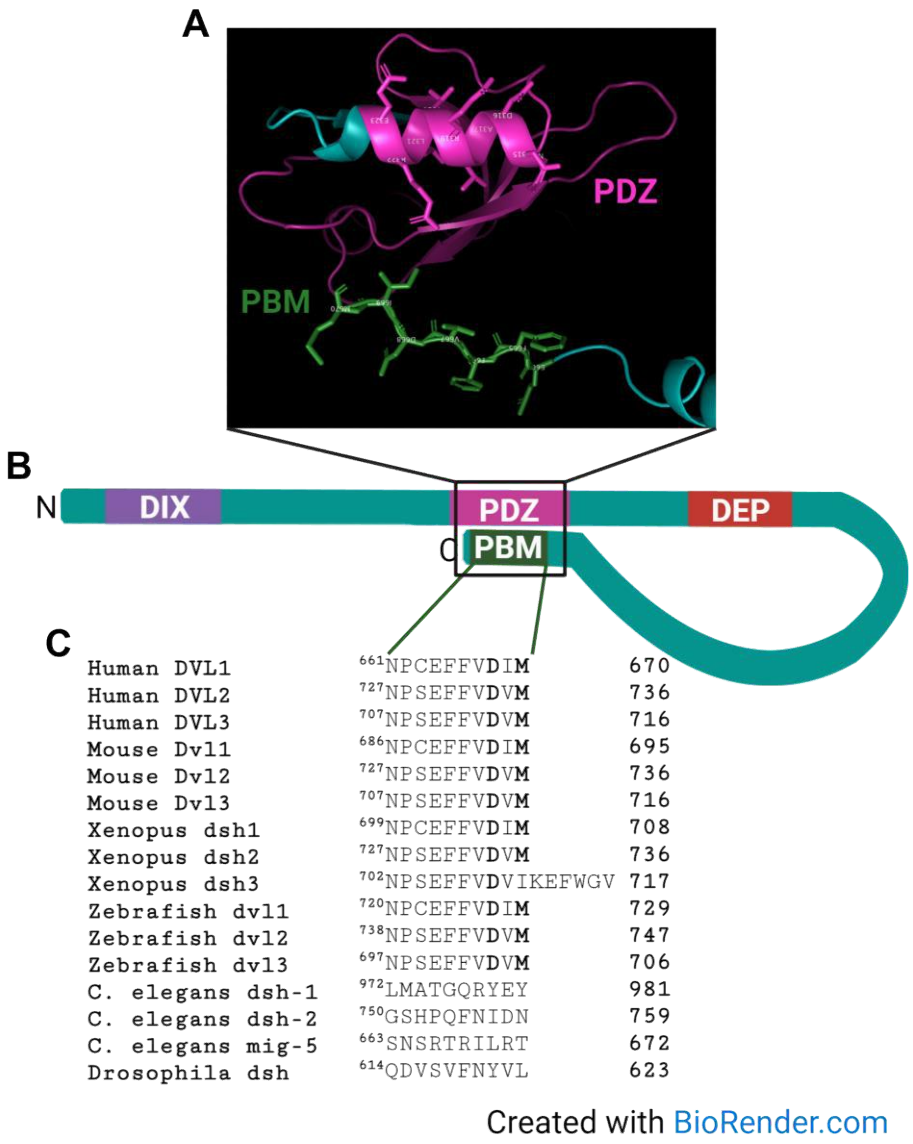

Figure 1.6. 3D predicted model and the schematic of the interaction between PDZ domain and the PDZ-binding motif (PBM)

(**A**) 3D predicted model of human DVL1 isoform 2, used in our studies. (**B**) Cartoon depiction of the protein structure of Dishevelled showing the 3 functional domains, important motifs and regions. (**C**) The table showing the conservation of the C-terminus in vertebrate DVL proteins. Model generated by ColabFold2. Mirdita, M., Schütze, K., Moriwaki, Y., Heo, L., Ovchinnikov, S., & Steinegger, M. (2022). ColabFold: making protein folding accessible to all. *Nature methods*, *19*(6), 679–682. https://doi.org/10.1038/s41592-022-01488-1

1.5.1. Dishevelled in Wnt signalling

Early genetic studies revealed that DVL proteins are involved in both canonical and non-canonical/PCP Wnt signalling pathways. Initially, it was unclear how DVL could participate in both pathways simultaneously. Later, it was discovered that DVL serves as

a switch and is essential for the proper activity of both types of Wnt signalling (Wallingford & Habas, 2005). DVL is also linked to other Wnt-related signalling pathways, such as Wnt-GSKβ-microtubule, Wnt-calcium, Wnt-RYK (related to tyrosine kinase), Wnt-aPKC (atypical protein kinase C), and Wnt-mTOR (mammalian target of rapamycin) pathways (Gao & Chen, 2010). Only the canonical (β-catenin-dependent) and noncanonical PCP pathways are of interest for this study (Fig. 1.4). Both pathways were well identified in *Drosophila*, especially in the processes of segment polarity and development (Wallingford & Habas, 2005; Sharma et al., 2018), hence there are many assays, reporters and well-established phenotypes we could utilize in our studies.

1.5.1.1. Canonical Wnt Signalling

After being recruited to the membrane with the activation of the signalling cascade, DVL proteins act as a platform for Axin and the rest of the degradation complex; GSK3β, Adenomatous polyposis coli (APC), Casein kinase 1 (Ck1). This helps inhibit β-catenin degradation in the cytoplasm. DVL proteins can also shuttle between the cytoplasm and the nucleus (Habas & Dawid, 2005; Itoh et al., 2005; Gan et al., 2008). Recent research has revealed that DVL proteins contain both a nuclear export sequence (NES) and a nuclear localization sequence (NLS) (Fig. 1.5), which are crucial for their function in the canonical Wnt signalling pathway (Itoh et al., 2005). Another study demonstrated that DVL-2 interacts with c-Jun and β-catenin to form a stable DVL-2/c-Jun/β-catenin/TCF complex that activates Wnt target genes in the nucleus (Gan et al., 2008) (Fig. 1.4). DVL also modulates Wnt signalling by interacting with various nuclear proteins, such as HIPK1 (Homeodomain-interacting Protein Kinase 1), xNET1 (Xenopus Nucleotide Exchange Factor 1), and FOXKs (Forkhead Box Transcription Factors) (Louie et al., 2009; Miyakoshi et al., 2004; W. Wang et al., 2015). Therefore, it appears that there are two DVL populations in a cell: one in the nucleus and another in the cytoplasm, both of which regulate the canonical Wnt pathway (Sharma et al., 2018).

1.5.1.2. Noncanonical/Planar Cell Polarity Wnt Signalling

In the non-canonical Wnt signalling pathway, also known as the Wnt/PCP (Planar Cell Polarity) pathway, DVL plays a crucial role in controlling planar cell polarity and cytoskeletal rearrangements. In vertebrates, the Wnt signal is first received by the Frizzled receptor, which then relays the signal to DVL and its associated proteins, Diego and Strabismus (Vangl in vertebrates)-Prickle (Pk). These interactions help define the

polarity of epithelial cells within a sheet or plane of cells (Wallingford et al., 2002; Veeman et al., 2003; Klein & Mlodzik, 2005; Gao & Chen, 2010). In Drosophila, Wnt ligands are not essential for this signal transduction to occur, yet other global cues must exist for tissue polarity to be established (Yu et al., 2020). It should be noted that the noncanonical/PCP pathway is distinct from the apico-basal polarity of epithelial cells.

For this pathway, DVL again acts as a switch for two distinct signalling cascades that lead to the activation of small GTPases Rho and Rac. For the Rho signalling branch, the Wnt signal causes DVL to form a complex with Daam1 (Dishevelled Associated Activator of Morphogenesis 1). This complex then interacts with the Rho guanine nucleotide exchange factor WGEF, which activates downstream effectors like Rho GTPase and Rho-associated kinase (ROCK) (Habas et al., 2001; Tanegashima et al., 2008). Activated Rho/ROCK signalling alters the actin cytoskeleton, affecting cell structure (Habas et al., 2003). In the other branch, DVL also activates the Rac GTPase independently of Daam1. Activated Rac stimulates the downstream effector c-Jun N-terminal kinase (JNK), which regulates cell polarity and movement during Xenopus gastrulation (Habas et al., 2003). In both *Drosophila* and higher organisms, JNK exerts pleiotropic effects in processes such as apoptosis, proliferation, differentiation, cell migration, tumorigenesis, and cell competition (Igaki, 2009; Pinal et al., 2019; La Marca & Richardson, 2020). Moreover, JNK pathway activation is essential for epithelial regeneration in flies (Hariharan & Serras, 2017) (Fig. 1.4).

As mentioned earlier, many genes implicated in Robinow Syndrome are components or regulators of the Wnt/PCP pathway (Zhang et al., 2022). However, several of these genes, like Dishevelled and Frizzled, are also active in the canonical Wnt pathway.

1.5.1.3. DVL in other signalling pathways

DVL interacts with proteins from other signalling pathways to regulate key cell processes. For example, DVL helps remodel the cell's cytoskeleton by inhibiting GSK3β and stabilizing microtubule-associated proteins MAP1B and MAP2 (Goold et al., 1999; Lucas et al., 1998). DVL also partners with a Ring finger protein called XRNF185 to support cell migration during *Xenopus* gastrulation (Iioka et al., 2007). In the Wnt/Ca^{2+} pathway, DVL increases intracellular calcium levels, which activates calcium-sensitive enzymes such as protein kinase C (PKC) and calcium-calmodulin-dependent kinase

(CamKII) (Sheldahl et al., 2003). This increase in Ca2+ ions regulates tissue separation and cell movements during early embryonic development (Slusarski & Pelegri, 2007). Additionally, DVL interacts with the RYK (Related to Tyrosine Kinase) receptor to mediate axonal repulsion and cell migration in neuronal cells (Lu et al., 2004). DVL also binds to and stabilizes atypical PKC (aPKC), which promotes microtubule assembly and axon formation. Studies in hippocampal neurons show that reducing DVL leads to fewer axons, while increasing DVL causes the formation of multiple axons (Zhang et al., 2007).

Overall, DVL is central to distribute the Wnt signal which will influence various fundamental developmental processes in cells. Due to its involvement in multiple pathways, DVL can be considered a master router of complex signals.

1.6. Robinow Syndrome-associated *Dishevelled1* variants

The majority of dominant Robinow Syndrome (RS) cases involve *de novo* frameshift mutations in the genes encoding cytoplasmic adaptor proteins (DVL) (Bunn et al., 2015; Hu et al., 2022; White et al., 2015; White et al., 2016; Zhang et al., 2022). These mutations result in an abnormal long peptide replacing portions of the C-terminus. Recently, DVL2 has also been proposed as a candidate gene, with a mutation identified in one RS patient (Zhang et al., 2022). Among the three DVL genes, DVL1 is the most frequently mutated in RS and is accountable for roughly one third of the cases (Bunn et al., 2015; Hu et al., 2022; White et al., 2015; White et al., 2016; Zhang et al., 2022). The functional link between skeletal phenotypes and frameshift mutations in DVL genes has not been extensively studied, except by our lab together with the Richman lab using chicken embryo and *Drosophila* models (Gignac et al., 2023).

Each DVL1 variant associated with RS has a unique single nucleotide deletion in the second to the last exon, exon 14, causing a -1 frameshift that replaces the highly conserved C-terminal region with a novel peptide sequence and introduces a translation-termination codon at a different location (Fig. 1.7. It should be noted that 109 amino acids of this novel sequence are identical across each variant (Bunn et al., 2015; Hu et al., 2022; Mansour et al., 2018; White et al., 2015; White et al., 2016, 2018). This fframeshift also slightly truncates the protein compared to the wild-type full-length DVL1. These heterozygous mutations do not affect key functional domains in the protein, such as the DIX, PDZ, or DEP domains, and are compatible with life, as patients survive into

adulthood. While some researchers have suggested that the abnormal C-terminus is responsible for the phenotypes (Bunn et al., 2015), it is also possible that abnormalities in protein folding might affect the interactions of the three conserved domains of DVL (Fig. 1.7) (Hu et al., 2022).

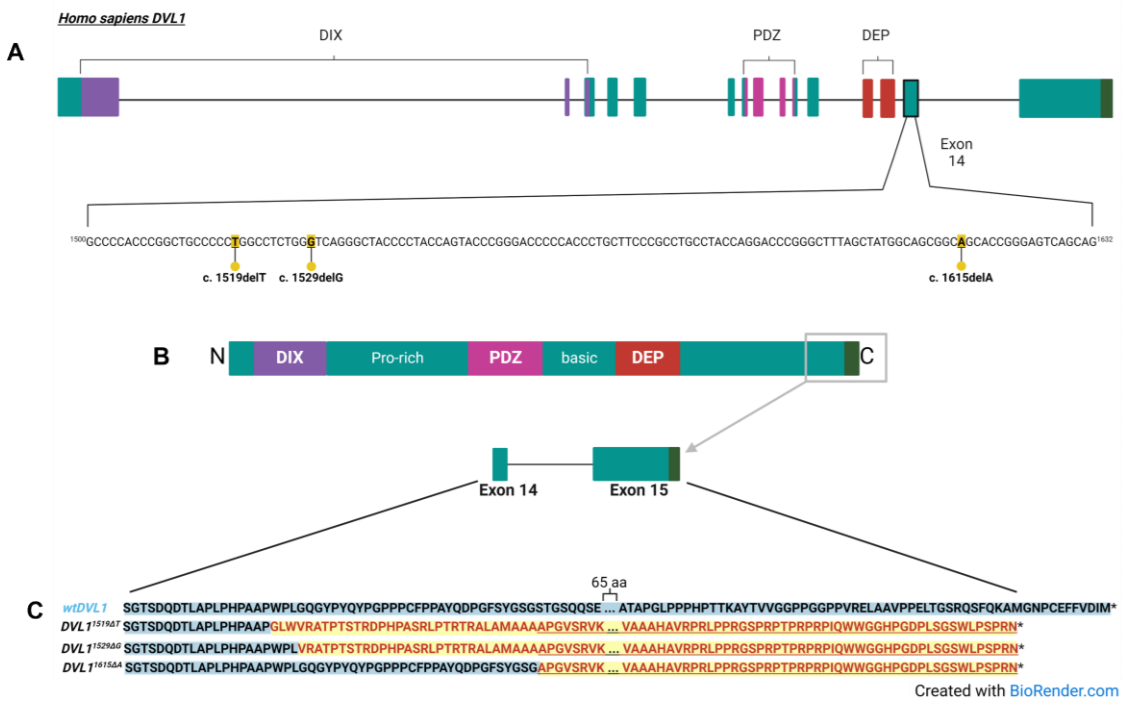

Figure 1.7. Schematic of RS-associated DVL1 mutations and frameshifts
A) Diagram depicting the exon-intron structure of the human DVL1 gene and the deletions of nucleotide 1519, 1529 and 1615 in Exon 14 that causes the frameshift mutations creating a different termination codon in Exon 15. **B)** Cartoon depiction of Dishevelled protein showing the parts corresponding to the transcripts of exon 14 and 15. **C)** Alignment of human wild type DVL1 C-terminal amino acid sequence with the variants, showing the homology of the novel peptide sequence at the C-termini of the variants.

Given that all DVL1-associated RS cases are autosomal dominant, with each patient carrying one mutant and one wildtype *DVL1* allele, we can express the human genes on top of the *Drosophila* genome during development to mimic the nature of autosomal dominant disorders. The current literature on RS primarily focuses on identifying new mutations and characterizing patient clinical phenotypes, resulting in a gap between the identification of RS-associated alleles and understanding their functional impact on development. The research from our lab and our collaborators aims to bridge this gap by elucidating how signalling pathways are disrupted by RS-associated DVL1 proteins and how this disruption corresponds to RS phenotypes.

Our earlier study of RS emphasized the significant roles of the DVL1 gene in morphogenesis, skeletogenesis, and PCP-JNK signalling (Gignac, et al., 2023). This thesis describes research which has expanded on previous findings which demonstrated that RS DVL1 variants induce a dominant negative reduction in canonical signalling while simultaneously increasing JNK-PCP signalling. This imbalance in WNT signalling may be central to the pathogenesis of all forms of RS, whether caused by DVL genes or other genes in the WNT pathway. Additionally, we provided evidence of the neomorphic activity of these DVL1 variants *in vivo* within a developmental context (Gignac et al., 2023).

1.7. Gal4-UAS Expression System

Humanized model organisms have been a powerful tool for the study of human diseases. These models are a powerful tool for our understanding of how a mutated gene can cause pathologies. They also provide insights into fundamental human biology (Oparin, 1957; Mukherjee et al., 2022). In this project, in order to model a rare genetic disease, Robinow Syndrome, we expressed human genes in fruit flies, thus making humanized fly models. For the expression of the wildtype and the variant *DVL1* genes, we used the Gal4-Upstream activating sequence (UAS) system (Brand & Perrimon, 1993). Inspired by baker's yeast, this binary expression tool was generated for controlled gene expression in eukaryotes. As the name suggests, there are two components in this tool: a Gal4 transcription factor that is under a native promoter and UAS-transgene construct. For a gene of interest that is cloned after the UAS site to be expressed, the Gal4 protein needs to bind the UAS site and activate the expression (Fig. 1.8). A large number of Gal4 insertion strains have been generated that drive expression in various patterns ranging from ubiquitous to very small subsets of cells. These lines are publicly available and allow us to design experiments to express transgenes in subsets of cells within a tissue, providing an internal control of normal tissue neighboring Gal4-expressing cells. To drive gene expression, the Gal4 protein and the UAS site must be present in a cell at the same time. However, the UAS and Gal4 components are carried in separate fly lines. This way, we can target the expression of our gene of interest to stages of development, specific tissues or sub-tissue cell types by just crossing together different fly lines (Brand & Perrimon, 1993) (Fig. 1.8).

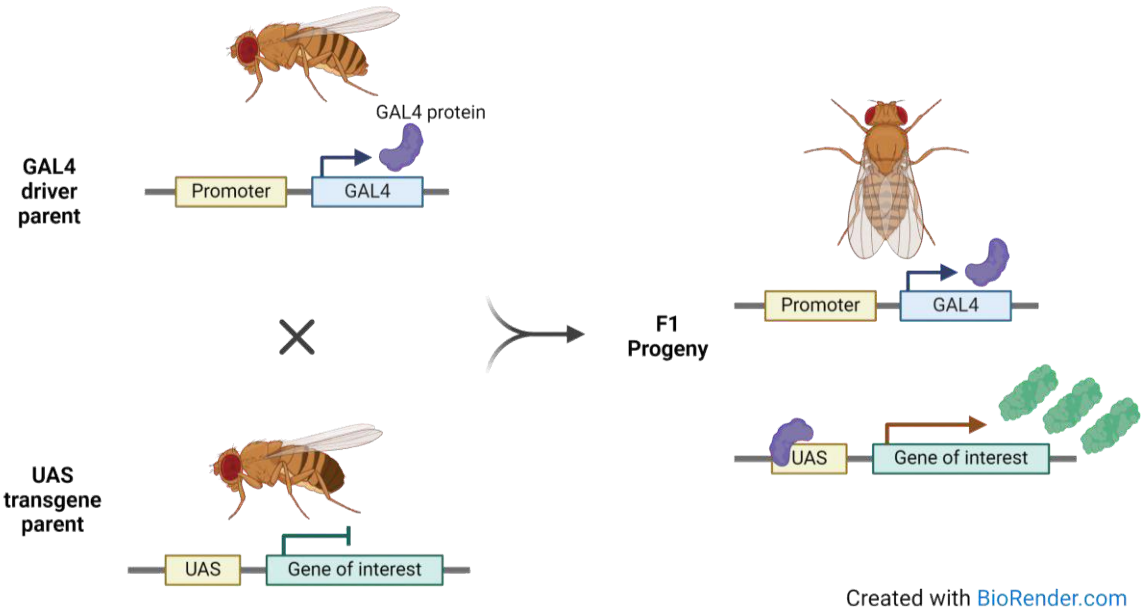

Figure 1.8. Gal4-UAS expression system
The parent flies that carry the Gal4 or the UAS lines are crossed together to induce the expression of the target gene in the tissue of interest of the progeny.

Many improvements and modifications were done on the basic model of Gal4-UAS system after its nature was better understood and use for the benefit of researchers. One such finding was the temperature sensitivity of Gal4 in fruit flies. Minimal Gal4 activity was found to be at 16°C while 29°C brought the maximal activity while not affecting the fly's overall health and fertility dramatically. So simply by changing the temperature the flies were grown in, we can achieve a range of expression levels (Duffy, 2002). With this logic, we've grown our flies in 22°C, 25°C and 29°C incubators for different experiments. We benefited from this temperature sensitivity in order to compare the levels of severity that could be observed phenotypically.

1.8. *Drosophila* wing development

In this project, we characterized wing development in fruit flies for the investigation of the functions of human wildtype and pathogenic DVL1 variants. We did experiments on all three stages of *Drosophila* wing development: late L3 wing imaginal discs, pre-expansion pupal wings, and adult wings (Fig. 1.9). The majority of my work has focused on the alterations in wing imaginal disc morphology.

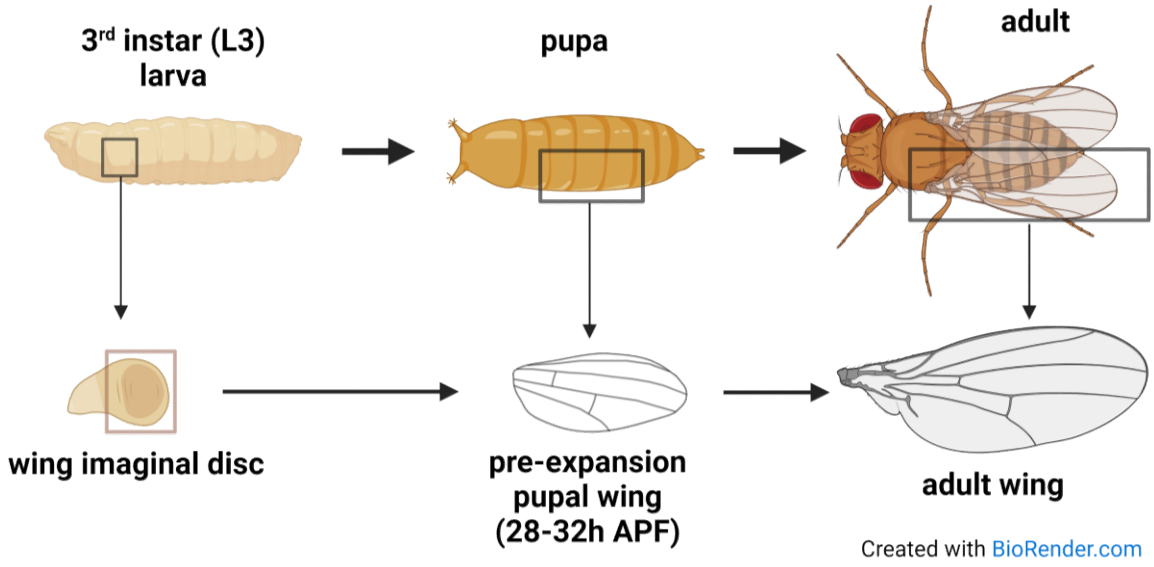

Figure 1.9. Stages of *Drosophila* wing development
The basic schematic of how the wing tissue changes during three stages of metamorphosis. The wing precursor tissue in the larval stage is called the wing imaginal disc which folds and expands to form the pupal wing structure that will become the adult wings after the flies eclosed from their pupal cases.

The wing precursor tissue forms during mid embryogenesis from a cluster of about 30 cells. This group of cells later invaginate to form a sac-like structure called an imaginal disc (Bate & Arias, 1991; Cohen et al., 1993; Requena et al., 2017). These cells then proliferate extensively during the larval stages and form the mature larval wing disc which consists of around 35,000 cells (Weigmann et al., 1997). Each larva possesses 2 wing discs. In the larval stages, the wing imaginal disc morphology becomes more complex and different regions of the wing imaginal discs are assigned different cell fates (Butler et al., 2003). After pupation, the wing disc goes through largescale morphogenetic changes by folding and expanding ultimately forming the adult wing structure (Waddington, 1940).

Wing imaginal discs are initially formed as a flat tiny bag of epithelial cells in the embryo. The morphology of these epithelial cells and the shape of the tiny bag changes as the wing disc grows through oriented cell divisions during the larval stages. On one side, cells form a flat squamous epithelium that is called the peripodial membrane (McClure & Schubiger, 2005). The cells on the other side lay in an apico-basal direction forming a columnar epithelium called the disc proper (Fig. 1.10). The peripodial

membrane is not considered a part of the disc proper in most studies, hence the wing imaginal disc is taken as an epithelial monolayer (McClure & Schubiger, 2005; Aldaz & Escudero, 2010). In this study, we are also referring to the disc proper only when we mention the wing imaginal disc.

The cells of the monolayer keep growing and form a tall epithelial layer especially around the center of the wing imaginal disc, which is called the pouch. Because of the dense packing of the tall columnar cells, the tension between the cells makes them narrower than the width of the nuclei hence their nuclei do not locate on the same plane, forming a pseudostratified appearance. In order for this tissue to grow, the tall columnar cells around this part of the imaginal disc relocate their nuclei before division and adapt their shape accordingly to maintain the epithelial monolayer (Meyer et al., 2011; Chanet et al., 2017) (Fig. 1.10).

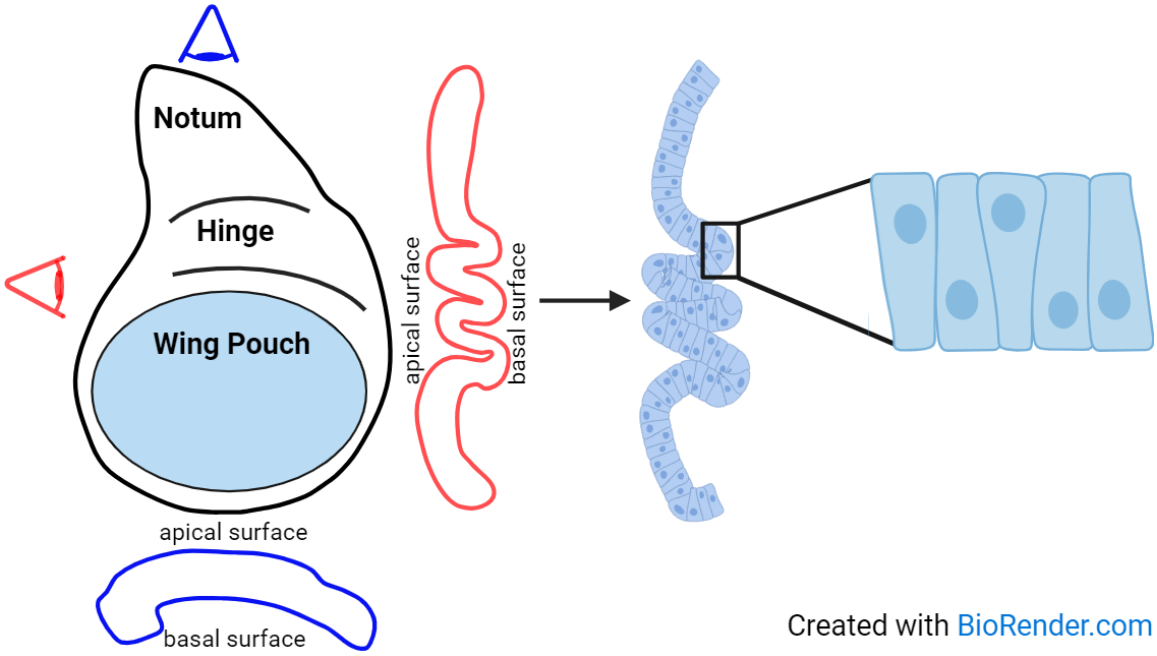

Figure 1.10. Wing imaginal disc morphology
A simple schematic of the wing imaginal disc morphology during the larval stage. The wing imaginal disc composed of columnar epithelial cells (shown on the right) obtains a 3D structure with a well conserved folding pattern. The cells that form the epithelial monolayer of the wing imaginal discs follow the folds of the wing imaginal disc in the 3D structure. The tension in the tissue stretches the cells and creates pseudostratified tall columnar cell morphology.

As the wing imaginal disc grows, the embryonic sac structure becomes a lot more complex and forms the highly controlled 3D structure of the late larval wing

imaginal disc. This 3D structure is formed by the folds that occur at precise locations (Fig. 1.10). Several morphogens and signalling pathways like IroC, Omb, Jak-Stat and Wg play important roles in the structuring of the wing imaginal disc while forming the folds between notum, hinge and the wing pouch (Villa-Cuesta et al., 2007; Johnstone et al., 2013; D. Wang et al., 2016; Sui & Dahmann, 2020).

The fold formation is associated with several cellular mechanisms. The conserved 3-fold pattern is governed by the local degradation of the basal membrane, apical-basal shortening of the cells and the rearrangement of cytoskeleton by mainly the redistribution of microtubules (Sui et al., 2012, 2018; Wang et al., 2016). Computational and experimental studies also showed that the differential growth of different regions governed by the intricate morphogen activity and the tension between the disc proper and ECM membranes also contribute to the fold formation and the morphology of the wing imaginal discs (Tozluoğlu et al., 2019; Kumar et al., 2024).

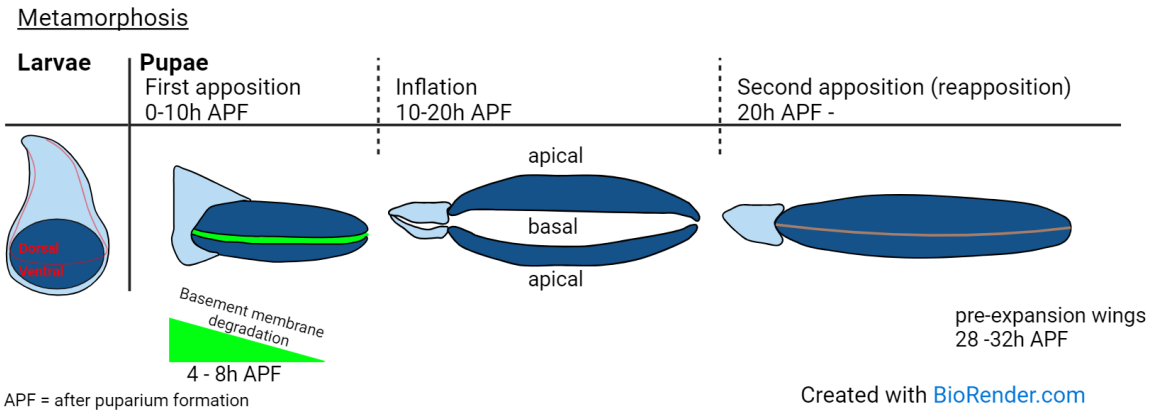

Figure 1.11. Simple schematic of *Drosophila* pupal wing development
During *Drosophila* metamorphosis, the dorsal and ventral surfaces of the wing imaginal disc undergo a complex process of eversion, adhesion, separation, and reapposition. This paradoxical process involves cell-matrix adhesion, matrix production and degradation, as well as the formation of long cellular projections. Figure inspired by: Gui, J., Huang, Y., Montanari, M., Toddie-Moore, D., Kikushima, K., Nix, S., Ishimoto, Y., & Shimmi, O. (2019). Coupling between dynamic 3D tissue architecture and BMP morphogen signaling during *Drosophila* wing morphogenesis. *Proceedings of the National Academy of Sciences of the United States of America*, *116*(10), 4352–4361. https://doi.org/10.1073/pnas.1815427116

During the pupal stage, the wing imaginal disc everts to form a two-layered structure composed of epithelial cells. These wings are flat appendages formed by the mutual adhesion of intervein regions on their dorsal and ventral surfaces (Pastor-Pareja et al., 2004; Blair, 2007; Aldaz et al., 2010; Matamoro-Vidal et al., 2015). Previous

research suggests that pupal wing development is divided into three phases during the first 24 hours of pupal development (Waddington, 1940; Fristrom et al., 1993; Blair, 2007; Gui et al., 2019) (Fig. 1.11). In the first phase, known as first apposition (0–10 hours after puparium formation, APF), a single-layered wing epithelium everts and forms the dorsal and ventral epithelia, creating a rudimentary two-layered wing. During this phase, around 4–8 hours APF, matrix metalloproteinases (Mmps) degrade the dorsal and ventral basement membranes (BMs), enabling adhesion (De Las Heras et al., 2018; Diaz-de-la-Loza et al., 2018; Thompson, 2021) (Fig 1.11). In the next phase, called inflation (10–20 hours APF), the two epithelia physically separate and form a cavity between the two layers of epithelial cells, before fusing in the third phase, second apposition or reapposition, at around 20 hours APF. After BM degradation that brings the two surfaces together, adhesion is mediated by laminin spots that do not contain other main BM components (Sun et al., 2021).

Pre-expansion pupal wings (28h – 32h after pupal formation) were of interest for my study. At this stage, the wings are still composed of living epithelial cells along with the vein structures formed to make them look like a mini adult wing that is ideal for visualizing the morphogenetic and physical abnormalities occurring in the wing development (Blair, 2007; Diaz de la Loza & Thompson, 2017). We can also visualize the hexagonal packing of the epithelial cells, the established proximal-distal polarity and early growth of the actin hairs controlled by Wnt/PCP signalling pathway activity (Classen et al., 2005). A short time after this stage of pupal development (around 40h after pupal formation), the pupal wing goes through a fast and complex expansion and folding that is induced by the contraction of the hinge region within the cuticle secreted in the pupal case, which makes it harder to visualize clearly (Diaz de la Loza & Thompson, 2017).

The final form of the adult wing is formed after eclosion and it is composed of non-living cells and cuticle (Sobala & Adler, 2016; Diaz de la Loza & Thompson, 2017). This stage is a robust readout for visualizing the PCP defects and abnormalities in the vein patterning of the wing blade.

1.9. Autosomal Dominant Robinow Syndrome-*DVL1* Animal Models

In this project, we aim to investigate the mechanistic and phenotypic alterations induced by RS-associated Robinow Syndrome by modelling the disease in fruit flies. The results presented in this thesis are the continuation of the master's project of Katja MacCharles, a former graduate student in our lab. The RS project started as a collaboration with Dr. Joy Richman's laboratory at University of British Columbia, who is modelling the disease in chicken embryos (*Gallus gallus*) to study bone morphology and skeletogenesis. A paper was published in 2023 from this study, by co-first authors Sarah Gignac and Katja MacCharles, with the title "Mechanistic studies in *Drosophila* and chicken give new insights into functions of DVL1 in dominant Robinow Syndrome", which I also had the opportunity to work on (Gignac et al., 2023). More about this paper will be explained in this section.

As mentioned earlier, genetics studies based on clinical reports have been the main focus of RS studies which helped identify the *DVL1* variants. However, functional studies of these variants are required in order to decipher the role of these mutations in disease development. After the identification of some DVL1 variants, researchers carried out cell culture studies and showed that the gene product of the variants were translated into proteins (White et al., 2015). Another study showed an increase in canonical Wnt signalling when the variants were co-transfected with wild type DVL1 *in vitro* (Bunn et al., 2015).

In terms of animal models that had defects in *DVL1*, a homozygous null *Dvl1*$^{-/-}$ mouse model is present in the literature. These mice do not show any alterations in the development of their skeleton while having some behavioural and social abnormalities (Lijam et al., 1997; Wynshaw-Boris, 2012). The results from these mouse model studies support the idea of RS-associated *DVL* variants not causing a strict loss-of-function or haploinsufficiency. Hence, to model DVL1-RS, a system where the variants of *DVL1* are expressed is necessary. So far, no mouse models were generated where the RS-DVL1 variants have been knocked into the equivalent loci of the mouse genome. Until the beginning of our work on RS modelling together with our collaborators, no RS-DVL1 animal models were generated.

This project succeeded in establishing two complementary model systems in which the gene function is investigated. Both models were generated by expressing human genes in addition to the endogenous genes in the chicken and *Drosophila* genomes, which is an advantageous methodology for studying autosomal-dominant mutations that are thought to interfere with the wild type protein's function. The *DVL1* variants used in this study carry frameshift mutations caused by a deletion as described in section 1.6. The specific variants investigated are called $DVL1^{1519\Delta T}$, $DVL1^{1529\Delta G}$ and $DVL1^{1615\Delta A}$, which have the nucleotide 1519, 1529 and 1615 deleted, respectively, which were identified in separate clinical studies (Fig. 1.7) (White et al., 2015).

The investigation of the molecular activities of these variants in chicken embryos showed that the injection of DVL1 variants caused disorganized hypertrophic chondrocytes in chicken skeleton. It also caused shortening in forelimb bones and dysplastic cartilage morphology. Since the transgene expression in chicken limbs are done by using viruses, the chicken embryo is not a genetic model. In order to carry out experiments in which we can control the level of variant expression, tissue location and developmental stage, a genetic model such as *Drosophila melanogaster* was necessary. The complementary experiments carried out in our lab in fruit flies found wing hair misalignment and abnormal wing morphology with abnormal veins and ectopic bristles induced by the expression of DVL1 variants. *In vivo* readouts used in fruit fly tissues showed an increase in noncanonical/PCP-JNK Wnt signalling and a decrease in canonical Wnt signalling induced by the expression of DVL1 variants. These results were supported by the *in vitro* luciferase reporter assays in HEK293 cells (Gignac et al., 2023).

In conclusion this work showed that the expression of DVL1 variants in two different model systems caused an imbalance between canonical and noncanonical Wnt signalling and induced neomorphic phenotypes that were not observed with the expression of wild type human *DVL1* gene (Gignac et al., 2023). In fruit flies, overexpression of the *DVL1* ortholog *dsh* induces ectopic Arm stabilization, which can be used as a readout of Dsh activity (Yanagawa et al., 1997). In our study, we showed that the overexpression of wild type human *DVL1* together with the overexpression of *dsh* does not affect the ectopic Arm levels induced by *dsh* while in contrast the expression of variants does interfere with the activity of elevated Dsh. It should be noted that while being at different severities, possibly due to the location of the frameshift, all variants

induced the same phenotypes in tissues and in the signalling activity (Fig. 1.12). These data together suggested that the variants have dominant-negative activity (Gignac et al., 2023).

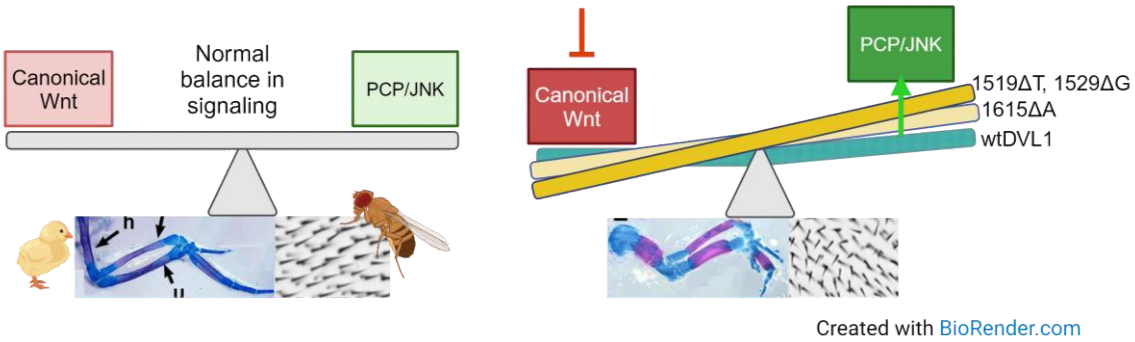

Figure 1.12. Animal models of autosomal dominant Robinow Syndrome associated with mutations in DVL1 showed an imbalance in Wnt signalling and alters development of the skeleton.

Basic schematic of the phenotypes and the Wnt imbalance induced by DVL1 variants in chicken and fruit fly animal models. Adapted from: Gignac, S. J., MacCharles, K. R., Fu, K., Bonaparte, K., Akarsu, G., Barrett, T. W., Verheyen, E. M., & Richman, J. M. (2023). Mechanistic studies in *Drosophila* and chicken give new insights into functions of DVL1 in dominant Robinow syndrome. Disease models & mechanisms, 16(4), dmm049844. https://doi.org/10.1242/dmm.049844

This study was significant in the study of RS since it introduced two animal models for studying autosomal dominant RS caused by the mutations in DVL1. The study of RS also highlighted the roles of *DVL1* in skeletogenesis and Wnt signalling pathway, especially PCP-JNK signalling activity (Gignac et al., 2023).

1.10. C-terminal truncated proteins generated to investigate DVL1 function

Our investigation on the effects of RS DVL1 variants in model organisms raised more questions in terms of the change of protein structure in DVL1 variants compared to its wildtype form. As mentioned earlier, the frameshift mutations that these DVL1 variants have, introduces an early stop codon and also creates an abnormal C-terminus. The novel peptide sequence that replaces the highly conserved C-terminus is mostly the same among all three variants (Bunn et al., 2015; Hu et al., 2022; Mansour et al., 2018; White et al., 2015; White et al., 2016, 2018).

Model organism studies with fruit flies, chicks and mice showed that the protein products of these variants are not affected by nonsense mediated decay, which is conserved mechanism to recognize and get rid of abnormal transcripts containing early termination codons, hence the transcripts are translated into functional proteins (Lykke-Andersen & Jensen, 2015; Bunn et al., 2015; Gignac et al., 2023). Our studies have shown that the expression of all RS DVL1 variants shows similar effects: they all had dominant negative effects in Wnt signalling while also creating phenotypes in the both chick and fly tissues that the expression of wildtype DVL1 did not cause (Gignac et al., 2023).

In the light of all these data, we questioned whether this dominant negative effect and the neomorphic phenotypes are caused by the lack of the highly conserved C-terminus or the novel peptide sequence that replaces it. We also wanted to understand how important the role of the C-terminus of DVL1 is to the protein's cellular function. To investigate these, our collaborators designed two constructs to isolate the role of the novel C-terminal peptide sequence: *DVL1*^{1519*} and *DVL1*^{1431*} (Fig. 1.13).

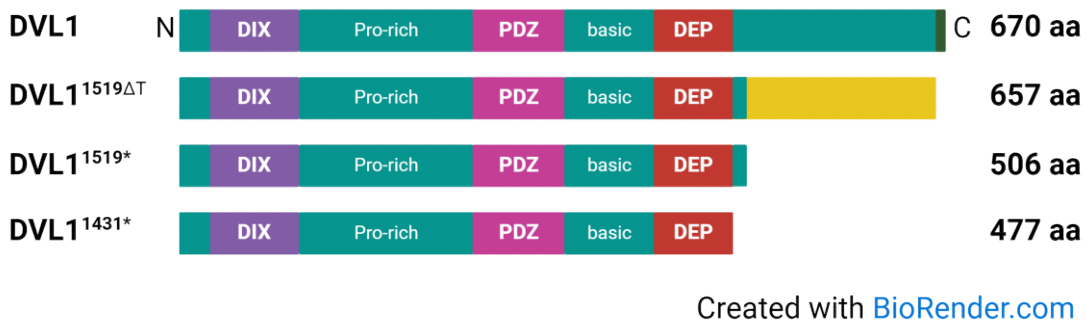

Figure 1.13. Schematic of all DVL1 proteins used in this study, showing the difference between the C-terminal truncated proteins, DVL1 variant and the wild type protein

1.10.1. DVL1^{1519*}

This construct contains the sequence that is common among all the variants and also the wildtype DVL1. For this construct, a stop codon is inserted right after the position of the earliest deletion (c. 1519ΔT) among the RS DVL1 variants that causes the -1 frameshift. *DVL1*^{1519*} contains all three domains and also the first 29 amino acids of

the C-terminus. This construct is specifically designed to help us understand if the neomorphic phenotypes we have shown with the variants (Gignac et al., 2023) are caused by the lack of original C-terminus or the novel 109 amino acid long peptide sequence that replaces it.

1.10.2. DVL1^{1431*}

This second construct contains only the three domains of DVL1, and a stop codon is inserted right after the sequence coding the DEP domain. It lacks the whole C-terminus; hence it is 29 amino acids shorter than *DVL1*^{1519*}. With this product, we are able to compare a DVL1 protein without its C-terminus to the normal DVL1 to further investigate the role of the highly conserved C-terminus in DVL1's cellular function.

1.11. Objectives

There are two main aims to this project. Firstly, we would like to understand how the DVL1 variants affect the development and morphology of fly tissues. We hope that this will provide insights for us understand the underlying mechanisms that causes Robinow Syndrome and also the cellular function of DVL1. Second, by using the C-terminal truncated products, we want to investigate which alteration in the structure of DVL1 protein is causing the previously shown neomorphic phenotypes.

1.11.1. Investigating the morphological alterations caused by DVL1 variants

The fruit fly system was validated by former lab members (Thalia W. Barret, Katja R. MacCharles) for the study of RS DVL1 variants. The mode of dominance of the DVL1 variants was previously shown to be neomorphic, meaning that the mutant proteins have novel functions that the wildtype protein does not display. After establishing these, the studies have shown that the expression of RS DVL1 variants resulted in altered tissue morphology in larval, pupal and adult tissues (Gignac et al., 2023). Based on novel wing imaginal disc, wing, bristle and thorax phenotypes induced by the variants and comparisons to the literature, we hypothesized that the variants are altering overall development and growth of fly tissues. Hence, we aimed to further investigate how the tissue structure is changed upon expressing the RS DVL1 variants.

1.11.2. Investigating the signalling network affected by DVL1 variants

Based on the morphological alterations and the neomorphic phenotypes induced by the variants, we hypothesized that multiple signalling pathways beyond Wnt signalling are being altered in the presence of RS *DVL1* variants. We addressed this hypothesis by conducting RNA sequencing and transcriptional readouts of other signalling pathways that are involved in development and growth.

1.11.3. Identifying the mode of dominance of the truncated DVL1 proteins

The C-terminal truncated *DVL1* constructs designed for investigating the role of C-terminus in DVL1 are synthetic, hence needs to be validated on the organism level. We hypothesize that the activity of these constructs will be more similar to the wild-type DVL1 rather than the variants, since they contain 3 of the functional domains of the wildtype protein while lacking the C-terminus hence the PDZ-binding motif (PBM). Because the fly C-terminus and the PBM are quite different than the vertebrate protein, the interactions between the human DVL1 C-terminus and the fly proteins are expected to be not effective in a disruptive way.

1.11.4. Investigating how the truncated DVL1 proteins function relative to wtDVL1 in Wnt signalling

The C-terminus of DVL1 is highly conserved among vertebrates and it contains functional sites and binding motifs. The lack of C-terminus in DVL1 was shown the reduce canonical Wnt signalling in the literature in a different animal model (Bunn et al., 2015). We also want to investigate the effect of the C-terminus and to distinguish whether the reduced canonical and induced noncanonical Wnt signalling pathway activity phenotypes are caused by the loss of the C-terminus or the addition of the novel peptide or a combination of the two. We will be able to shed light to our questions by using the C-terminal truncated DVL1 constructs *DVL1*^{1519*} and *DVL1*^{1431*}.

Chapter 2. Results: DVL1 variant alters *Drosophila* tissue morphology

The initial goal of this project was to introduce wild-type DVL1 into the fly via transgenesis and compare its effects to those of the variant forms and wild-type controls. By conducting these studies in a wild-type background with endogenous Dishevelled (Dsh) present, we were able to model the interaction between wild-type and mutant proteins, a crucial aspect of the human autosomal dominant RS genetics. The studies conducted by Katja MacCharles have shown that the variants displayed dominant interference by disrupting the normal function of endogenous fly Dsh and introducing novel functions in Wnt signalling and neomorphic phenotypes during fly development which are not seen by the expression of wt*DVL1* (Gignac et al., 2023). To continue, we aim to further investigate the alterations in the role of DVL1 in cell signalling and the mechanisms involved in the altered morphology of fly tissues by using the same system.

Part of the data presented here was collected by the generous and much appreciated help of Dr. Kenneth Kin Lam Wong during the experimental process. Some of the initial experiments were also carried out by Katja MacCharles (Katja MacCharles author, 2022) and repeated by me in the thesis project. Unless stated otherwise, all the images shown in this thesis are produced by me.

2.1. Re-validation of transgenic RS-DVL1 fly lines

As previously mentioned, we utilized the Gal4-UAS binary expression system to induce transgene expression in our fruit fly model. To generate the UAS-transgenic lines, all DVL1 transgenes were inserted into the same attp40 chromosomal site on Chromosome II. Transgene generation was caried out by the Richman Lab at UBC, and injections were performed by BestGene Inc., as detailed in the Materials and Methods chapter of this thesis.

In summary, three autosomal dominant RS *DVL1* patient mutations were selected, and site-directed mutagenesis was used to introduce these specific mutations (c.1519delT, c.1529delG, c.1615delA) into wild-type *DVL1* (wt*DVL1*) cDNA. This resulted in the creation of four transgenes: wt*DVL1* and three variants, respectively *DVL1*$^{1519\Delta T}$, *DVL1*$^{1529\Delta G}$, and *DVL1*$^{1615\Delta A}$. These specific mutations were chosen due to

their association with severe clinical phenotypes. N-terminal FLAG tags were also added to the constructs. Following the successful incorporation of the patient mutations and tags into the wild-type cDNA, the alleles were cloned into destination vectors suitable for transfection into *Drosophila* embryos or chicken embryos, where complementary experiments were conducted. All chicken-related experiments were performed by our collaborators in the Richman Lab and will not be discussed in this thesis.

Transgene expression was initially driven using the *decapentaplegic-Gal4* (*dpp-Gal4*) driver, which is expressed along the border between anterior and posterior compartments, reaching from the tip of the notum to the bottom of the wing pouch of the larval imaginal discs. qRT-PCR analyses confirmed that all transgenes were expressed at comparable mRNA levels (Fig. 2.1A).

Next, we aimed to determine whether the full-length human proteins were expressed in the fly using western blotting. Antibody staining against the FLAG tag present in the DVL1 transgenes was used to visualize DVL1 proteins on the membrane. The western blots showed that both the wild-type and variant DVL1 proteins were expressed at the expected size of 85 kD. However, analysis of the signal intensity on the western blots showed that the expression of the protein at DVL1$^{1615\Delta A}$ both 25 and 29°C was consistently lower than that of the other transgenes, suggesting decreased stability, as mRNA levels were comparable (Fig. 2.1B).

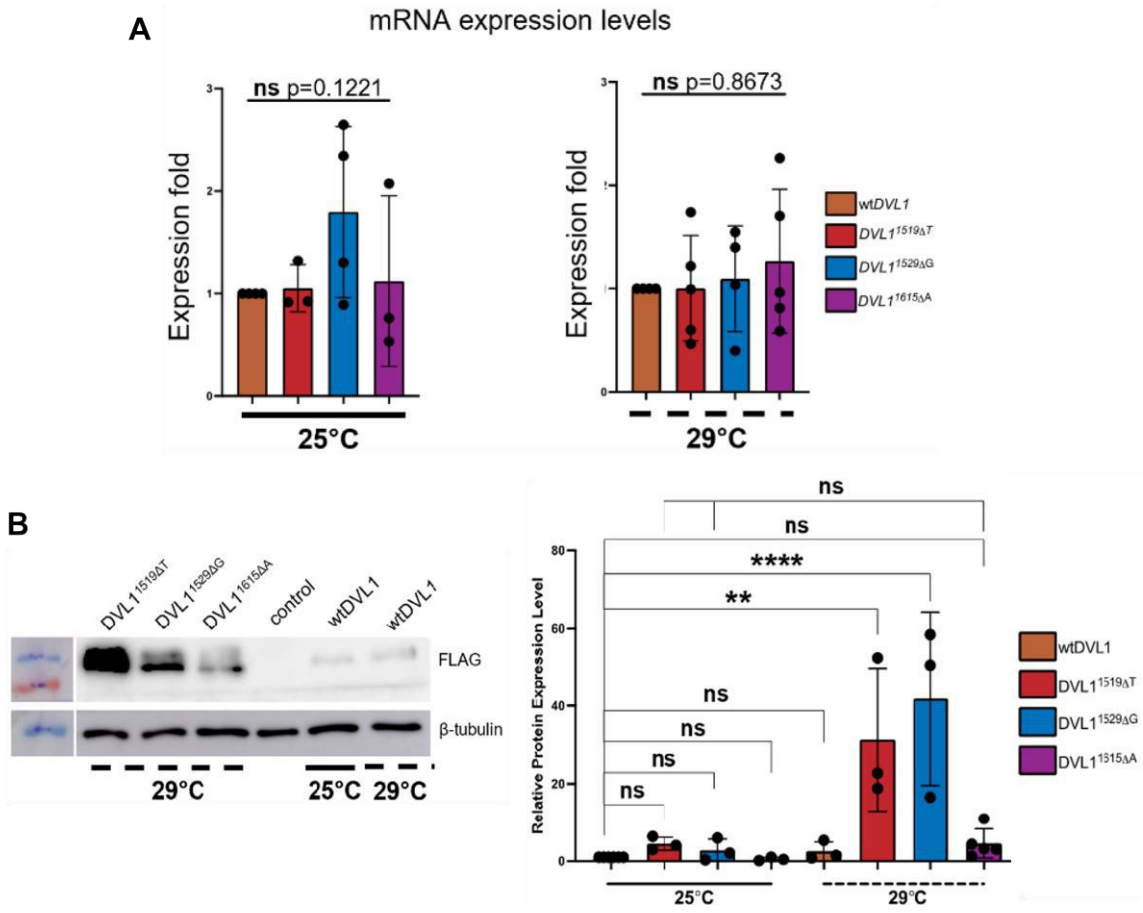

Figure 2.1. mRNA and protein expression levels of human DVL1 transgenes in salivary glands

(**A**) mRNA expression of *DVL1* variants expressed with *dpp-Gal4* relative to control discs that expresses wt*DVL1*. The results for the crosses performed at 25°C are shown on the left and 29°C on the right. All experiments were performed in triplicates. n=3-5 independent experiments, indicated on the graph by circles with samples comprising 5 salivary glands per genotype. Error bars show mean with SD. Statistics were performed with a one-way ANOVA test. (**B**) Western blot analysis of DVL1 protein levels from salivary gland extracts. *Dpp>DVL1* crosses were performed at 25°C or 29°C as indicated. Salivary glands were dissected from 2-10 larva per genotype and the equivalent of 2 salivary glands was loaded onto the gel. β-tubulin was used as a loading control. On the right, plot of DVL1 protein levels in variant DVL1-expressing tissue relative to control (*dpp*>wt*DVL1*) tissue. Crosses were performed at 25°C or 29°C as indicated. n=3-5 independent experiments as indicated. Error bars show mean with SD. Statistics were performed with a one-way ANOVA test. This figure corresponds to Fig. S8 in Gignac et al., 2023.

These results also suggested *DVL1*$^{1519\Delta T}$ as a suitable candidate for studying the phenotypic alterations caused by RS-associated DVL1 variants since the gene products are stable at both temperatures.

For the following experimental results presented in this chapter, we used *DVL1*$^{1519\Delta T}$ as the only variant. Considering these expression levels and the earlier study

from our lab that showed all three RS-DVL1 variants to be inducing the same phenotypes in different frequencies, we chose to continue our investigation with the strongest variant.

2.2. DVL1 variant induce abnormal morphology in adult fly tissues

Earlier work has shown that when DVL1 variant expression was driven by *dpp-Gal4*, the adult wings displayed additional neomorphic phenotypes such as longitudinal vein thickening, abnormalities in tanterior cross vein, ectopic bristles on the wing margin of L3 longitudinal vein and a crease between L3-L4 veins. These phenotypes were exclusive to the variants only (Gignac et al., 2023). Since the *dpp-Gal4* expression domain corresponding to the adult tissue is quite narrow, we wanted to drive the variant expression by using drivers with larger expression domains, such as *apterous (ap)-Gal4* and *hedgehog* (*hh)-Gal4* (Fig. 2.2).

He

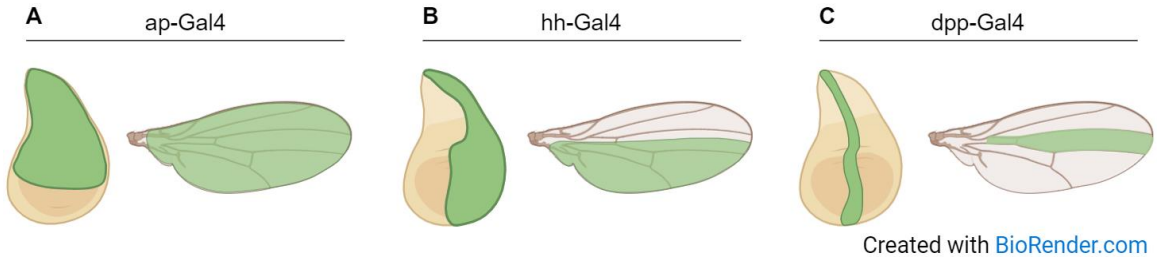

Figure 2.2. Cartoon depiction of the Gal4 drivers used in the following experimental results
The green coloured parts show the regions where *ap-Gal4* (**A**), *hh-Gal4* (**B**) and *dpp-Gal4* (**C**) is expressed in wing imaginal discs and what part it corresponds to in adult wings *ap-Gal4* is expressed in the dorsal compartment, *hh-Gal4* in the posterior domain and *dpp-Gal4* along the anterior-posterior boundary.

Expectedly, we observed more dramatic phenotypes when expressing the variant in larger parts of several tissues with both drivers. PCP disruptions in the form of misaligned hairs and bristles were observed in *wtDVL1* expressing tissues however the neomorphic phenotypes were not induced. We performed our crosses both at 25°C and 29°C. When expressed with the *ap-Gal4* driver, the $DVL1^{1519\Delta T}$ variant restricted the

growth of the wings and wing expansion did not occur properly after eclosion, hence the wings appeared shrivelled and blistered (Fig. 2.3C). Together with this wing phenotype, the thorax of the flies was also abnormally developed. The flies had missing or malformed scutellum and some of the thorax bristles were missing. No leg malformations were observed, the flies were able to eclose and survive after eclosion (Fig. 2.3).

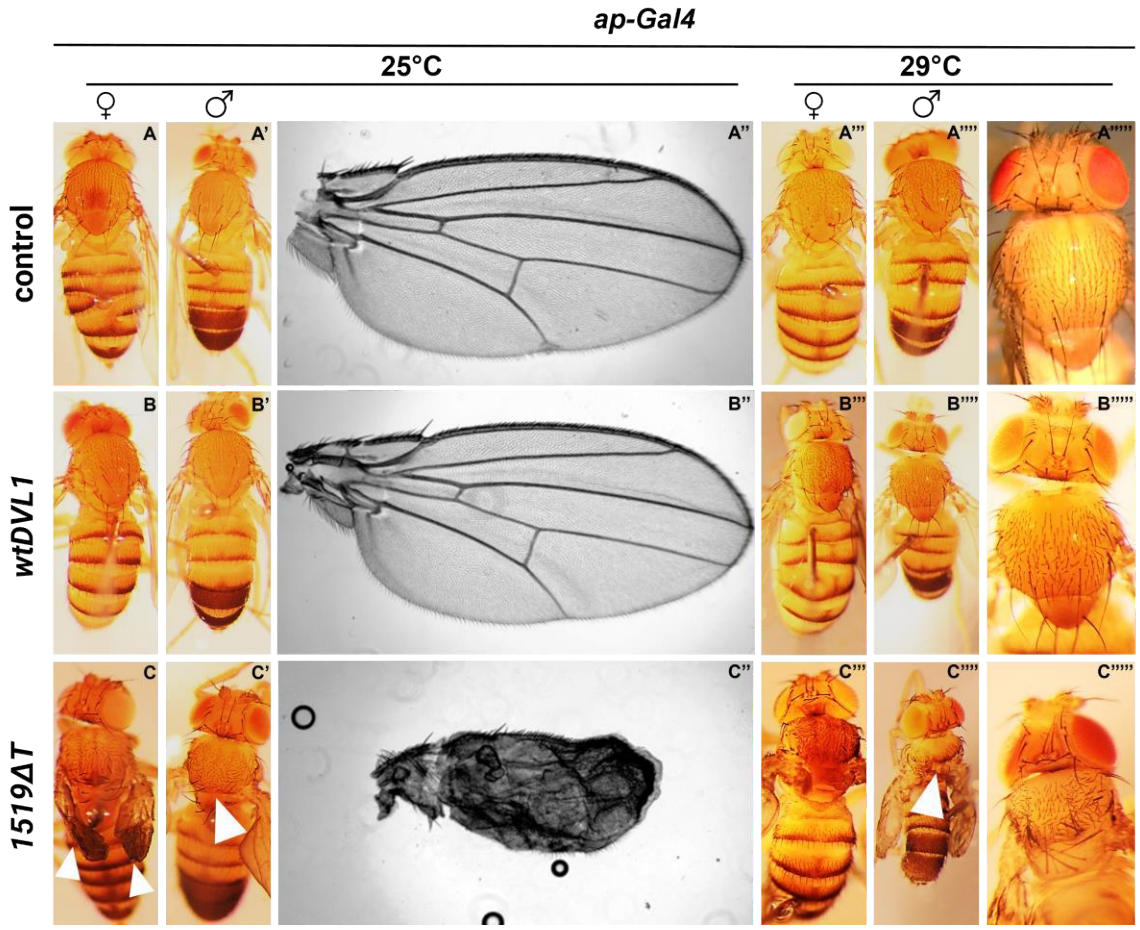

Figure 2.3. Expression of DVL1 variant with the *ap-Gal4* driver disrupts adult structures

(**A-A''**) 25°C control adult phenotypes. (**A'''-A'''''**) 29°C control adult phenotypes. (**B-B'''''**) The representative images from female and male adult phenotypes from *ap*>wt*DVL1* crosses performed at 25 and 29°C. (**B-B'''''**) The representative images from female and male adult phenotypes from *ap>DVL1*$^{1519\Delta T}$ crosses performed at 25 and 29°C. (**A''-C''**) The adult wing phenotypes from 25°C, representative pictures for all genotypes. (**A'''''-C'''''**) Zoomed in images of the thorax phenotypes from crosses grown at 29°C. Arrowheads in **C**-**C'''''** points to reduced thoraxes with missing bristles and reduced scutellums. n=25 minimum for both sexes at both temperatures.

When expressed with the *hh-Gal4* driver at 25°C, the *DVL1*$^{1519\Delta T}$ variant led to development of smaller, blistered wings that had abnormally enlarged veins (Figs. 2.4C, 2.5C). In addition to these wing phenotypes, the flies had difficulties eclosing from the pupal case. They could not walk after eclosing which led them to die after falling on the food. This eclosion problem was due to their abnormal leg morphology. All 3 pairs of legs (L1-3) were observed to be malformed (Figs. 2.4C, 2.5C). The most distal part of the *Drosophila* leg, tarsus contains 5 tarsal segments. In flies that expresses the *DVL1*$^{1519\Delta T}$ variant in the *hh-Gal4* domain, the tarsi of all legs formed a curved structure that appears like a hook. Especially In the L1 legs, the tarsi were compressed, and the tarsal segments were indistinguishable. For ease of visualization, the pictures of female (Fig. 2.4) and male (Fig. 2.5) fly parts are presented in separate figures below.

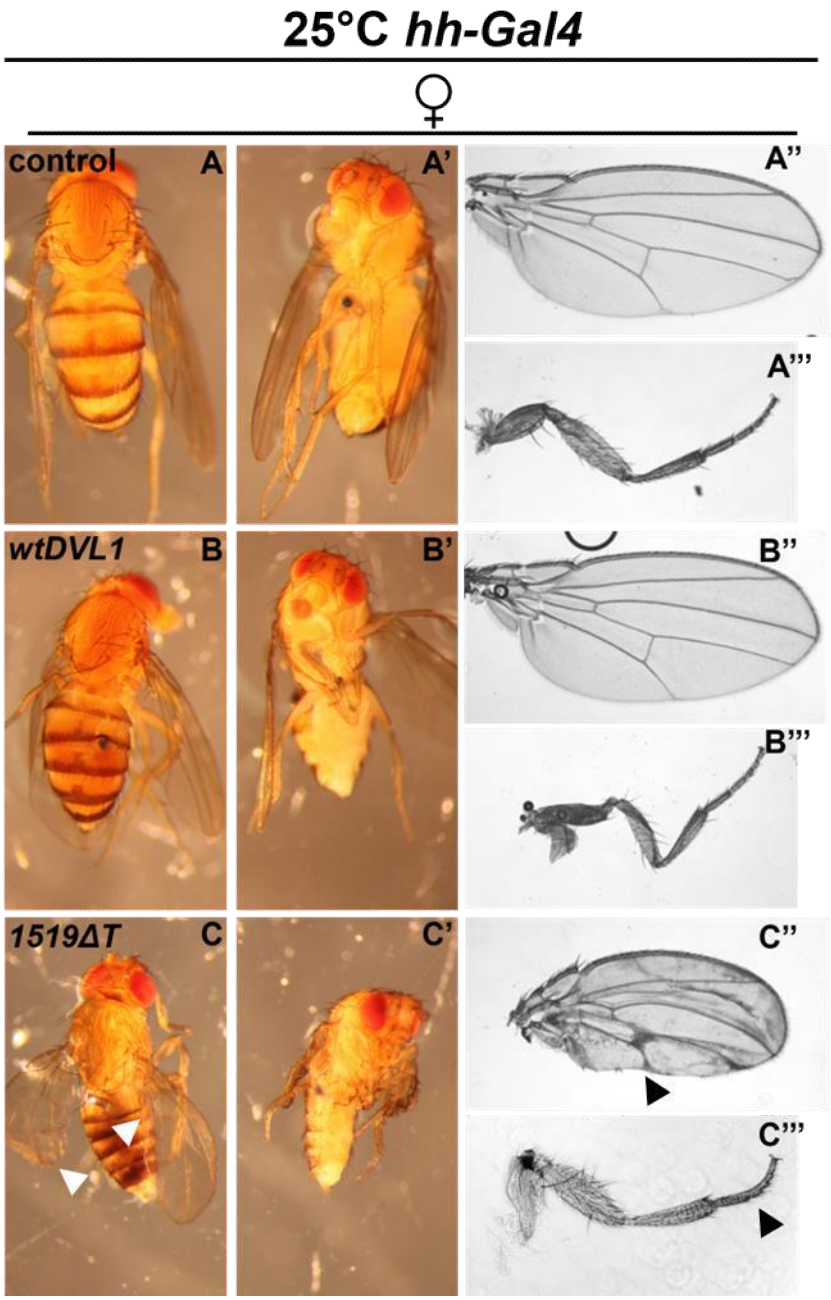

Figure 2.4. Expression of DVL1 variant with the *hh-Gal4* driver at 25°C disrupts adult structures in females

(**A-A'''**) 25°C control adult phenotypes. (**B-C'''**) The representative images from female adult phenotypes from transgene expressing crosses performed at 25°C. (**A''-C''**) The adult wing phenotypes, representative pictures for all genotypes. (**A'''-C'''**) The adult L1 leg phenotypes, representative pictures for all genotypes. Arrowheads in **C**-**C'''** points to malformed wings and the leg tarsa in *hh>DVL1*$^{1519\Delta T}$ flies. Part of the leg pictures were taken by Dr. Kenneth Kin Lam Wong. n=25.

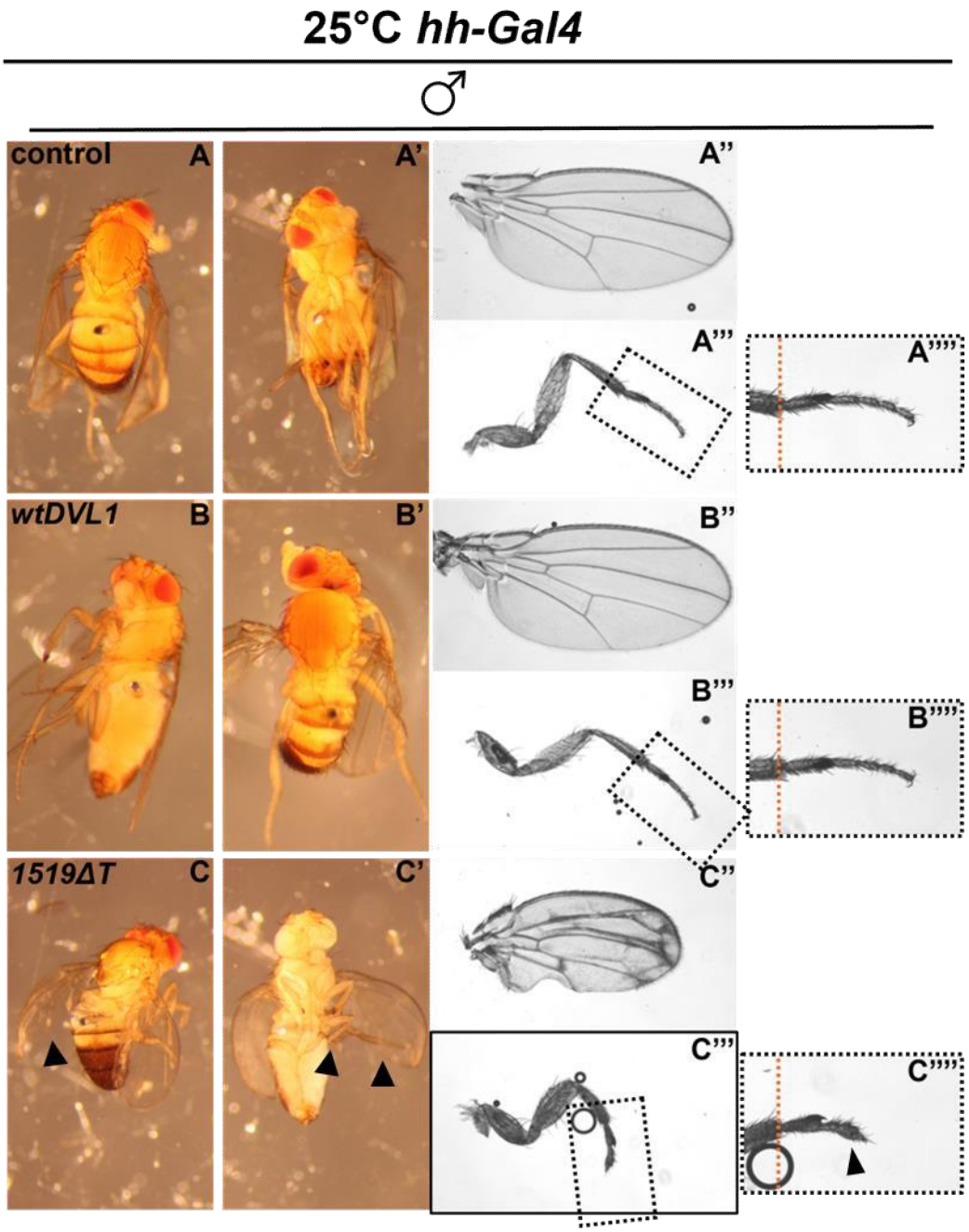

Figure 2.5. Expression of DVL1 variant with the *hh-Gal4* driver at 25°C disrupts adult structures in males

(A-A''') 25°C control adult phenotypes. (B-C''') The representative images from male adult phenotypes from transgene expressing crosses performed at 25°C. (A''-C'') The adult wing phenotypes, representative pictures for all genotypes. (A'''-C''') The adult leg phenotypes, representative pictures for all genotypes. (A''''-C'''') Zoomed in pictures of the tarsal segments of L1 legs. Arrowheads in C-C'''' points to malformed wings and the leg tarsa in hh>DVL1$^{1519\Delta T}$ flies. Part of the leg pictures were taken by Dr. Kenneth Kin Lam Wong. n=25.

When we expressed the *DVL1*$^{1519\Delta T}$ variant in the *hh-Gal4* domain at higher levels by growing the flies at 29°C, we observed more severe phenotypes compared to the flies grown at 25°C (Fig. 2.6C). Variant expressing flies failed to eclose from their pupal case and died inside of it. Since the expansion of wings and legs are completed after expansion, we were not able to image the tissues separately. None of the wt*DVL1* expressing flies had difficulties eclosing at 29°C (Fig. 2.6B). The variant expressing flies imaged were dissected out of their pupal cases (Fig. 2.6C).

Figure 2.6. Expression of DVL1 variant with the *hh-Gal4* driver at 29°C disrupts adult structures

(**A-A'''**) 29°C control adult phenotypes. (**B-B'''**) The representative images from female and male adult phenotypes from *hh*>wt*DVL1* crosses performed at 29°C. (**C-C'''**) The representative images from female and male adult phenotypes from *hh>DVL1*$^{1519\Delta T}$ crosses performed at 29°C. Arrowheads in **C**-**C'''** points to malformed wings and the legs in *hh>DVL1*$^{1519\Delta T}$ flies. n=15 for both sexes.

2.3. DVL1 variant disrupt morphology in larval wing imaginal discs

The phenotypes observed in adult flies with the expression of the *DVL1*$^{1519\Delta T}$ variant led us to investigate the morphology of wing precursor tissues in larvae. Since *dpp-Gal4* has a narrow expression domain along the anterior-posterior border, we investigated the wing imaginal discs that expresses the variant in larger domains with *ap-Gal4* and *hh-Gal4* drivers. We used *UAS-GFP* in these crosses to mark the domains in which transgenes were expressed.

When the *DVL1*$^{1519\Delta T}$ variant was expressed with the *ap-Gal4* at 25°C, we observed that the expression domain in the wing disc (marked by GFP) was distorted, and the dorso-ventral border was expanded towards the ventral compartment. We also observed that the highly regulated folding structure of the wing imaginal disc was altered, and more layers were formed above the wing pouch especially on the posterior side of the wing imaginal discs (Fig. 2.7C). The abnormal folding was also present on the dorsal domain, in the notum. When we looked at the orthogonal view, the discs were compressed even with the bridged slides hence this abnormal morphology appeared to be an overgrowth in the wing disc epithelium. However, the morphology of the wing imaginal discs that expressed *wtDVL1* was comparable to the control discs (Fig. 2.7B).

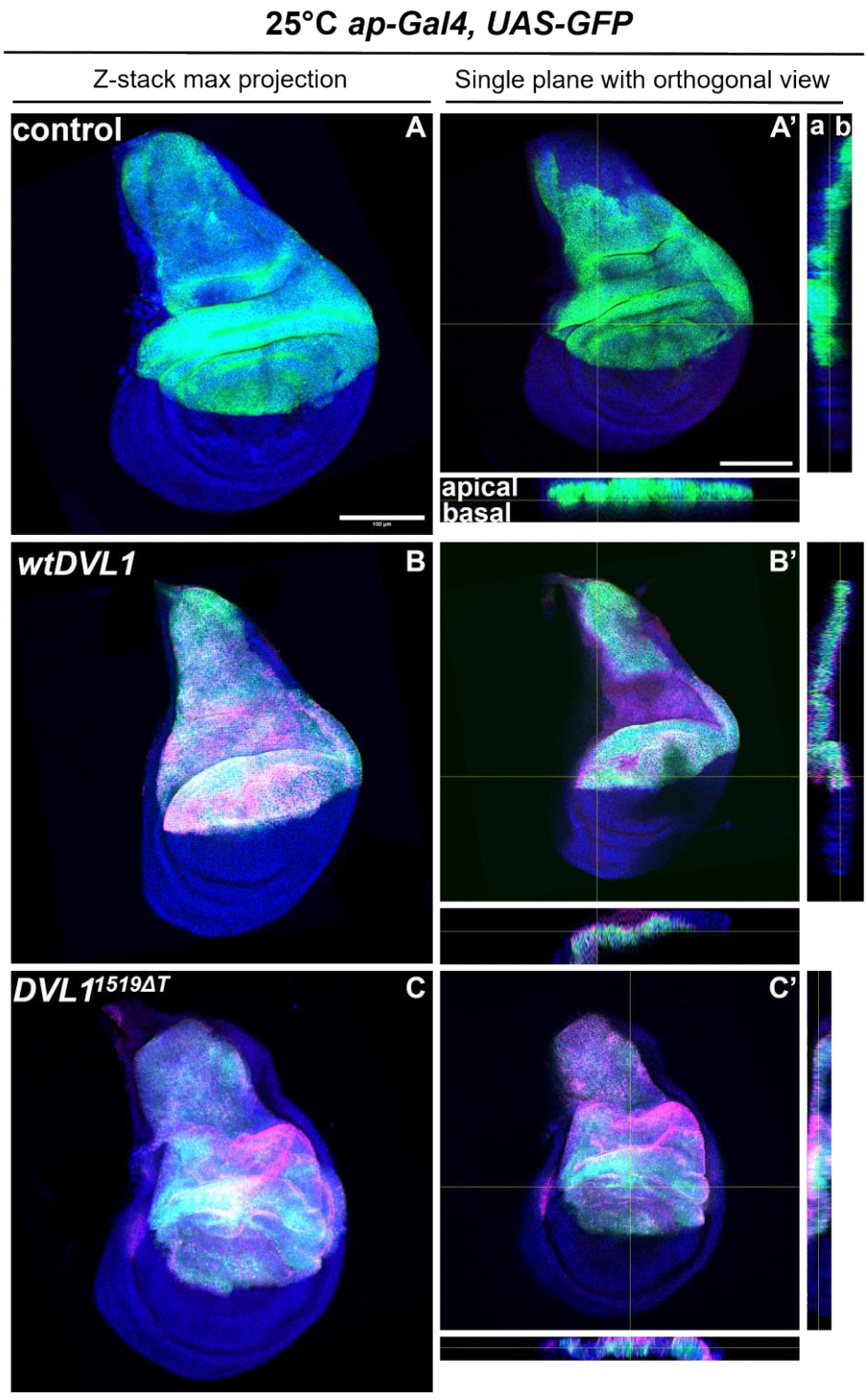

Figure 2.7. Expression of DVL1 variant with the *ap-Gal4* driver at 25°C disrupts wing imaginal disc morphology

Microscopy images showing DNA (blue), *ap>GFP* expression (green) and FLAG (magenta) staining in control (**A, A'**) and DVL1-expressing (**B-C'**) wing discs mounted on bridged slides. (**A-C**) Show maximum projections. (**A'-C'**) Show single plane images with orthogonal views of the tissue. Crosses were performed at 25°C and only female wing discs were used. Scale bar = 100 µm. n=10 minimum.

We also wanted to see the effects of the variant when it's expressed in higher levels at 29°C since the adults grown at this temperature had more severe thorax and wing phenotypes. The wing imaginal discs that express the *DVL1*$^{1519\Delta T}$ variant at higher levels showed more severe alteration in the folding motif both in the apical-basal and anterior-posterior directions (can be seen in the C' orthogonal view in Fig. 2.8C). The discs and the folds appeared thicker in the orthogonal view as well. None of these morphological alterations were displayed when the *wtDVL1* was expressed in higher levels at 29°C (Fig. 2.8B).

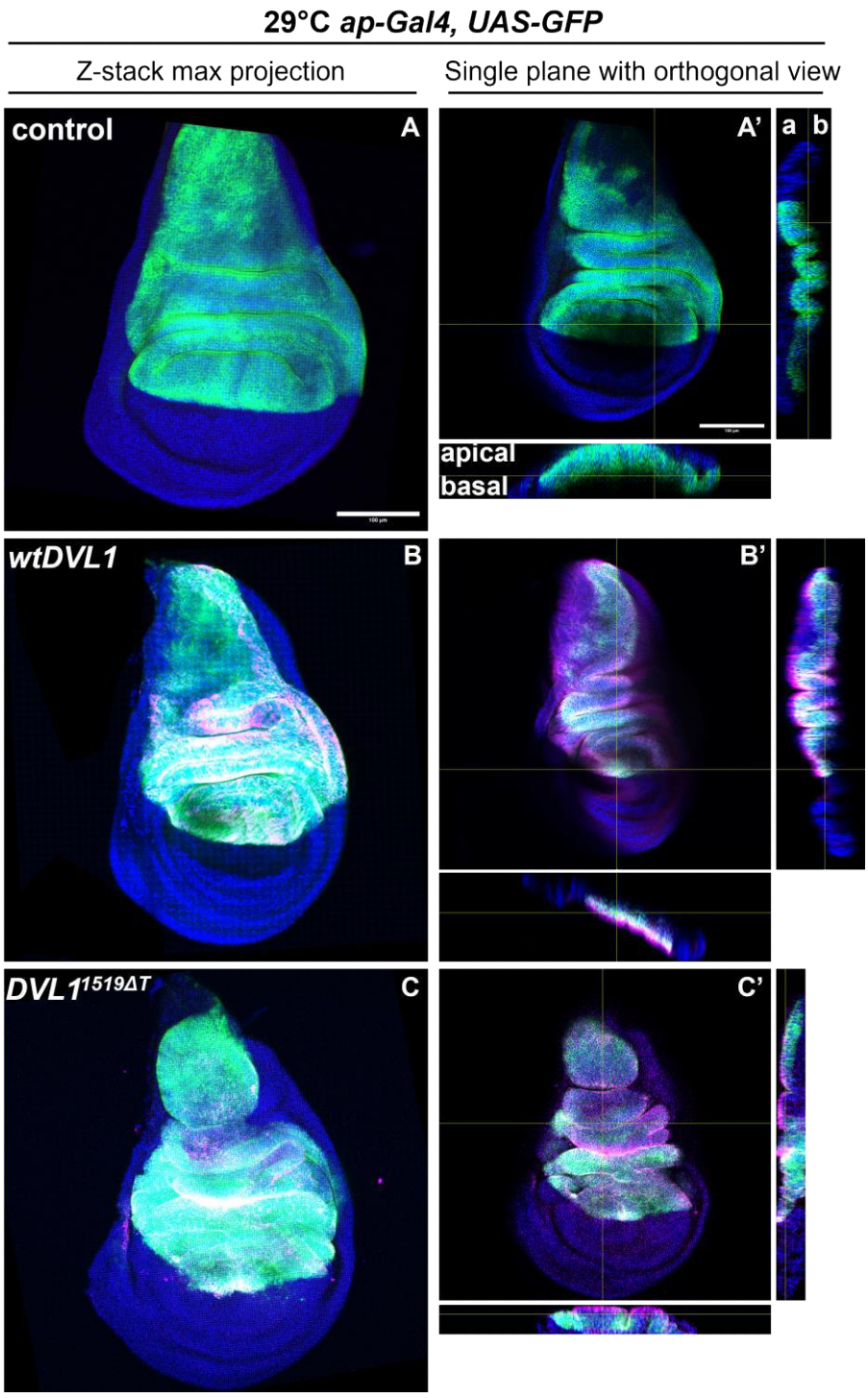

Figure 2.8. Expression of DVL1 variant with the *ap-Gal4* driver at 29°C disrupts wing imaginal disc morphology

Microscopy images showing DNA (blue), *ap>GFP* expression (green) and FLAG (magenta) staining in control (**A, A'**) and DVL1-expressing (**B-C'**) wing discs mounted on bridged slides. (**A-C**) Show maximum projections. (**A'-C'**) Show single plane images with orthogonal views of the tissue. Crosses were performed at 29°C and only female wing discs were used. Scale bar = 100 µm. n= 10.

We found that the expression of the *DVL1*$^{1519\Delta T}$ with the *hh-Gal4* driver caused severe wing phenotypes in adults at 25°C. We wanted to investigate how the expression of the DVL1 variant in the same domain affected the development of wing imaginal discs. The tissue in the notum and hinge above the wing pouch appeared highly misfolded on the basal surface of the wing imaginal discs (Fig. 2.9C). On the orthogonal view, the wing disc morphology appeared aberrant but less abnormal compared to the discs that expresses the variant in the *ap-Gal4* domain. The misfolded tissue above the wing pouch seemed to be pushing the pouch towards the anterior side of the wing imaginal disc, disrupting the normal shape of the wing disc. The discs did not appear thicker in the orthogonal view, however the overall tissue seemed to be overgrown. These morphological alterations were not induced by the expression of *wtDVL1*, which appeared very similar to the control discs (Fig. 2.9B).

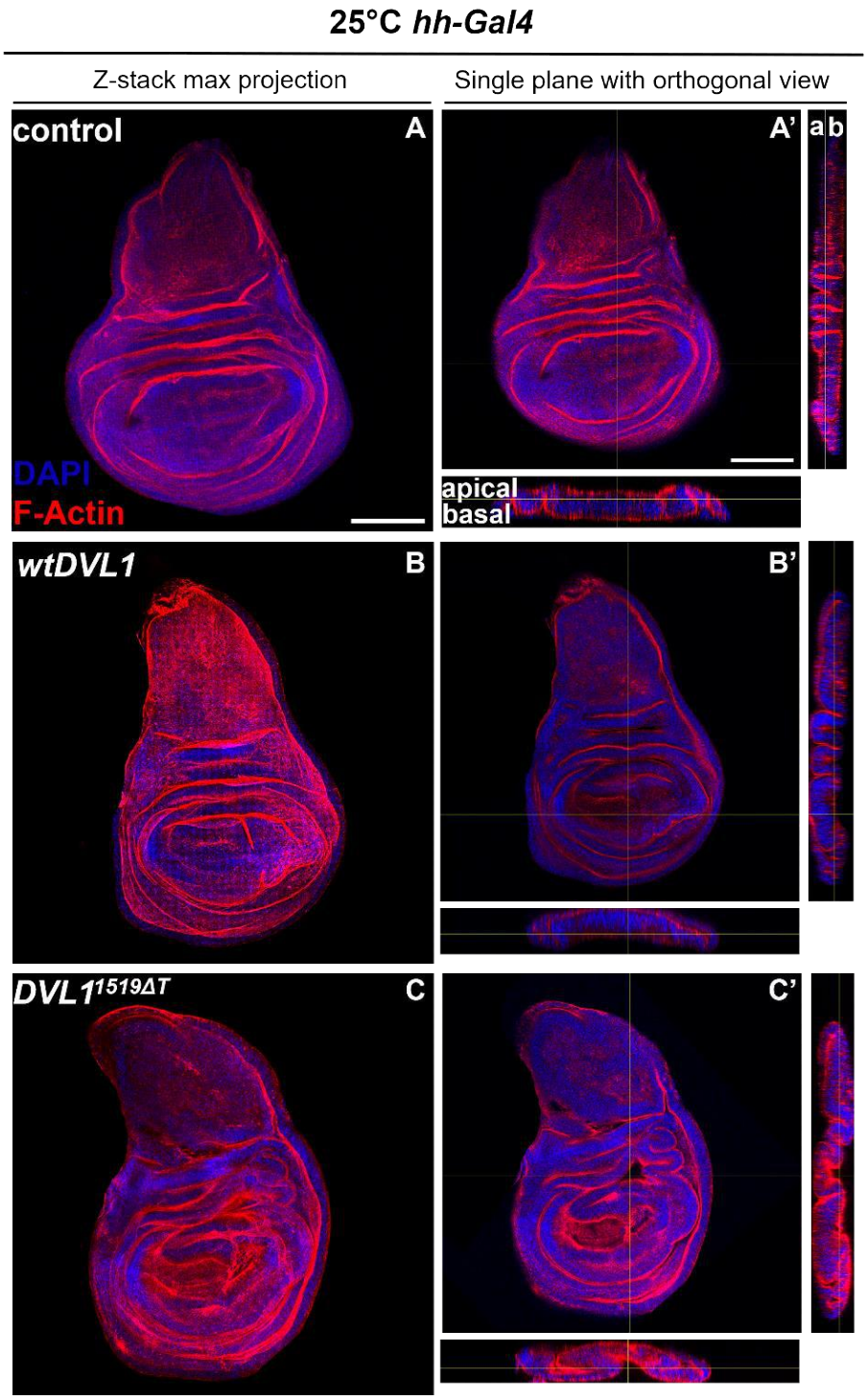

Figure 2.9. Expression of DVL1 variant with the *hh-Gal4* driver at 25°C disrupts wing imaginal disc morphology

Microscopy images showing DNA (blue), F-actin (red) in control (**A, A'**) and DVL1-expressing (**B-C'**) wing discs mounted on bridged slides. (**A-C**) Show maximum projections. (**A'-C'**) Show single plane images with orthogonal views of the tissue. Crosses were performed at 25°C and only female wing discs were used. Scale bar = 100 µm. n= 10 minimum.

When the *DVL1*$^{1519\Delta T}$ variant expression was driven by the *hh-Gal4* driver in higher levels at 29°, the hh domain itself appeared enlarged (Fig. 2.10C). The activity of *DVL1*$^{1519\Delta T}$ in the posterior side of the wing imaginal discs induced extra folds in every direction, making the wing disc appear highly distorted. All parts of the wing disc, notum, hinge and wing pouch showed abnormal morphology, affecting the overall look of the wing discs. The orthogonal view from above the wing imaginal discs showed disruption of the arc-like form of the wing discs. With all the extra folds, the wing discs appeared highly overgrown. These morphological alterations did not occur with the expression of wt*DVL1* (Fig. 2.10B).

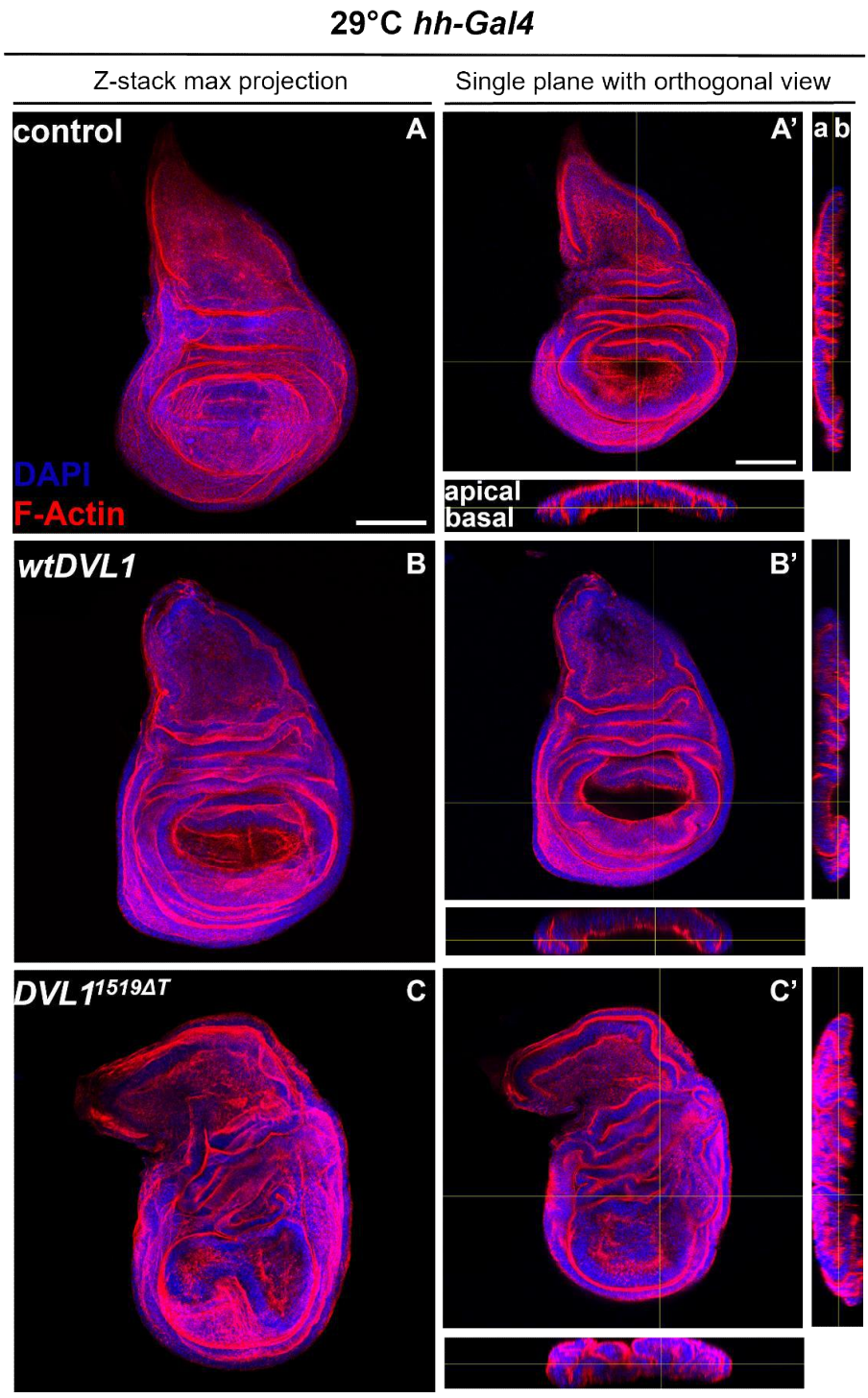

Figure 2.10. Expression of DVL1 variant with the *hh-Gal4* driver at 29°C disrupts wing imaginal disc morphology

Microscopy images showing DNA (blue), F-actin (red) in control (**A, A'**) and DVL1-expressing (**B-C'**) wing discs mounted on bridged slides. (**A-C**) Show maximum projections. (**A'-C'**) Show single plane images with orthogonal views of the tissue. Crosses were performed at 29°C and only female wing discs were used. Scale bar = 100 µm. n=10.

2.4. DVL1 variant does not induce cell proliferation in wing imaginal discs

After observing the highly altered morphology in wing imaginal discs that express the *DVL1*$^{1519\Delta T}$ variant in apterous and hedgehog domains, we wanted to investigate whether cell proliferation was being induced to cause the extra fold formation. To assess the relative amount of cell proliferation occurring between the wild type *DVL1* and variant expressing wing imaginal discs, we used an antibody against a commonly used specific mitotic marker, Phospho-Histone 3 (PH3).

Again, we induced the expression of wt*DVL1* and *DVL1*$^{1519\Delta T}$ by using the *ap-Gal4* driver at 25°C. We counted the number of PH3 puncta in the apterous domain of the control, wt*DVL1* and *DVL1*$^{1519\Delta T}$ expressing wing imaginal discs (Fig. 2.11). We found the PH3 levels in control wing discs to be variable, but the average was similar to the PH3 levels measured in the wt*DVL1* and *DVL1*$^{1519\Delta T}$ expressing wing imaginal discs. No significant differences were found between the genotypes.

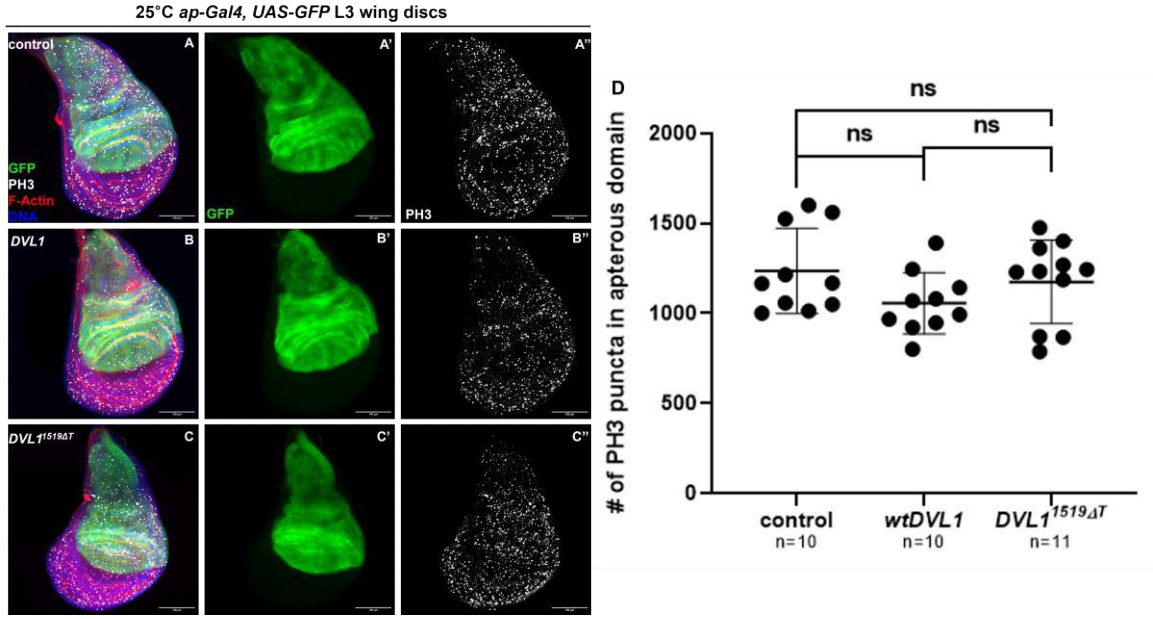

Figure 2.11. Expression of DVL1 variant with the *ap-Gal4* driver at 25°C does not alter cell proliferation levels in wing imaginal discs

Confocal microscopy images showing *ap>GFP* (green), F-actin (red), DNA (DAPI, blue) and PH3 (white) stainings merged together in one image in control (**A**) and transgene expressing discs grown at 25°C (**B-C**). (**A'-C'**) The *apterous* domain of the representative wing disc images are shown with the GFP images. (**A''-C''**) PH3 staining for all genotypes are shown. (**D**) The number of PH3 puncta counted within the apterous domain are plotted. Sample size is shown under each genotype. Statistics were performed with ANOVA. Scale bar = 100 µm.

We continued by counting the number of PH3 puncta in wing imaginal discs that expresses the variant in the apterous domain in higher levels at 29°C and comparing the results to the PH3 levels measured in control and wt*DVL1* expressing discs (Fig. 2.12). We found higher numbers of PH3 puncta compared to the discs grown at 25°C, yet again there were no significant difference between the genotypes.

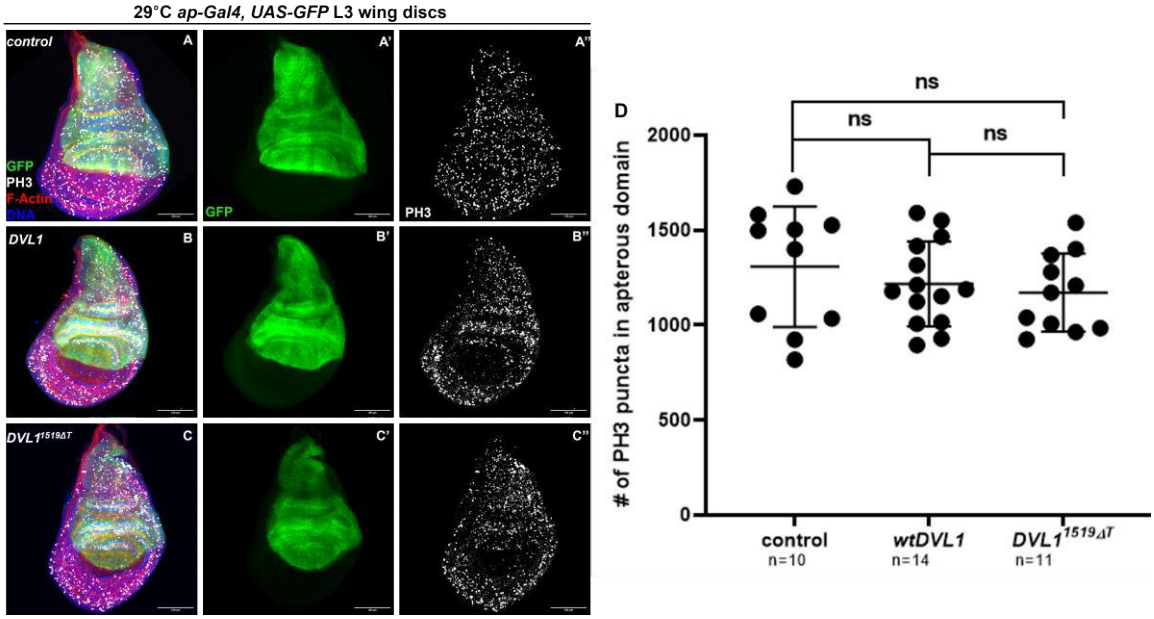

Figure 2.12. Expression of DVL1 variant with the *ap-Gal4* driver at 29°C does not alter cell proliferation levels in wing imaginal discs

Confocal microscopy images showing *ap>GFP* (green), F-actin (red), DNA (DAPI, blue) and PH3 (white) stainings merged together in one image in control (**A**) and transgene expressing discs grown at 29°C (**B-C**). (**A'-C'**) The *apterous* domain of the representative wing disc images are shown with the GFP images. (**A''-C''**) PH3 staining for all genotypes are shown. (**D**) The number of PH3 puncta counted within the apterous domain are plotted. Sample size is shown under each genotype. Statistics were performed with ANOVA. Scale bar = 100 μm.

We proceeded to investigate the levels of cell proliferation in wing imaginal discs that expresses either wt*DVL1* or *DVL1*$^{1519\Delta T}$ variant in the *hedgehog* domain in comparison to the control discs at 25°C (Fig. 2.13). The number of PH3 puncta in all three genotypes were very similar and the variance was very small. Statistical analyses showed no significant difference between the discs that express the *DVL1*$^{1519\Delta T}$ and

wt*DVL1.* The expression of the transgenes did not cause any difference in the number of PH3 puncta compared to the control either.

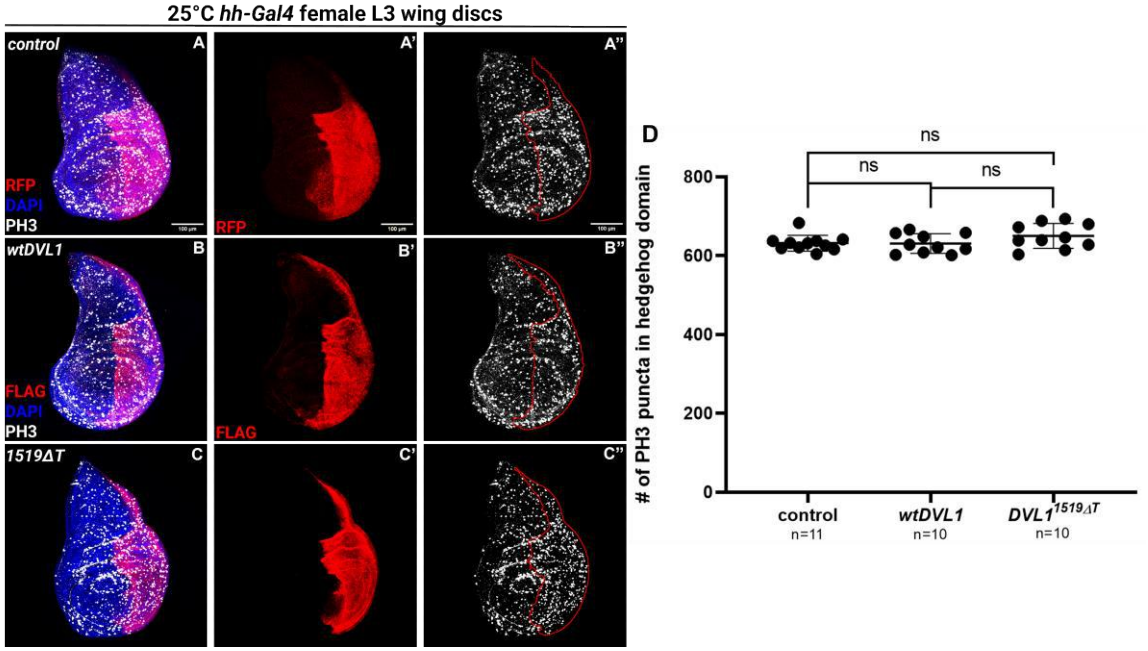

Figure 2.13. Expression of DVL1 variant with the *hh-Gal4* driver at 25°C does not alter cell proliferation levels in wing imaginal discs

Confocal microscopy images showing UAS transgene expression domain (red), DNA (DAPI, blue) and PH3 (white) stainings merged together in one image in control (**A**) and transgene expressing discs grown at 25°C (**B-C**). (**A'-C'**) The *hedgehog* domain of the representative wing disc images are shown with the RFP or FLAG staining images. (**A''-C''**) PH3 staining for all genotypes are shown. (**D**) The number of PH3 puncta counted within the hedgehog domain are plotted. Sample size is shown under each genotype. Statistics were performed with ANOVA. Scale bar = 100 μm.

We also counted the PH3 puncta in wing discs that expresses the transgenes in higher levels in the hedgehog domain at 29°C (Fig. 2.14). We observed increased PH3 puncta numbers in all genotypes compared to the wing discs grown at 25°C. Again, no significant difference was observed between the different genotypes.

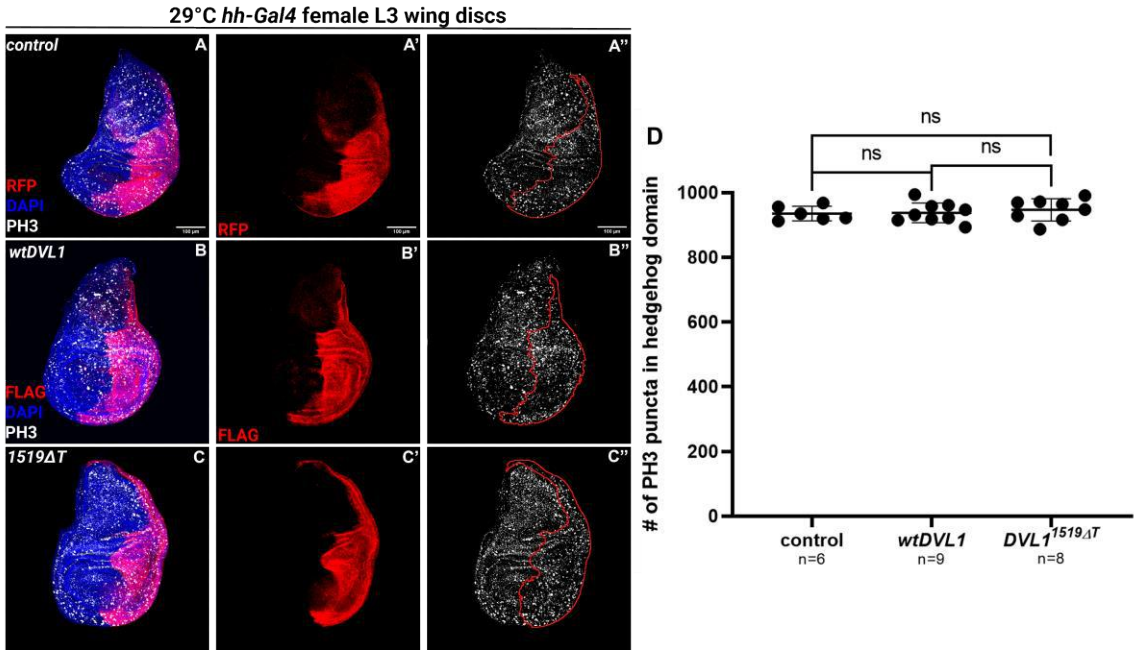

Figure 2.14. Expression of DVL1 variant with the *hh-Gal4* driver at 29°C does not alter cell proliferation levels in wing imaginal discs

Confocal microscopy images showing UAS transgene expression domain (red), DNA (DAPI, blue) and PH3 (white) stainings merged together in one image in control (**A**) and transgene expressing discs grown at 29°C (**B-C**). (**A'-C'**) The *hedgehog* domain of the representative wing disc images are shown with the RFP or FLAG staining images. (**A''-C''**) PH3 staining for all genotypes are shown. (**D**) The number of PH3 puncta counted within the hedgehog domain are plotted. Sample size is shown under each genotype. Statistics were performed with ANOVA. Scale bar = 100 μm.

After these experimental results, we concluded that the abnormal morphology of the wing imaginal discs induced by the expression of *DVL1*$^{1519\Delta T}$ variant is not due to cell proliferation. One possibility we have considered for the cause of the abnormal morphology in wing imaginal discs was the tension induced from the part of the disc that is overgrown while the other part was normal. Since we do not observe over proliferation, we partly eliminated this possibility, however the tension could be occurring due to the inverse of this. The less grown DVL1 variant expressing tissue could be pulled by the normal tissue in the other part of the wing discs, as in the case of the discs expressing the variant in the *hedgehog* domain.

2.5. DVL1 variant induces cell death in wing imaginal discs

To further investigate the reasons underlying the altered morphology in the wing imaginal discs and the adult tissues induced by the expression *DVL1* variant, we investigated the relative amount of cell death occurring between wild type and variant forms of *DVL1*. Our earlier work has found that the *DVL1* variant expression causes an imbalance in Wnt signalling and increases the activity of noncanonical Wnt signalling, which mediates cytoskeletal organization and apoptosis. It also showed that when *DVL1* variants were expressed, JNK signalling was ectopically induced, which also regulates apoptosis (Gignac et al., 2023). Considering these alterations in signalling and the smaller thorax and adult wing phenotypes induced by the expression of *DVL1* variant in different domains, we stained the adult precursor tissue in the larval wing imaginal discs against the cleaved death caspase-1 (Dcp1) protein. Dcp1 is an effector caspase, activated after the cell goes into apoptosis by getting cleaved into two fragments (Song et al., 1997).

We first induced the expression of wt*DVL1* and $DVL1^{1519\Delta T}$ by using the *ap-Gal4* driver at 25°C (Fig. 2.15). We counted the number of Dcp1 puncta in the apterous domain of the control, wt*DVL1* and $DVL1^{1519\Delta T}$ expressing wing imaginal discs. We found no significant difference between the Dcp1 levels in control and wt*DVL1* expressing wing imaginal discs. The number of Dcp1 puncta in the discs that expresses wt*DVL1* was found to be more variable compared to the other genotypes, but the average was similar to the Dcp1 puncta counted in the control discs. We found that the number of Dcp1 puncta in wing imaginal discs that expresses $DVL1^{1519\Delta T}$ in the apterous domain is significantly higher than both control and wt*DVL1* expressing discs (Fig. 2.15C, D).

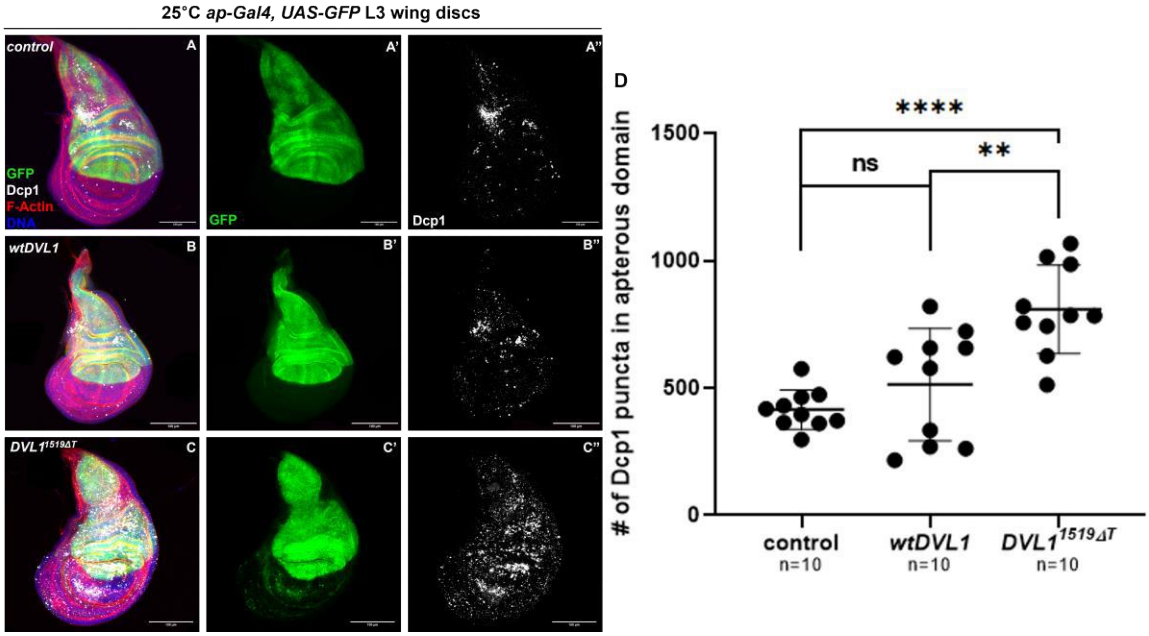

Figure 2.15. Expression of DVL1 variant with the *ap-Gal4* driver at 25°C does significantly increases apoptosis levels in wing imaginal discs

Confocal microscopy images showing *ap>GFP* (green), F-actin (red), DNA (DAPI, blue) and Dcp1 (white) stainings merged together in one image in control (**A**) and transgene expressing discs grown at 25°C (**B-C**). (**A'-C'**) The *apterous* domain of the representative wing disc images are shown with the GFP images. (**A''-C''**) Dcp1 staining for all genotypes are shown. (**D**) The number of Dcp1 puncta counted within the *apterous* domain are plotted. Sample size is shown under each genotype. Statistics were performed with ANOVA. Scale bar = 100 μm.

We then investigated the number of Dcp1 puncta in wing imaginal discs that expresses the variant in the *apterous* domain in higher levels at 29°C (Fig. 2.16). We found higher numbers of Dcp1 puncta in all genotypes compared to the numbers at 25°C, but the trend was similar to the discs grown at 25°C. We observed a significant increase in the number of Dcp1 puncta in variant expressing wing discs (Fig. 2.16C). It should be noted that the difference between the wt*DVL1* and variant expressing discs was more significant at 29°C (Fig. 2.16D).

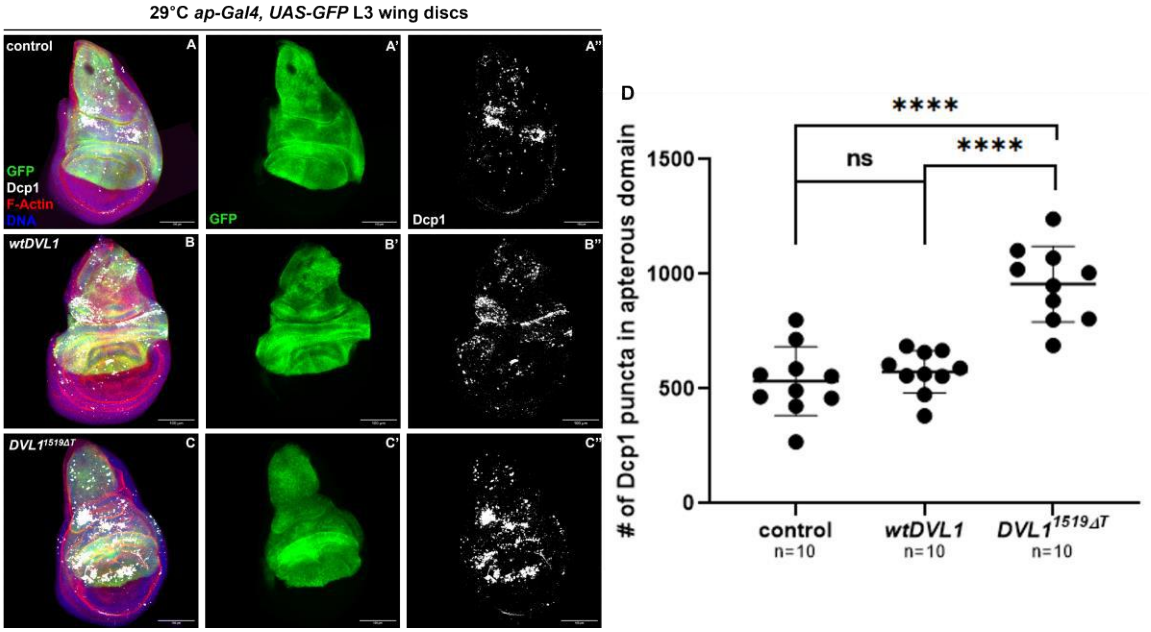

Figure 2.16. Expression of DVL1 variant with the *ap-Gal4* driver at 29°C does significantly increases apoptosis levels in wing imaginal discs

Confocal microscopy images showing *ap>GFP* (green), F-actin (red), DNA (DAPI, blue) and Dcp1 (white) stainings merged together in one image in control (**A**) and transgene expressing discs grown at 29°C (**B-C**). (**A'-C'**) The *apterous* domain of the representative wing disc images are shown with the GFP images. (**A''-C''**) Dcp1 staining for all genotypes are shown. (**D**) The number of Dcp1 puncta counted within the *apterous* domain are plotted. Sample size is shown under each genotype. Statistics were performed with ANOVA. Scale bar = 100 µm.

We proceeded to investigate the levels of cell death in wing imaginal discs that expresses either wt*DVL1* or *DVL1*$^{1519\Delta T}$ variant in the *hedgehog* domain in comparison to the control discs at 25°C (Fig. 2.17). The number of Dcp1 puncta in all three genotypes were overall lower than the numbers we counted for the discs expressing the transgenes in the apterous domain as the hedgehog domain is smaller than the apterous domain. We found that both wt*DVL1* and *DVL1*$^{1519\Delta T}$ expression caused a significant increase in the Dcp1 puncta numbers compared to the control discs (Fig. 2.17D). *DVL1*$^{1519\Delta T}$ variant expressing discs had significantly higher numbers of Dcp1 puncta than the wt*DVL1* expressing discs.

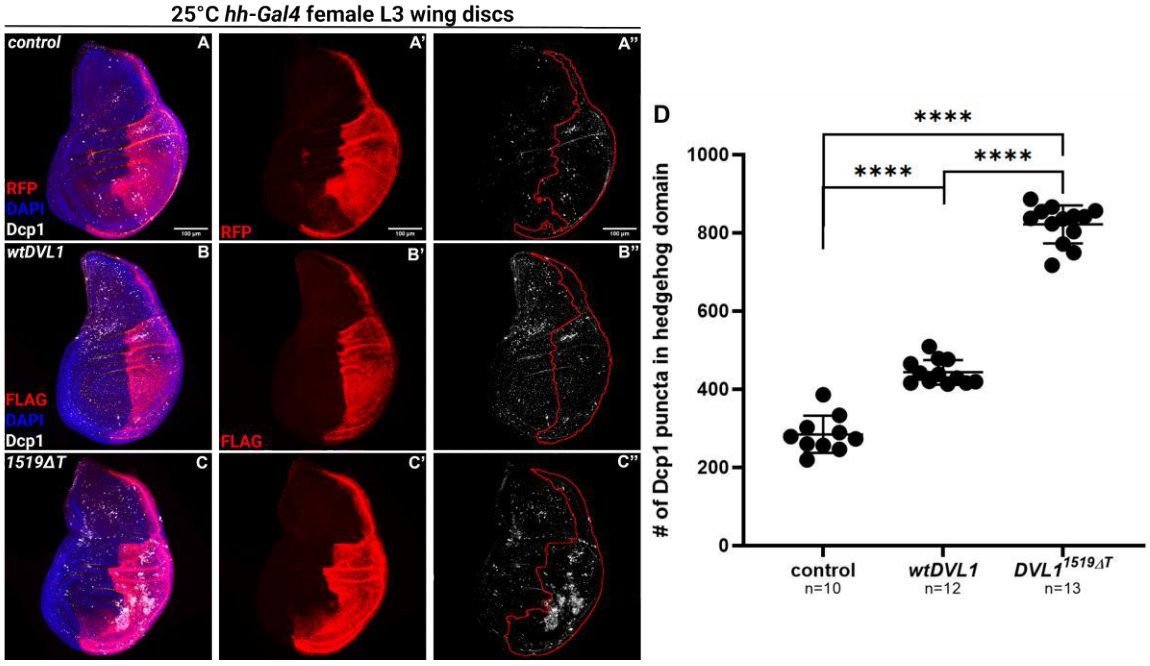

Figure 2.17. Expression of DVL1 variant with the *hh-Gal4* driver at 25°C does significantly increases apoptosis levels in wing imaginal discs

Confocal microscopy images showing UAS transgene expression domain (red), DNA (DAPI, blue) and Dcp1 (white) stainings merged together in one image in control (**A**) and transgene expressing discs grown at 25°C (**B-C**). (**A'-C'**) The *hedgehog* domain of the representative wing disc images are shown with the RFP or FLAG staining images. (**A''-C''**) Dcp1 staining for all genotypes are shown. (**D**) The number of Dcp1 puncta counted within the hedgehog domain are plotted. Sample size is shown under each genotype. Statistics were performed with ANOVA. Scale bar = 100 μm.

Again, we also counted the Dcp1 puncta in wing discs that expresses the transgenes in higher levels in the hedgehog domain at 29°C (Fig. 2.18). We have observed increased Dcp1 puncta numbers in all genotypes compared to the wing discs grown at 25°C, however, the trend was the same. *DVL1*$^{1519\Delta T}$ variant expression in the *hedgehog* domain significantly increased the number of Dcp1 puncta compared to both control and wt*DVL1* expressing wing discs (Fig. 2.18C, D).

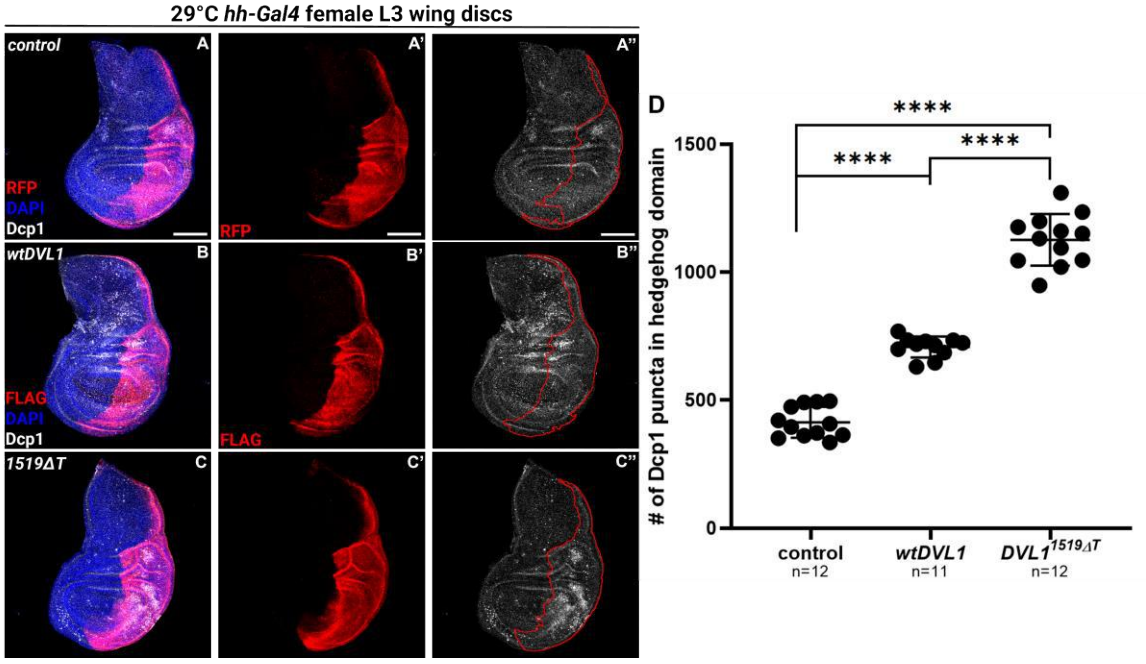

Figure 2.18. Expression of DVL1 variant with the *hh-Gal4* driver at 29°C does significantly increases apoptosis levels in wing imaginal discs

Confocal microscopy images showing UAS transgene expression domain (red), DNA (DAPI, blue) and Dcp1 (white) stainings merged together in one image in control (**A**) and transgene expressing discs grown at 29°C (**B-C**). (**A'-C'**) The *hedgehog* domain of the representative wing disc images are shown with the RFP or FLAG staining images. (**A''-C''**) Dcp1 staining for all genotypes are shown. (**D**) The number of Dcp1 puncta counted within the hedgehog domain are plotted. Sample size is shown under each genotype. Statistics were performed with One-Way ANOVA. Scale bar = 100 μm.

With these results, we can conclude that the expression of *DVL1* variant leads to increased levels of apoptosis in wing imaginal disc epithelium. These results support our finding that the abnormal morphology is not caused due to an increase in cell proliferation. *DVL1* variant expression possibly also disrupts cytoskeletal organization by altering noncanonical Wnt/PCP-JNK signalling and alters the mechanistic forces that govern the wing disc morphology and hence induces the altered shape and folding of the discs.

2.6. DVL1 variant disrupts pupal wing development

When expressed in the *hh-Gal4* domain, the *DVL1*$^{1519\Delta T}$ variant caused dramatic phenotypes in adult wings by altering the wing development, creating enlarged veins and decreasing the overall size of the wing blade. It also resulted in a curved wing blade rather than the fully expanded flat wings. We also showed that the variant induces apoptosis in wing imaginal discs. After these results, we wanted to look at the pupal wings of the flies that expresses the variant in the *hh-Gal4* domain at 25°C.

The pupal wing developmental stages are well described for the flies grown at 25°C (Waddington, 1940; Diaz de la Loza & Thompson, 2017). We looked at the wings of pupae 30-32 hours after puparium formation (APF) since the wings at this stage have the actin hairs and the veins formed. These wings reflect the “definitive shape” of the adult wings.

We observed that the pupal wings of the flies that expresses the variant in the *hh-Gal4* domain has the same wing shape as the corresponding adult wings: curved wing blade and the invagination on the proximal end of the posterior side of the wing (Fig. 2.19C). The variant altered the vein formation, resulting in thicker veins, especially the L4 longitudinal vein. The bent shape of the wing also pulled the anterior side of the wing via the mechanical forces applied during the hinge contraction, which made the L3 vein thicken as well. Wild type *DVL1* expressing wings appeared similar to the controls except for the disorganization of the actin hairs on the posterior side of the wing blade (Fig. 2.19B). The vein structure of control and wt*DVL1* expressing wings were also similar.

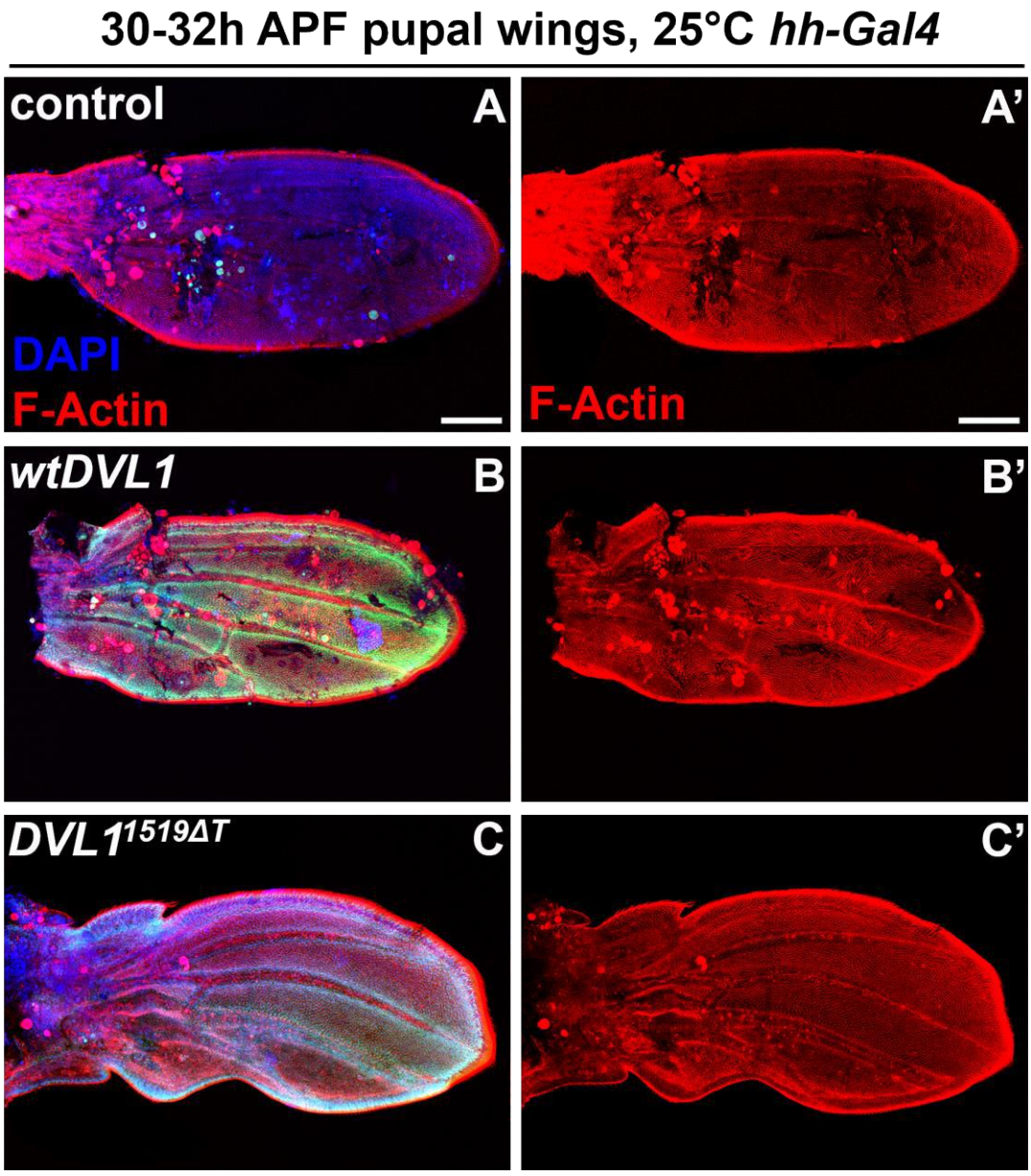

Figure 2.19 Alteration of pupal wing development induced by the expression of DVL1 variant with the hh-Gal4 driver

Confocal microscopy images of F-actin (red), FLAG (green), DNA, (DAPI, blue) in control (**A-A'**), wt*DVL1* (**B-B'**) and *DVL1*$^{1519\Delta T}$ (**C-C'**) expressing pupal wings. Scale bar = 100 μm.

2.7. DVL1 variant disrupts cell adhesion in pupal wings

To further investigate the pupal wing phenotypes in DVL1 variant expressing flies, we used the driver with the narrower expression domain, *dpp-Gal4*. When the

variant is expressed in this domain, it caused a blistering phenotype in the 30 hr APF pupal wings (Fig. 2.20B). At this stage of the pupal wing development, the vein patterning is established. This blister phenotype appears to be enlargement of the L3 longitudinal vein. It seems, in this region of the wing, the dorsal and ventral layers of the wing were unable to adhere together to form the proper vein and wing blade structures separately hence they appear merged and non-adhered.

Earlier studies in literature have shown that the overexpression of Matrix-metalloproteases (Mmp) can induce blister formation in pupal wings (Sun et al., 2021). Our lab has shown that the variant expression induces ectopic Mmp1 expression in wing imaginal disc pouches (Gignac, et al., 2023). Hence, we wanted to investigate if the overexpression of Mmp1 is also present in the pupal wing blisters. We found that the variant induced blister is filled with the Mmp1 protein in 30hr APF pupal wings (Fig. 2.20B). This phenotype was not observed in wt*DVL1* expressing pupal wings (Fig. 2.20A).

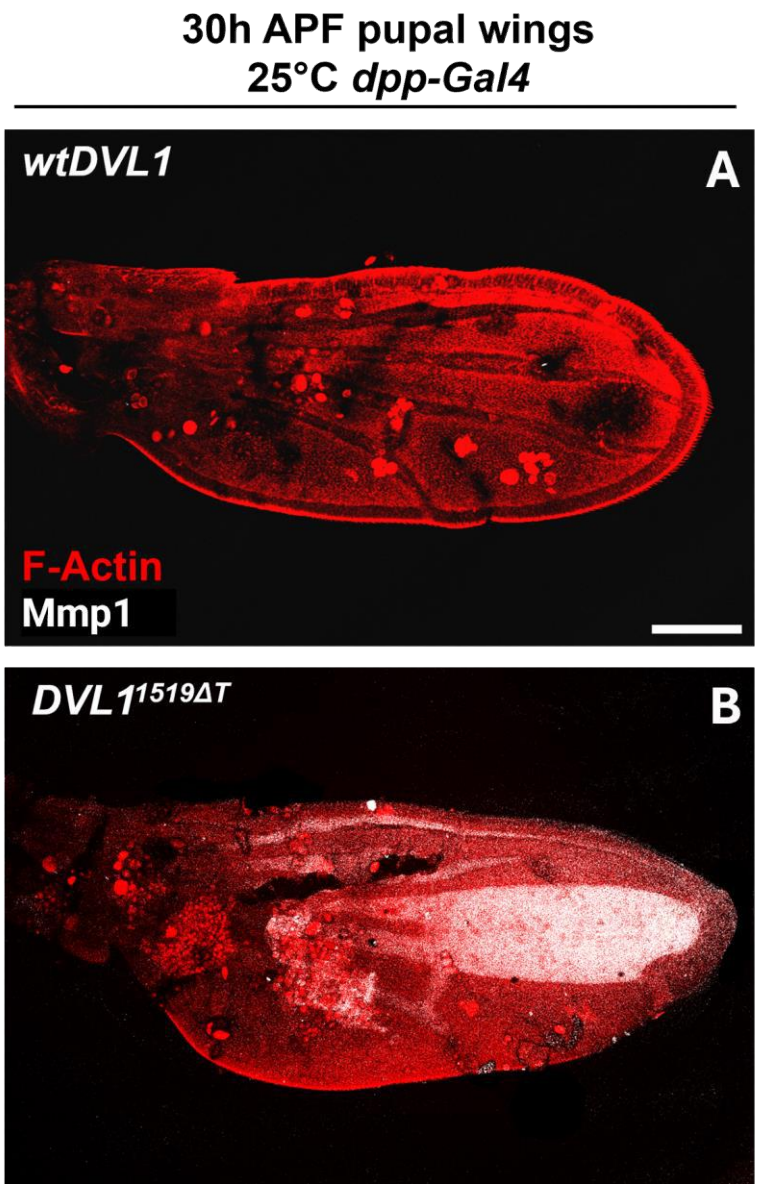

Figure 2.20 The expression of DVL1 variant disrupts dorso-ventral adhesion and induces Mmp1 expression in pupal wings

F-Actin (red) and Mmp1 (white) stainings of 30h APF pupal wings that express wt*DVL1* (**A**) and *DVL1*$^{1519\Delta T}$ (**B**) in the *dpp-Gal4* domain at 25°C. Scale bar = 100 µm. n=10 for each genotype.

We proceeded our investigation by looking at the blisters more closely. The proper adhesion of the dorsal and ventral layers of the wings can occur with the slow degradation of the basement membrane (Sun et al., 2021). Since we hypothesized that there was an alteration in the adhesion process, we wanted to look at the basement membrane. We chose to target *Drosophila* Collagen IV called *Viking* (*Vkg*) as a proxy for the basement membrane since it is the most abundant component. We used Vkg-GFP

expressing flies, which expresses the endogenously tagged Vkg-GFP fusion protein to visualize the basement membrane in pupal wings.

The variant and wt*DVL1* expression were driven by *dpp-Gal4* driver (Fig. 2.21). We found that the Vkg-GFP is not abundant in the control pupal wing, we only observed a faint GFP signal withing the veins (Fig. 2.21A). We observed a sharper GFP signal in the veins of the wt*DVL1* expressing pupal wings (Fig. 2.21B). The vein pattern was mostly comparable to control wings, however, L4 longitudinal vein of wt*DVL1* expressing pupal wings appeared malformed and sometimes bent (Fig. 2.21B). The pupal wings that express the $DVL1^{1519\Delta T}$ variant had the most intense GFP signal (Fig. 2.21C). The veins and the area around the veins seemed to be filled with Vkg-GFP. The L3 longitudinal vein appeared enlarged, forming a blister-like structure. The region between the L3 and L4 longitudinal veins appeared much narrow supporting the idea that the blister is formed by the non-adhered epithelial layers merging with the L3 vein.

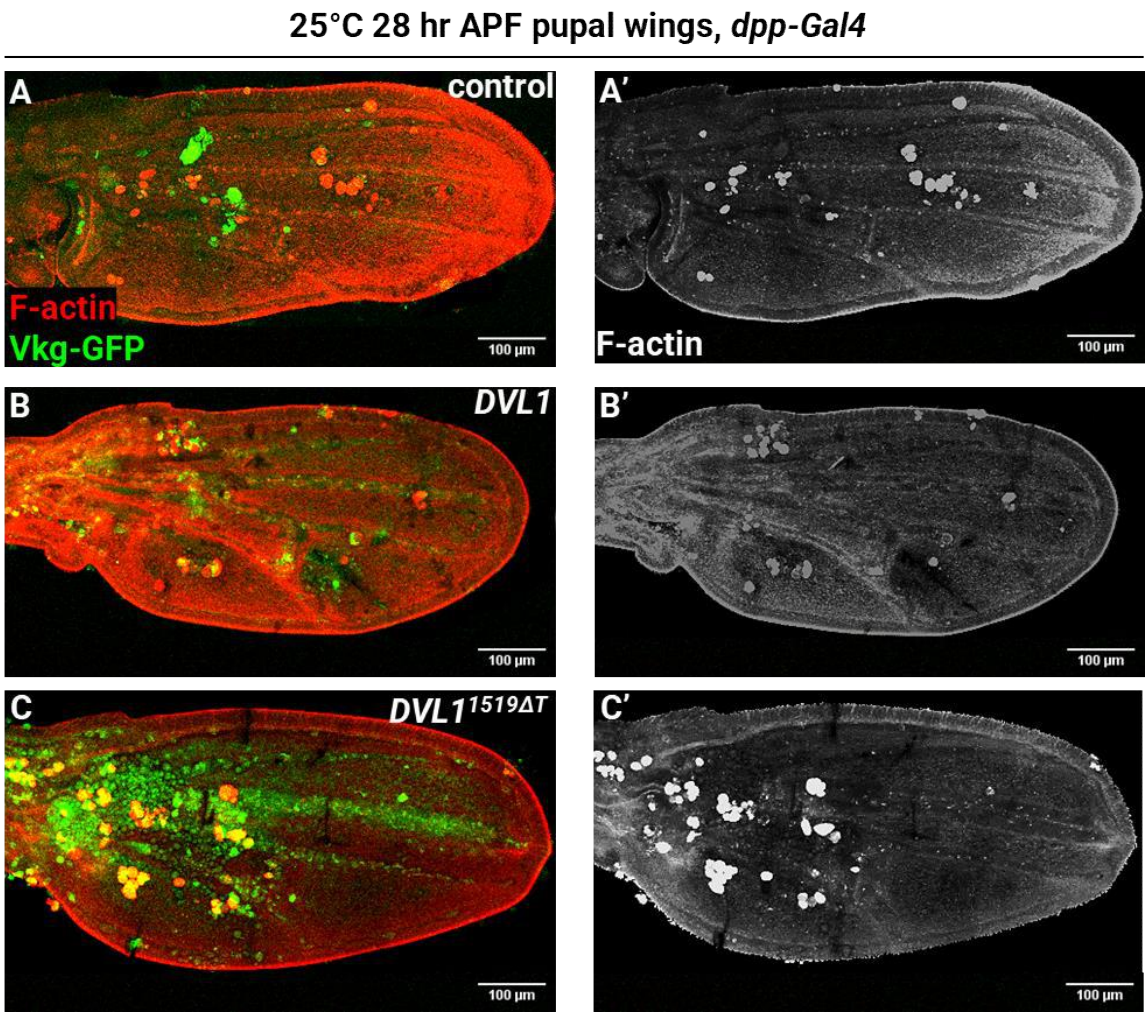

Figure 2.21. The expression of DVL1 variant leads to increased Vkg-GFP levels in pre-expansion pupal wings

28hr APF pupal wings showing F-Actin (red/grey) and Vkg-GFP (green) staining in control (**A**), wt*DVL1*- expressing (**B**) or $DVL1^{1519\Delta T}$ -expressing (**C**) tissue with single channel F-Actin staining shown in **A'-C'**. Crosses were performed at 25°C. Scale bar = 100 µm. n=10 per genotype.

We then took a closer look at the veins and the Vkg-GFP expression in these pupal wings. We found that the blister in the variant expressing pupal wings is filled with basement membrane component Vkg protein (Fig. 2.22C). A slight thickening of the L4 longitudinal vein in the wt*DVL1* expressing wings was observed with the orthogonal view, which also showed the abundance of Vkg-GFP in this region (Fig. 2.22B). However, the intensity was much lower than the variant expressing pupal wings. Vkg-GFP signals were also observed around the adhered epithelia closer to the L3 veins in

the variant expressing pupal wings. This shows that the expression of the variant reduces the basement membrane degradation during pupal wing development.

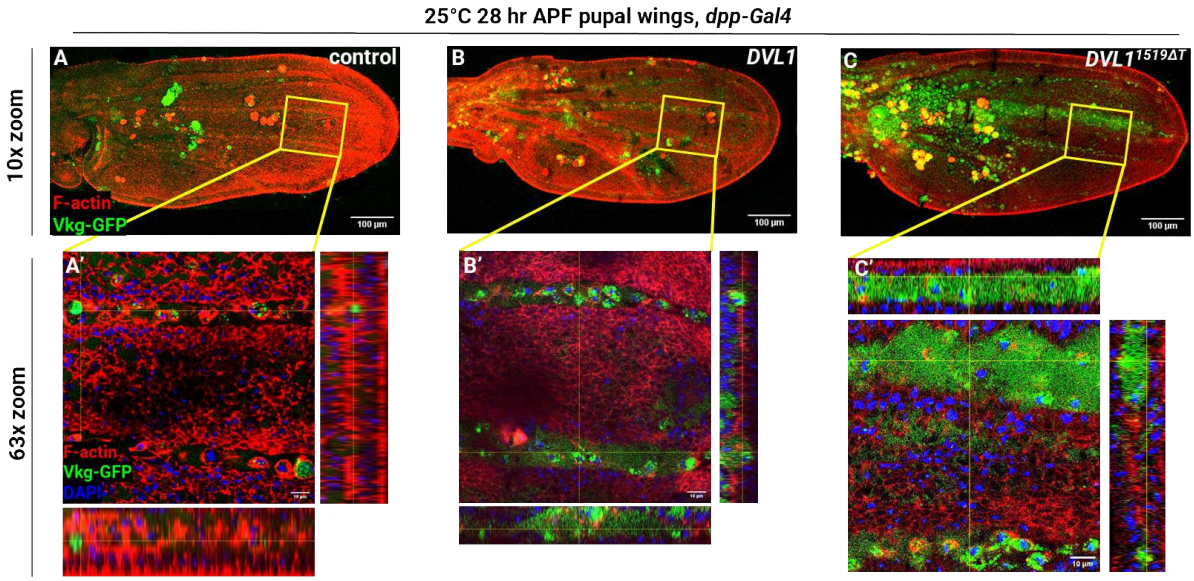

Figure 2.22. The expression of DVL1 variant disrupts basement membrane degradation

28hr APF pupal wings showing F-Actin (red) and Vkg-GFP (green) staining in control (**A**), wt*DVL1*- expressing (**B**) or $DVL1^{1519\Delta T}$ -expressing (**C**) tissue at 10x zoom. 63x zoomed in images of the region marked by the yellow squres in **A**-**C** are shown in **A'**-**C'** respectively also with DAPI staining showing the cell nuclei in blue. Crosses were performed at 25°C. Scale bar = 100 µm. n=10 per genotype.

2.8. DVL1 variant expression alters other conserved signalling pathways and cellular processes

DVL1 is a well-established relay molecule in both canonical and noncanonical branches of Wnt signalling. Earlier work from our lab showed that DVL1 establishes a balance between these two branches and the variant expression disrupts this balance (Gignac et al., 2023). However, not all the phenotypes we have shown in our previous work and in Chapter 2 of this thesis can be justified by the imbalance in Wnt signalling branches. Especially the vein defects, ectopic bristles, scutellum and thorax malformation phenotypes indicate that many cellular processes during development are being altered by the variant expression. In the light of all these findings, we hypothesized that the expression of $DVL1^{1519\Delta T}$ variant alters other conserved signalling pathways and

cellular processes. To test this hypothesis, we conducted RNA-sequencing by using *Drosophila* tissue.

We chose to use late third instar wing imaginal discs as the epithelial cells are subject to more changes during development compared to pupal wings. Wing imaginal discs were also the tissue that we have assayed the most. Then we have decided to use the wing imaginal discs that expresses *wtDVL1* and $DVL1^{1519\Delta T}$ variant in the *apterous-Gal4* driver domain, since it's the largest expression domain and we observed dramatic alterations in adult tissues.

We used w^{1118} as wild type *Drosophila* for our control. We crossed our control, *UAS-wtDVL1* and *UAS-* $DVL1^{1519\Delta T}$ fly lines with *apterous-Gal4, UAS-GFP* fly line. Then the female larvae with the correct genotype were selected from the progeny. We dissected wing imaginal discs from larvae and extracted RNA from them. We sent the first batch to the School of Biomedical Engineering (SBME) Sequencing Core at the Biomedical Research Center (BRC) at UBC for quality control. This step helped us make sure if the samples were eligible for RNA sequencing by measuring the RNA integrity for all types of RNA. RNA integrity shows how much degradation occurred in your sample and a number from 1 to 10 is assigned after the measurement. This number is called the RNA integrity number (RIN) (Farrell, 2017). Our samples had a good RIN of ~8. After this step we proceeded to prepare more samples. We made sure to have 4 samples from each genotype. The synthesis of cDNA and library preparation followed by the sequencing was done at the SBME Sequencing Core using Illumina mRNA Next-generation sequencing systems, recording 10 million reads. The sequencing results were analysed by Dr. Stephane Flibotte at the Life Sciences Institute Bioinformatics Facility in UBC. The flowchart of this process can be seen in Figure 2.23 below.

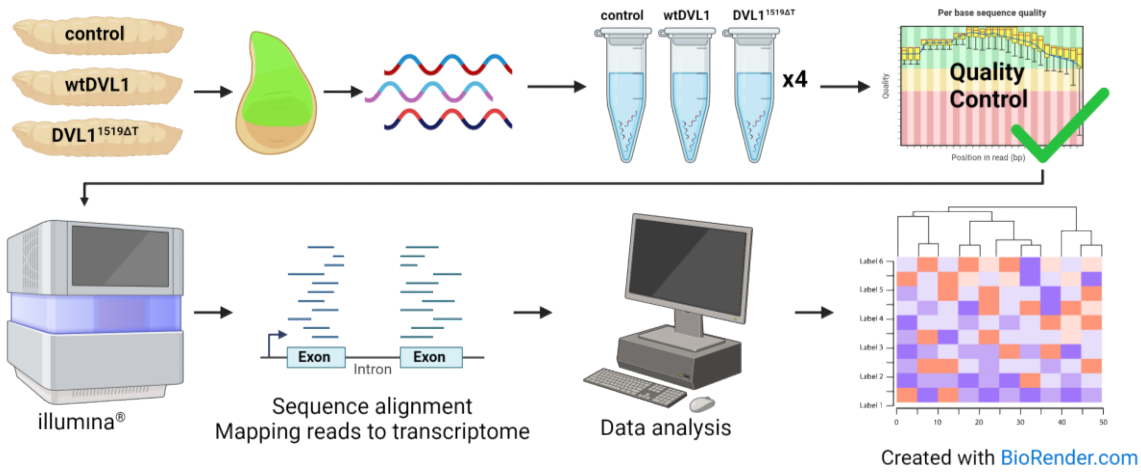

Figure 2.23. Simple schematic of RNA-Sequencing workflow

We first received the lists of genes that are differentially regulated in the wing imaginal disc samples that expresses wild type *DVL1* or *DVL1*$^{1519\Delta T}$ compared to the control wing disc samples and to each other. Without further looking in the detailed information regarding these genes, we checked the numbers of genes that are significantly differentially regulated between the genotypes. For these numbers we only considered the genes that are differentially regulated with q-values or adjusted p values lower than 0.05. This adjustment of the p-value is necessary since the data obtained from sequencing is subject to a multitude of statistical tests. The adjusted value indicates the number of tests that could produce a false positive result so the adjusted p-value is a higher number than the p-value and it helps us eliminate the false positive results (Koch et al., 2018). We found that the number of differentially expressed genes (DEGs) in wing imaginal discs that express wt*DVL1* compared to the control to be the lowest with 151. The highest number of DEGs were found to be 674 in wing imaginal discs that express *DVL1*$^{1519\Delta T}$ compared to the control discs. The number of DEGs in *DVL1*$^{1519\Delta T}$ discs compared to wt*DVL1* discs was 223. Even with the high stringency provided by the p-adjusted value, these numbers suggest that the expression of *DVL1*$^{1519\Delta T}$ variant causes a big change in the transcriptome of the fruit fly wing imaginal discs. It should be noted that there were DEGs common in both wt*DVL1* and *DVL1*$^{1519\Delta T}$ discs data compared to the control discs.

After obtaining these numbers, we wanted to look into the details of the differentially expressed genes, so we asked Dr. Flibotte to prepare a heatmap of the significantly differentially expressed genes. Among the DEGs with appropriate p-adjusted values (<0.05), a heatmap that shows 50 genes was plotted. The data was also clustered in the making of this map. Clustering of RNA sequencing data is used to identify patterns of gene expression by grouping the DEGs based on their distance to the cluster mean (Koch et al., 2018). This method helps us visually assess the results in the heat map, making it easier to see the trends of gene expression across different genotypes. The heatmap generated showed clear blocks of genes that are upregulated and downregulated only in the presence of the variant in wing imaginal disc tissues. There were also blocks of genes that are regulated in a similar pattern in both wt*DVL1* and $DVL1^{1519\Delta T}$ expressing wing imaginal discs (Fig. 2.24). The gene expression levels presented on this heatmap are presented in a 2-fold base with p value < 0.05 hence the data presented has high significance.

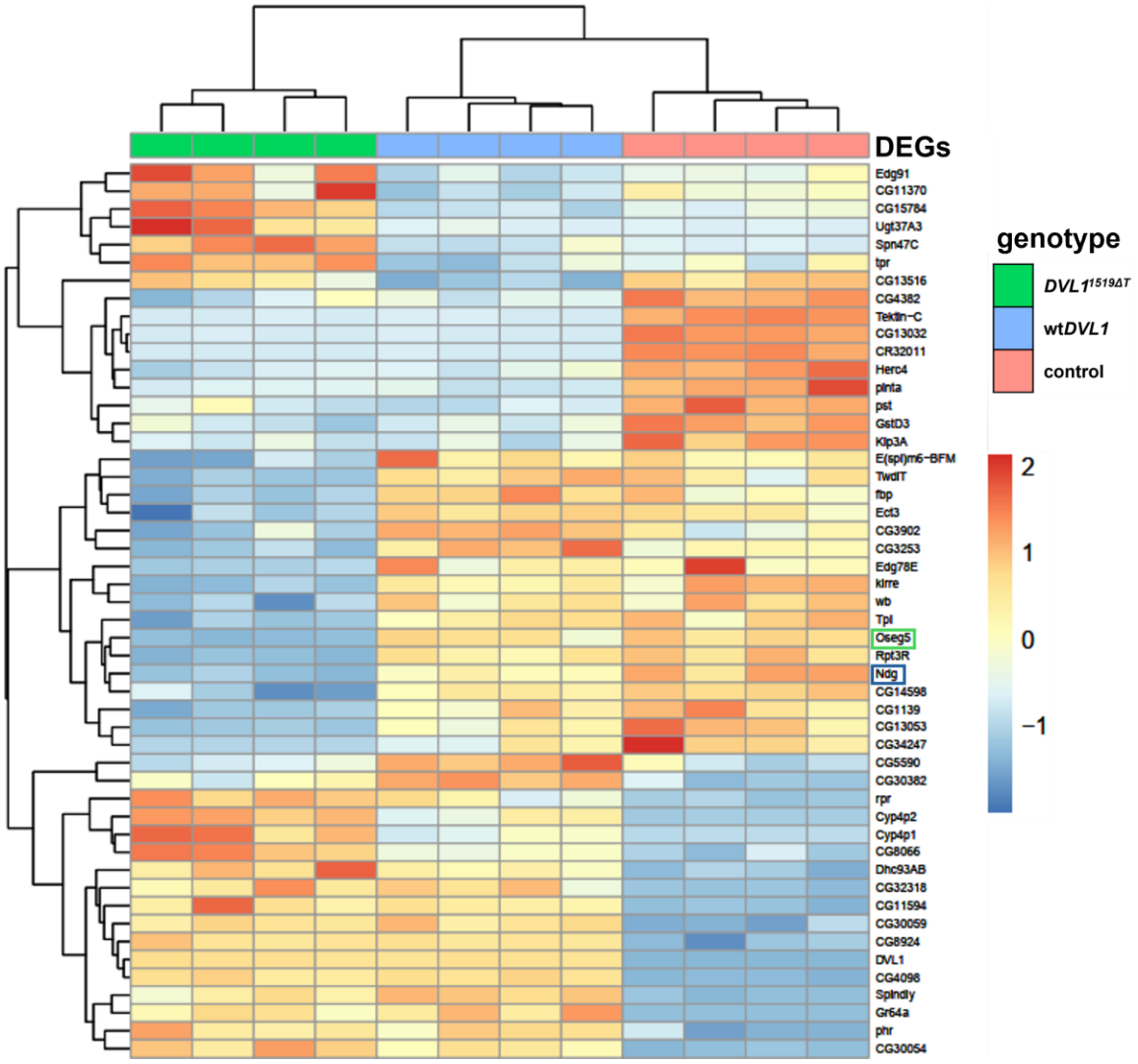

Figure 2.24. Heatmap of DEGs found in the RNA-sequencing results
The DEGs found in *DVL1*$^{1519\Delta T}$ –expressing wing discs (green), wt*DVL1*- expressing discs (blue) in the *apterous* domain and the control discs (pink) were plotted in the heatmap. The figure legend shows the colours from dark blue to dark red that shows the differential expression levels in the log2fold base from -2 to +2 respectively. p-value<0.05 for the significance of differential expression.

When we looked into the genes mapped on the heatmap, we expectedly found that the expression of genes involved in the formation of the basement membrane, morphogenesis of cuticle and epithelial tissues were altered with the expression of the variant. We also found genes that are associated with glycolysis and carbohydrate metabolism were differentially regulated in the presence of *DVL1*$^{1519\Delta T}$. Genes involved in the regulation of sexual reproduction in *Drosophila* were also found to be affected by

the expression of the variant (Fig. 2.25). These results suggest that the expression of *DVL1*$^{1519\Delta T}$ variant alters other metabolic processes and signalling pathways.

Among the DEGs on the heatmap, there were promising candidates we found in the list of DEGs. One of these were *Nidogen* (*Ndg*) (marked blue on the list of DEGs, Fig. 2.25), a component of the basement membrane together with Collagen IV ortholog *Vkg* (Hynes & Zhao, 2000). In the variant expressing wing discs, *Ndg* expression levels were found to be about 10 times (log2fold change = -3.35) lower compared to the control discs according to our RNA sequencing results. *Ndg* plays a crucial role in the maintenance of tissue homeostasis and dynamics by linking ECM components. It was found that loss of *Ndg* causes ruptures in the BM of *Drosophila* fat bodies and microperforations in the BM of larval visceral muscles (Dai et al., 2018; Wolfstetter et al., 2019). These findings go along with our finding regarding the disrupted basement membrane degradation in pupal wings and the dysregulated *Vkg* levels.

Another gene that was interesting among the DEGs was *Outer segment 5* (*Oseg5*) (marked green on the list of DEGs, Fig. 2.25), ortholog of human *IFT80* (Intraflagellar transport 80), which is involved in cilium assembly and located in non-motile cilium (Avidor-Reiss et al., 2004). We found that in the variant expressing wing discs, *Oseg5* expression levels were almost 20 times lower compared to the control. A study that aims to decipher cilia-independent functions of IFT components used *Drosophila* as their model since all cell types except for sensory neurons and sperm are non-ciliated. The researchers did a screen by knocking down ciliary genes and staining for markers of developmental signalling pathways in wing imaginal discs. They found that knocking down *Oseg5* caused loss of canonical Wnt signalling (Balmer et al., 2015) which is in line with our previous findings of lower Arm stability in the presence of *DVL1* variants (Gignac et al., 2023).

Due to time constraints, we were not able to pursue any of the hits we found in the RNA sequencing results.

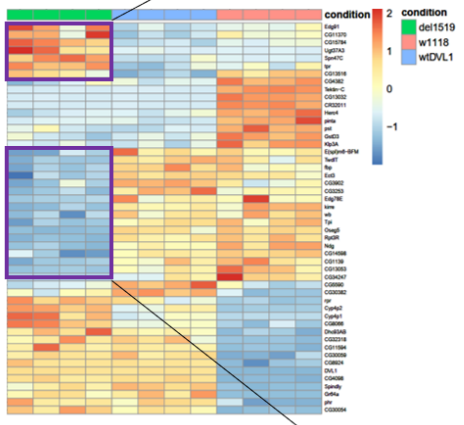

UPREGULATED IN *DVL1*$^{1519\Delta T}$ DISCS	DOWNREGULATED IN *DVL1*$^{1519\Delta T}$ DISCS
Edg91	E(spl)m6−BFM
CG11370	TwdlT
CG15784	fbp
Ugt37A3	Ect3
Spn47C	CG3902
tpr	CG3253
	Edg78E
	kirre
	wb
	Tpi
	Oseg5
	Rpt3R
	Ndg
	CG14598
	CG1139
	CG13053
	CG34247

Figure 2.25. The list of DEGs in *DVL1*$^{1519\Delta T}$–expressing wing discs extracted from the heatmap

The DEGs found to be significantly upregulated (red) and downregulated (blue) in DVL11519ΔT –expressing wing discs in the apterous domain in comparison to the wtDVL1-expressing and the control discs. The gene lists were extracted from the heatmap in Fig. 2.24.

We then wanted to be able to see the biological processes the DEGs induced by the expression of *DVL1*$^{1519\Delta T}$ are involved in. For this purpose, we requested a bar plot that shows the Gene Ontology (GO) Enrichment clustering of the DEGs by comparing all three genotypes. The GO Resource knowledgebase is the world's largest source of information on gene function. The GO Consortium assigns statements called GO terms about the function of genes by associating a gene or gene product a term on their vast database. These terms allow researchers to see a snapshot of the current biological knowledge regarding their gene/genes of interest (Ashburner et al., 2000; The Gene Ontology Consortium et al., 2023). A clustering based on the biological process GO terms assigned for the DEGs that showed up in our RNA sequencing data was done and this data was plotted (Thomas et al., 2022). A high stringency was ensured by keeping adjusted p-values low in this clustering (adjusted $p < 0.0006$). The list of biological terms showed up in the plot below expectedly included wing disc development, wing disc, appendage and wing morphogenesis as we showed with our experiments (Fig. 2.26).

The other biological process annotations on this plot also showed that the DEGs in the presence of *DVL1*$^{1519\Delta T}$ were involved in the morphogenesis of other organs and neurons (Fig. 2.26). These results also supported our hypothesis that the expression of *DVL1*$^{1519\Delta T}$ alters other biological processes during fruit fly development.

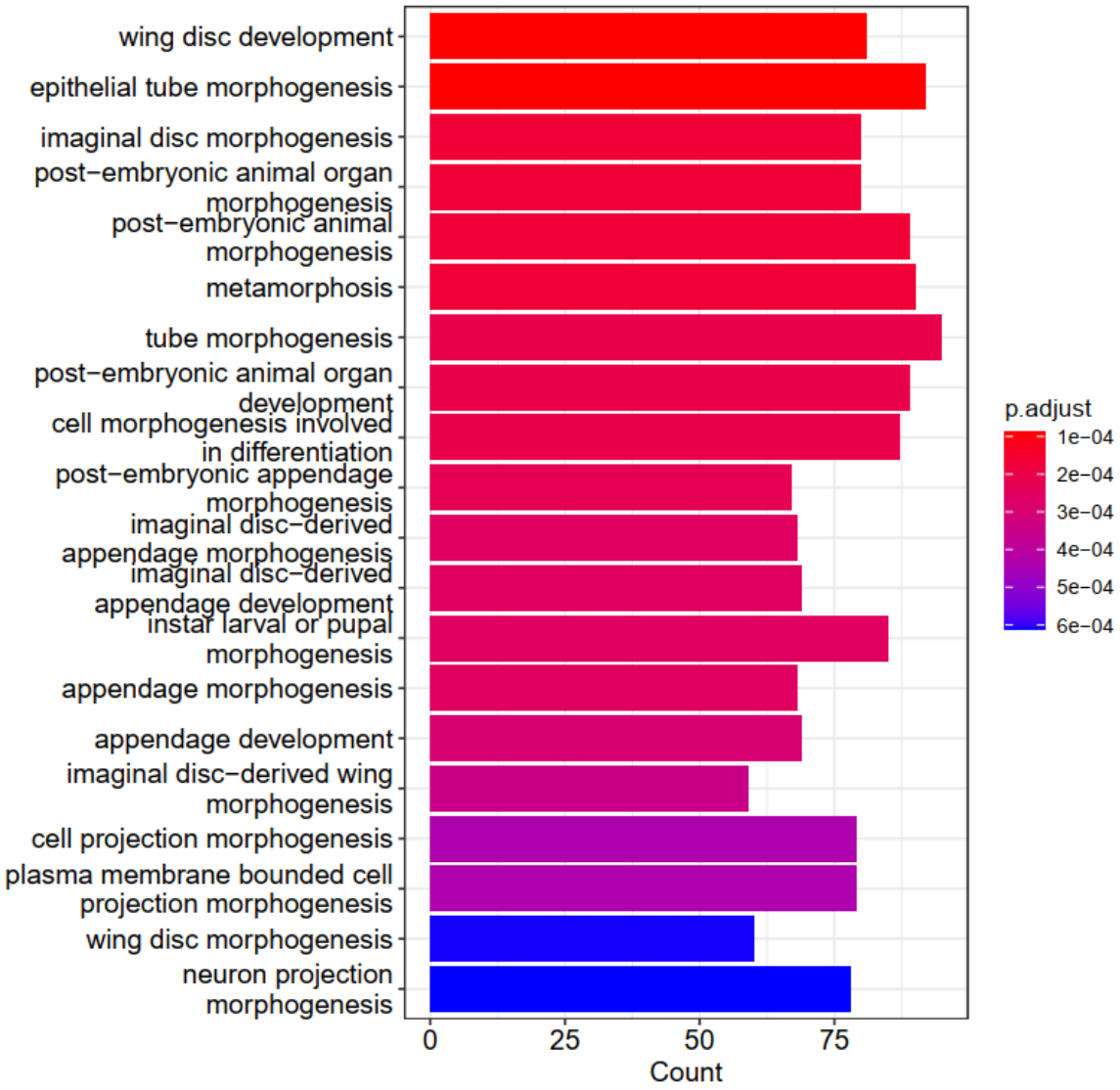

Figure 2.26. Barplot of the differentially regulated biological processes detected by GO Enrichment clustering in variant expressing wing discs in comparison to wt*DVL1* expressing discs

Barplot showing the Gene Ontology Enrichment clustering of DEGs according to the biological processes they are involved in on the GO Resource database. The y-axis shows the GO terms of the biological processes, y-axis shows the number of significantly differentially expressed genes. The figure legend on the right indicates the adjusted p-value selected for the genes plotted varies between 0.0001 and 0.0001, which indicated a very low possibility of false positives.

Chapter 3. Results: DVL1 variant C-terminus novel peptide sequence causes neomorphic phenotypes

Earlier work by Katja MacCharles has shown that that abnormal DVL1 variants cause an imbalance in two Wnt pathways without showing significant differences between the variants and displaying similar trends (Gignac et al., 2023). Hence, we questioned whether this consistent dominant negative effect and the neomorphic phenotypes caused by expression of the variants are because of the lack of the highly conserved C-terminus or due to the novel peptide sequence that replaces it. We also wanted to understand how important the role of the C-terminus of DVL1 is to the protein's cellular function. In order to address these further, our collaborators designed two constructs to isolate the role of the novel C-terminal peptide sequence: DVL1^{1519*} and DVL1^{1431*}, in which the nucleotide position indicated is followed by a stop codon to terminate the protein.

The experimental results presented in this chapter were obtained with the generous help of Dr. Kenneth Kin Lam Wong in the dissections.

3.1. Generation and validation of C-terminal truncated RS-DVL1 fly lines

Again, we utilized the Gal4-UAS system to express the C-terminal truncated proteins in fruit fly tissues. Generation of the UAS-transgenic lines was carried out by the Richman Lab at UBC, as detailed in the Materials and Methods chapter of this thesis. The coding sequences of the truncated protein constructs were inserted into the same attp40 chromosomal site on Chromosome II as the original variants. N-terminal FLAG tags were also added to the constructs.

To be able to compare to expression levels directly to the variants, the expression of these transgenes was driven using the *decapentaplegic-Gal4* (*dpp-Gal4*) driver.

We initially wanted to determine whether the proteins were expressed in the fly using western blotting. Antibody staining against the N-terminal FLAG tag present in the truncated DVL1 constructs was used to visualize DVL1 proteins on the membrane. The

western blots showed that both the DVL1^{1431*} and DVL1^{1519*}proteins were expressed at the expected sizes of ~60 and ~55 kDa respectively (Fig. 3.1) The analysis of the western blots showed high expression levels of DVL1^{1519*} at both temperatures, suggesting that the specific truncation made the protein more stable in this model system. The expression levels of DVL1^{1431*} protein was lower than the expression levels of wtDVL1 at 25°C, however, increasing the expression levels by growing the flies at 29°C increased the levels above physiological levels.

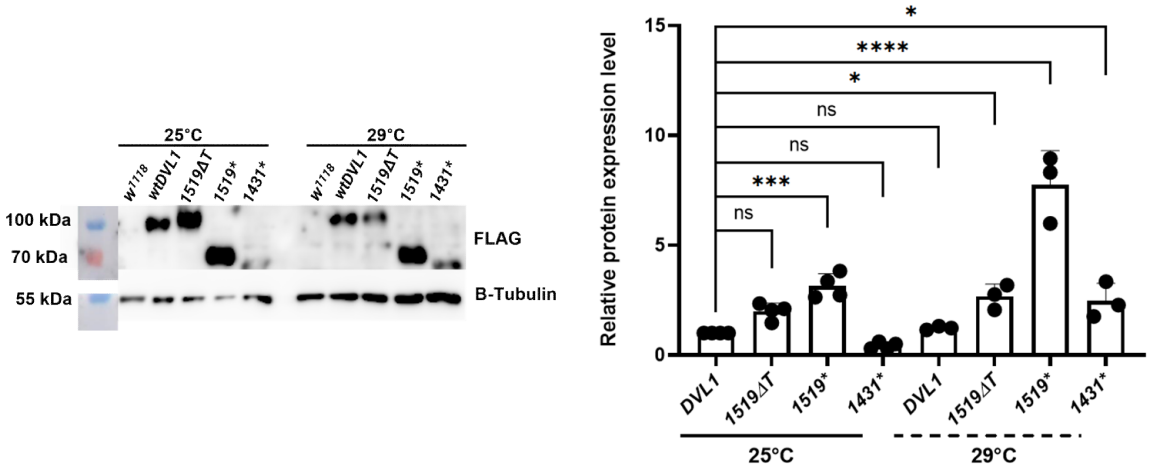

Figure 3.1. Protein expression levels of human *DVL1* transgenes in larval heads
Western blot analysis of wildtype, variant and C-terminal truncated DVL1 protein levels from larval head protein extracts. *Dpp>DVL1* crosses were performed at 25°C or 29°C as indicated. Larval heads were dissected from 5 female larvae per genotype and the equivalent of 2 larval heads was loaded onto the gel. β-tubulin was used as a loading control. On the right, plot of DVL1 protein levels in variant DVL1-expressing tissue relative to control (*dpp*>wt*DVL1*) tissue. Each dot on the bars represents one blot. Error bars show mean with SD. Statistics were performed with a one-way ANOVA test.

3.2. All DVL1 proteins induce planar cell polarity defects

In adult *Drosophila* wings the wing blade is covered with actin hairs called trichomes, which are parallel to each other and pointing distally. This orientation is governed by the PCP pathway (Simons & Mlodzik, 2008; L. L. Wong & Adler, 1993). Detection of wing hair polarity defects has been a well-established method for identifying disruptions in the larval and pupal PCP pathway. In our earlier studies, it was shown that all transgenes encoding wildtype and RS-associated DVL1 variants in the *dpp* domain induced defects in planar cell polarity (Gignac et al., 2023).

Here, we wanted to investigate whether the C-terminal truncated DVL1 proteins would also cause PCP defects manifested as misaligned trichomes in the adult wings. We again employed the *dpp-Gal4* driver to induce expression in the wing imaginal disc along the anterior/posterior boundary, which corresponds to the middle region of the adult wing between the L3 and L4 longitudinal veins (Fig. 3.2A, Fig. 3.3A). Wing hair alignment in this middle region can be compared to the neighbouring compartments where the transgenes are not expressed. We grew our crosses at 25°C and 29°C separately in order to see if any other alterations are induced by higher expression of the transgenes. Our results showed that all transgenes caused PCP defects, in all the wings scored (n=25 for all). To make it easier to visualize the phenotypes, the images taken from flies grown at 25°C and 29°C will be shown in separate figures (Fig. 3.2, Fig. 3.3)

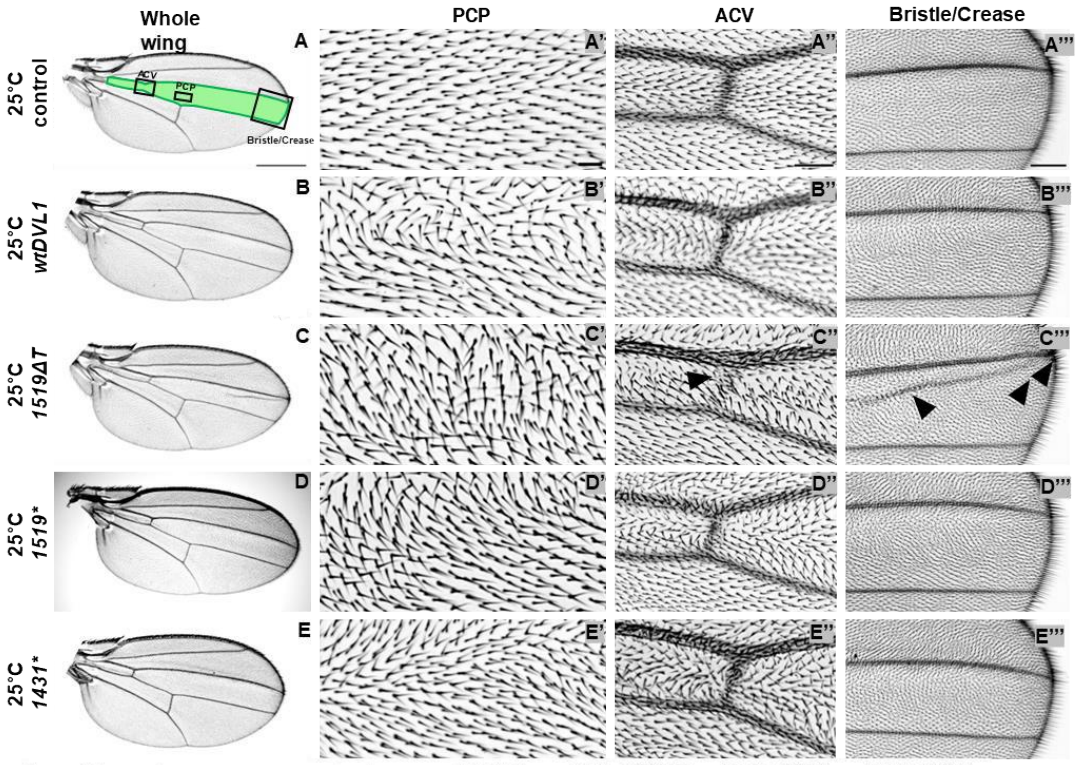

F Phenotype	control	*wtDVL1*	*DVL1*$^{1519\Delta T}$	*DVL1*^{1519*}	*DVL1*^{1431*}
PCP disruption	0	100	100	100	100
Ectopic bristles	0	0	96	0	0
Vein thickening	0	0	76	0	0
Wing crease	0	0	68	0	0
ACV abnormality	0	0	72	0	0

% of flies: 0 10 20 30 40 50 60 70 80 90 100

Figure 3.2. Adult wing phenotypes induced by the expression of DVL1 transgenes in the *dpp-Gal4* domain at 25°C

(**A**) Control wild-type wing with shaded *dpp-Gal4* expression domain (green) and black boxes that corresponds to zoomed in views presented in panels (**A'-E'''**). (**B-E**) Representative *dpp>DVL1*-expressing adult female wings at 25°C. (**A'-E'**) Zoomed in views of PCP defects within a fixed region above the posterior cross vein for control (**A'**) and *DVL1*-expressing (**B'-E'**) adult female wings from 25°C crosses. (**A''-E''**) Zoomed in views of anterior cross vein (ACV) in control (**A''**) and *DVL1*-expressing (**B''-E''**) adult female wings. Arrowhead in **C''** points to reduction of ACV. (**A''-E''**) Zoomed in view of adult wing between the L3 and L4 veins in control (**A'''**) and *DVL1*-expressing **(B'''-E''')** female wings from 25°C crosses where extra bristles and creases are indicated with arrowheads in **C'''**. Phenotypic frequencies are quantified in (**F**). 25 wings were scored per genotype across n=2 independent experiments. Scale bar = 500 µm (**A-E**), 20 µm (**A'-E'**), 50 µm (**A''-E''**), 100 µm (**A'''-E'''**).

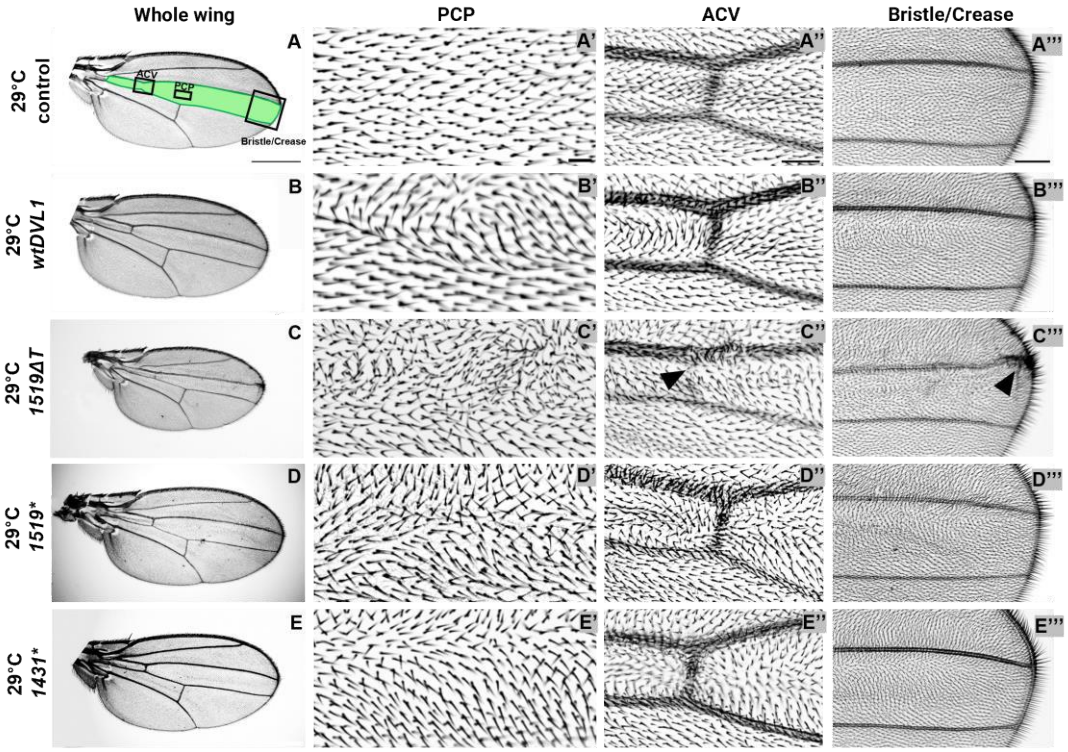

Phenotype	control	*wtDVL1*	*DVL1*$^{1519\Delta T}$	*DVL1*^{1519*}	*DVL1*^{1431*}
PCP disruption	0	100	100	100	100
Ectopic bristles	0	0	100	0	0
Vein thickening	0	0	92	0	0
Wing crease	0	0	84	0	0
ACV abnormality	0	0	88	4	0

% of flies: 0 10 20 30 40 50 60 70 80 90 100

Figure 3.3. Adult wing phenotypes induced by the expression of DVL1 transgenes in the *dpp-Gal4* domain at 29°C

(**A**) Control wild-type wing with shaded *dpp-Gal4* expression domain (green) and black boxes that corresponds to zoomed in views presented in panels (**A'-E'''**). (**B-E**) Representative *dpp>DVL1*-expressing adult female wings at 29°C. (**A'-E'**) Zoomed in views of PCP defects within a fixed region above the posterior cross vein for control (**A'**) and *DVL1*-expressing (**B'-E'**) adult female wings from 29°C crosses. (**A''-E''**) Zoomed in views of anterior cross vein (ACV) in control (**A''**) and *DVL1*-expressing (**B''-E''**) adult female wings. Arrowhead in **C''** points to reduction of ACV. (**A''-E''**) Zoomed in view of adult wing between the L3 and L4 veins in control (**A'''**) and *DVL1*-expressing **(B'''-E''')** female wings from 29°C crosses where extra bristles and creases are indicated with arrowheads in **C'''**. Phenotypic frequencies are quantified in (**F**). 25 wings were scored per genotype across n=2 independent experiments. Scale bar = 500 μm (**A-E**), 20 μm (**A'-E'**), 50 μm (**A''-E''**), 100 μm (**A'''-E'''**).

In our earlier studies, additional, neomorphic phenotypes were observed only in the wings of the flies that express the DVL1 variants while scoring the PCP phenotype (Gignac et al., 2023). These neomorphic phenotypes were thickening in veins, ectopic bristle formation on the edge of the L3 vein, alterations or absence of anterior cross vein (ACV) and a wing crease between the intervein region between L3 and L4 longitudinal veins (Figs. 3.2C, 3.3C). Since these mutant phenotypes were not observed in *dpp>wtDVL1* wings or the two truncated transgenes (*DVL1*^{1431*} and *DVL1*^{1519*}), even with elevated protein levels at 29°C, it was concluded that these phenotypes were novel effects of the variants (Gignac et al., 2023). With this experiment, we show that the PCP defects are induced by the presence of the DVL1 protein and its 3 functional domains, however, the neomorphic phenotypes are only induced by the novel peptide sequence at the C-terminus of *DVL1*$^{1519\Delta T}$.

3.3. Lack of C-terminus does not induce abnormal morphology in adult fly tissues

Since the region corresponding to the *dpp-Gal4* expression domain in the adult wing is narrow, we used a Gal4 driver, *hh-Gal4*, that span a larger region to look for adult phenotypes.

We performed our crosses at both 25°C and 29°C. In chapter 2 (Fig. 2.4, Fig. 2.5), we have shown that the flies that express the *DVL1*$^{1519\Delta T}$ variant in the hh domain had smaller wings with dramatically abnormal vein growth and a curved posterior structure. In addition to these wing phenotypes, we have also shown that the flies had difficulties eclosing from their pupae due to their abnormal leg morphology, most of them died trying to eclose or they fell on the food after eclosion. The flies expressing *DVL1*$^{1519\Delta T}$ at 25°C, were taken from the vials after seeing them eclose and fall onto the food. None of the *wtDVL1* expressing flies showed this phenotype. In this experiment we observed that the C-terminal truncated *DVL1*^{1519*} *and DVL1*^{1431*} expressing flies developed similarly to the *wtDVL1* expressing flies with no dramatic alteration in their wing or leg morphology (Fig. 3.4D, E). This experiment one more time showed that the altered morphology caused only by the expression of DVL1 variant, and it is due to the novel peptide sequence at its C-terminus, not the lack of the highly conserved C-terminus.

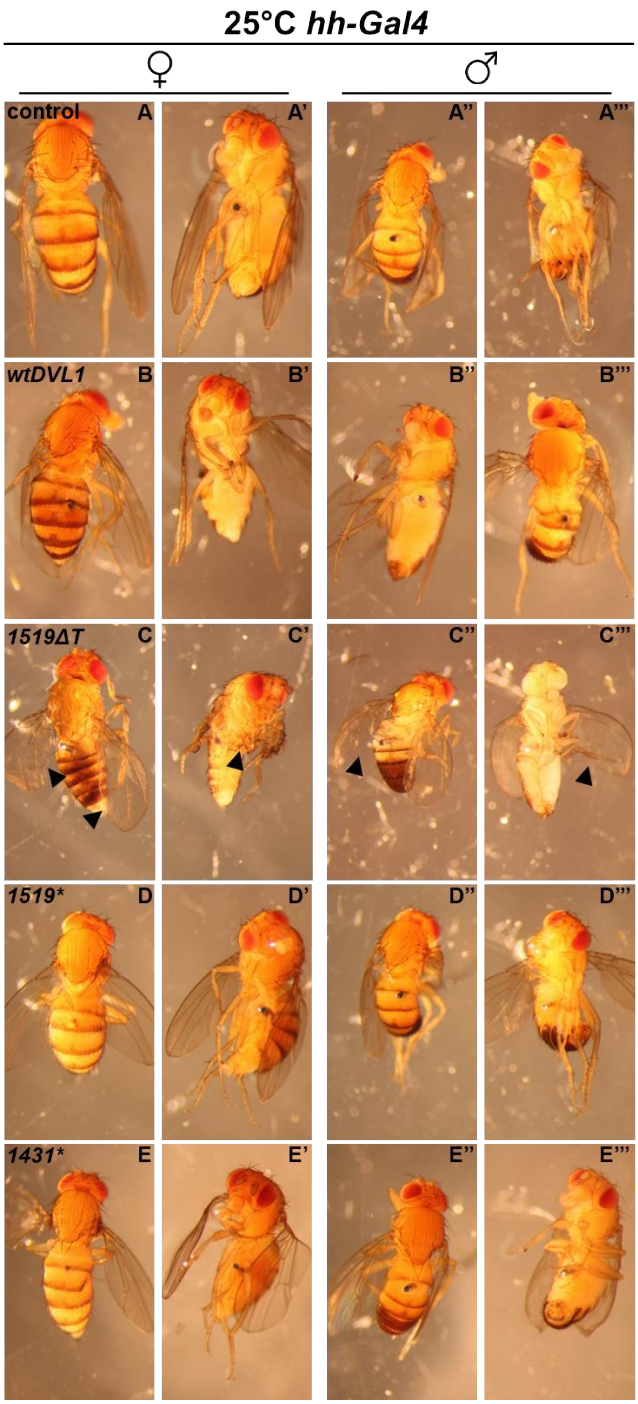

Figure 3.4. Expression of C-terminal truncated DVL1 proteins does not induce abnormal adult structures when expressed in the *hh-Gal4* domain at 25°C

(**A-A'''**) 25°C control adult fly phenotypes. (**B-B'''**) The representative images from female and male adult phenotypes from *hh*>wt*DVL1* crosses performed at 29°C. The representative images from female and male adult phenotypes from *hh>DVL1*$^{1519\Delta T}$ (**C-C'''**), *hh>DVL1*^{1519*} (**D-D'''**) and *hh>DVL1*^{1431*} (**E-E'''**) crosses performed at 25°C. Arrowheads in **C**-**C'''** points to malformed wings and the legs in *hh>DVL1*$^{1519\Delta T}$ flies. n=10 per each genotype and per sex.

The flies that expressed *DVL1*$^{1519\Delta T}$at higher levels at 29°C were not able to eclose and thus the flies were dissected out of the pupal case for imaging. The higher expression of *wtDVL1*, *DVL1*^{1519*} *and DVL1*^{1431*} did not cause any such alterations during the development of the flies (Fig. 3.5).

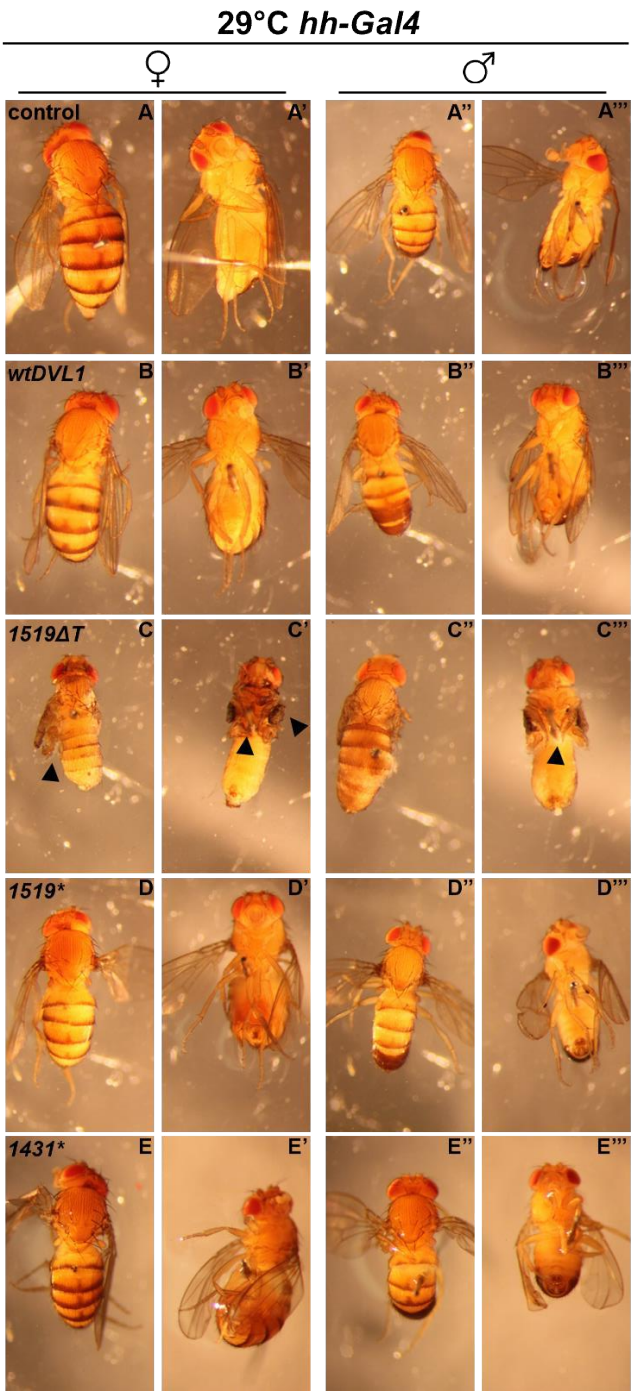

Figure 3.5. Expression of C-terminal truncated DVL1 proteins does not induce abnormal adult structures when expressed in the *hh-Gal4* domain at 29°C

(**A-A'''**) 29°C control adult fly phenotypes. (**B-B'''**) The representative images from female and male adult phenotypes from *hh*>wt*DVL1* crosses performed at 29°C. The representative images from female and male adult phenotypes from *hh>DVL1*$^{1519\Delta T}$ (**C-C'''**), *hh>DVL1*^{1519*} (**D-D'''**) and *hh>DVL1*^{1431*} (**E-E'''**) crosses performed at 29°C. Arrowheads in **C**-**C'''** points to malformed wings and the legs in *hh>DVL1*$^{1519\Delta T}$ flies. n=10 per each genotype and per sex.

3.4. Lack of DVL1 C-terminus does not alter JNK signalling

PCP defects in adult wing hairs can be caused both by loss or gain of Wnt/PCP pathway (Vinson & Adler, 1987; Krasnow & Adler, 1994; Axelrod et al., 1998), hence further investigation is required to decipher in which way the signalling is altered. Our previous work used two established reporters for this purpose, the JNK targets Mmp1 and *puckered-lacZ* (*puc-lacZ*) and both reporters were used to show that DVL1 variants ectopically induced JNK signalling in the wing pouch of wing imaginal discs while *wtDVL1* did not show any induction (Gignac et al., 2023). In this study, we did the same assays to see whether this induction is due to the lack of the original C-terminus which would cause the necessary PDZ-binding motif (PBM) interactions to not occur with the expression of both the variant and the C-terminal truncated DVL1 proteins.

We used *dpp-Gal4* to express the transgenes and quantified the expression of Mmp1. No induction of Mmp1 protein signal in controls, wt*DVL1*, $DVL1^{1519*}$ and $DVL1^{1431*}$ expressing wing imaginal discs were observed, while all the $DVL1^{1519\Delta T}$ expressing discs showed Mmp1 puncta in the wing pouch within the *dpp-Gal4* expression domain (Fig. 3.6).

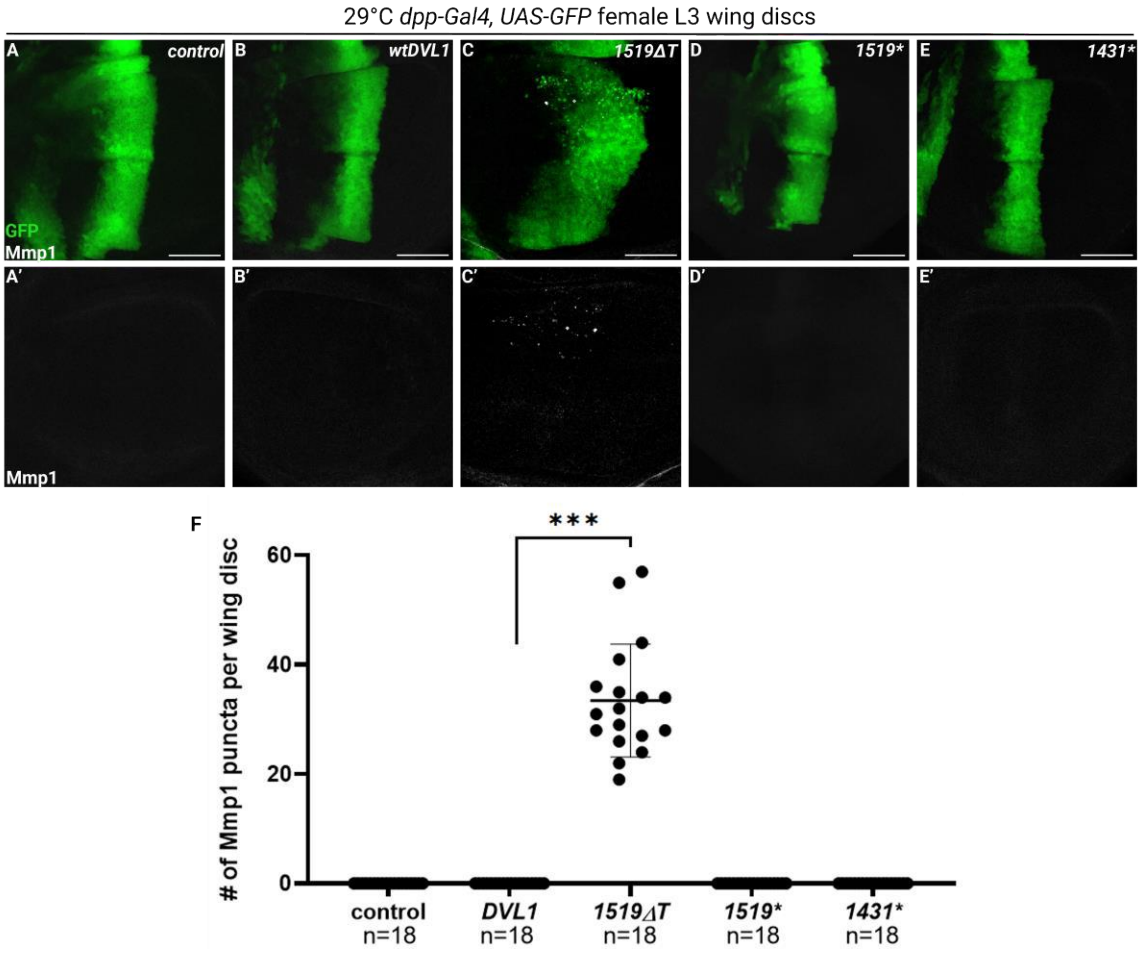

Figure 3.6. C-terminal truncated DVL1 proteins do not induce Mmp1 expression in wing imaginal discs

(**A-E**) Z-stack maximum projection of third instar wing imaginal discs showing Mmp1 (white) and *dpp>GFP* expression domain (green) in control (**A**) and *DVL1*-expressing female wing disc pouches (**B**-**E**). (**A'-E'**) Z-stack maximum projection of sşngle channel images showing Mmp1 staining in control (**A'**) and *DVL1*- expressing female wing discs (**B'-E'**). (**F**) Shows the number of Mmp1 puncta counted per wing disc. Crosses were performed at 29°C and 18 female wing discs were analyzed per genotype. Scale bar = 50 μm.

To further confirm these results and increase the expression of variants, we used the transcriptional reporter *puc-lacZ* by expressing the DVL1 proteins in the *apterous-Gal4* domain at 29°C. All discs showed *puc-lacZ* expression in the peripodial membrane, mostly in the notum of wing discs (not shown in figures). Only the $DVL1^{1519\Delta T}$ expressing wing discs showed a robust induction of *puc-lacZ* signal in the dorsal compartment of the wing pouch, where the *apterous-Gal4* drives the expression of the variant (Fig 3.7C).

.

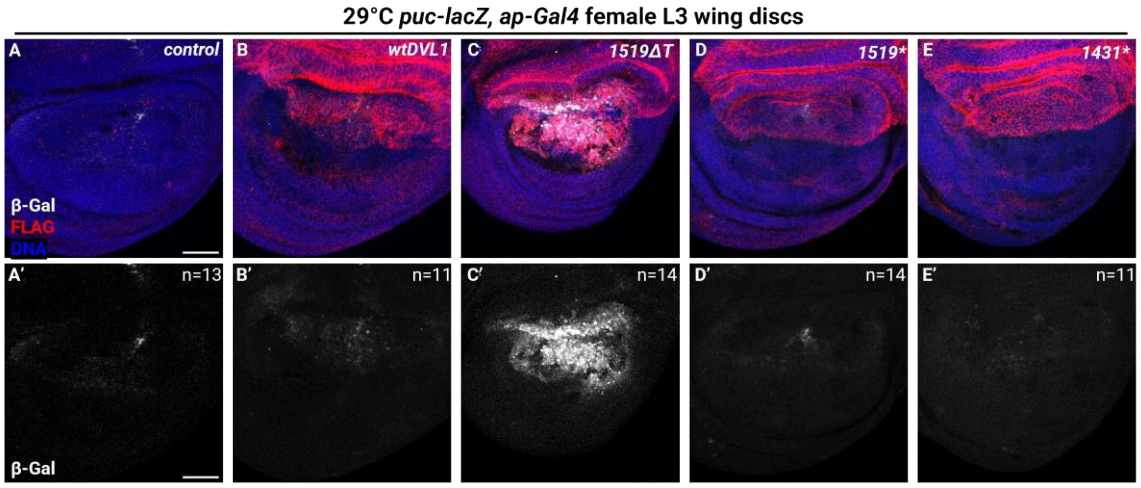

Figure 3.7. C-terminal truncated DVL1 proteins do not induce *puc-lacZ* expression in wing imaginal discs

(**A-E**) Z-stack maximum projection of imaginal wing discs showing DNA (DAPI, blue), β-gal (white) and UAS transgene expression domain (red) staining in control (**A**) and *DVL1*-expressing female wing discs (**B-E**). (**A'-E'**) Z-stack maximum projection of single channel images showing β-gal (white) staining in control (**A'**) and *DVL1*-expressing female wing discs (**B'-E'**). n numbers in bottom panels depict the number of wing discs that displayed the phenotype shown in the representative image. Crosses were performed at 29°C and 11-14 female wing discs were imaged per genotype across n=2 independent experiments. Scale bar = 50 μm.

We also observed that the expression of the C-terminal truncated proteins did not cause any of the morphological abnormalities (Figs. 3.8D and 3.8E) caused by the expression of $DVL1^{1519\Delta T}$ variant (Fig. 3.8C) in the wing imaginal discs when expressed in the *apterous* domain. In wing imaginal discs that express $DVL1^{1519*}$ or $DVL1^{1431*}$, the structure and number of folds were comparable to wild type discs. Unlike $DVL1^{1519\,\Delta T}$ variant expressing discs (Fig. 3.8C''), dorso-ventral boundary was not disrupted when the C-terminal truncated proteins were expressed (Figs. 3.8D'' and 3.8E'').

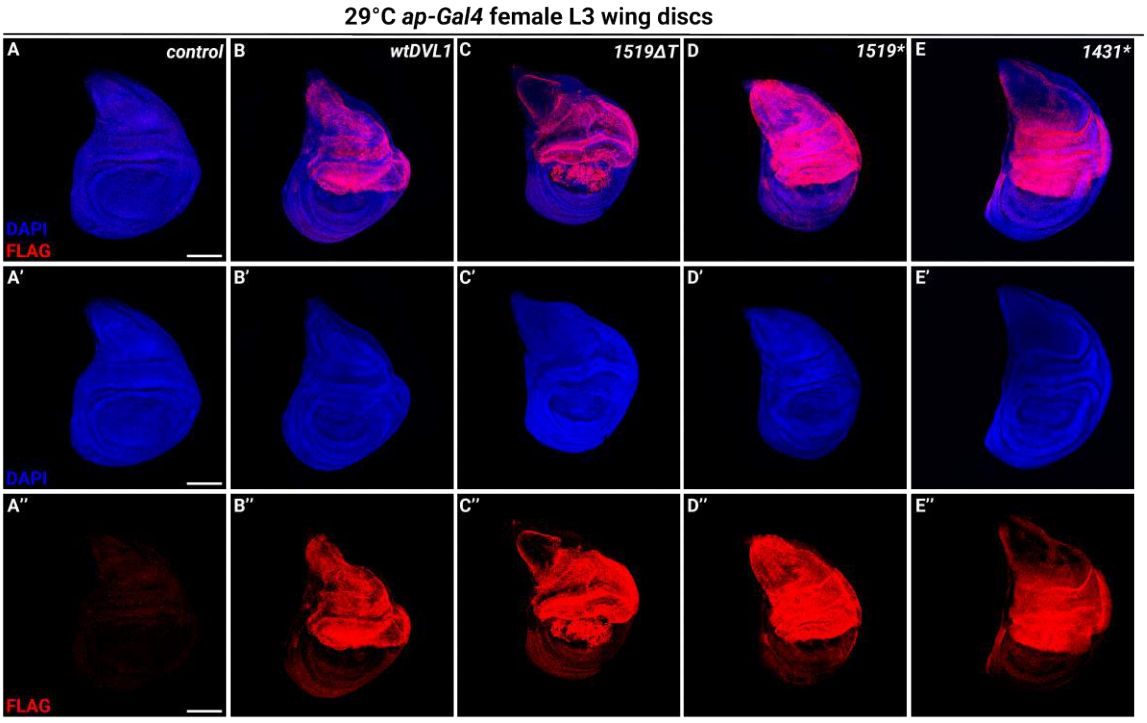

Figure 3.8. C-terminal truncated DVL1 proteins do not induce morphological alterations in wing imaginal discs

(**A-E**) Z-stack maximum projections of DNA (DAPI, blue) and *apterous* expression domain (red) shown with FLAG staining for the transgenes in control (*dpp>GFP*) (**A**) and *DVL1*-expressing female wing discs (**B**-**E**) with corresponding single channel DAPI (blue) staining shown in (**A'-E'**) and FLAG (red) in (**A''-E''**). Scale bar = 100 μm. n=10 per each genotype.

3.5. Lack of DVL1 C-terminus does not alter canonical Wnt/Wg signalling

The majority of RS-associated genes are components of non-canonical Wnt/PCP signalling. However, DVL1 is the branching point for both signalling pathways hence important for the balance between two signalling cascades. In *Drosophila*, Armadillo (Arm) protein stability can be measured to investigate canonical Wnt signalling activity. Arm is the fruit fly ortholog of β-catenin, which is stabilized in the cytoplasm after Wnt signalling pathway activation. Arm expression can be seen as two stripes flanking the dorso-ventral boundary in the wing imaginal disc pouch. In our earlier work, it was shown that the expression of 3 RS-*DVL1* variants caused a decrease in the Arm protein levels while the expression of *wtDVL1* did not have any such effects. Hence, it was concluded

that the canonical Wnt/Wg signalling is being disrupted by the expression of variants (Gignac et al., 2023).

In this study, we wanted to investigate whether this disruption in canonical Wnt signalling is due to the lack of conserved C-terminus of human *DVL1* gene or the novel peptide sequence in the DVL1 variants. Again, we used Arm protein levels in the wing imaginal disc pouch as a measure of canonical Wnt signalling activity. We used *dpp-Gal4* to drive the expression of our transgenes at 25°C. We observed a decrease in the level of Arm only in the presence of *DVL1* variant $DVL1^{1519\Delta T}$. However, it was not very robust (Fig.3.9).

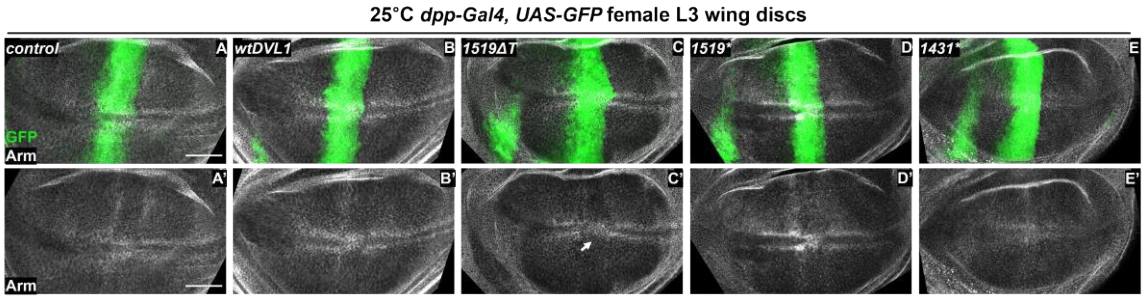

Figure 3.9. C-terminal truncated DVL1 proteins do not disrupt Arm stabilization in wing imaginal discs when expressed at 25°C

(**A-E**) Z-stack maximum projections of Arm protein (white) and *dpp>GFP* expression domain (green) staining in control (*dpp>GFP*) (**A**) and *DVL1*-expressing female wing discs (**B**-**E**) with corresponding single channel Arm (white) staining shown in (**A'-E'**). Significant decrease in Arm levels relative to control is indicated with white arrow in **C'**. The crosses were performed at 25°C. Scale bar = 50 µm. n=10 per each genotype.

In order to increase the expression levels of all transgenes, we performed our crosses at 29°C and measured the Arm signal intensity as shown in the figure below. We confirmed that only the $DVL1^{1519\Delta T}$ variant altered the canonical/Wnt signalling while the C-terminal truncated proteins showed a similar phenotype to the control and *wtDVL1*. In the light of this finding, we concluded that the disruption in canonical Wnt signalling in *Drosophila* is not caused by the lack of the original C-terminus in RS-associated *DVL1* variant but the presence of the new peptide sequence (Fig 3.10).

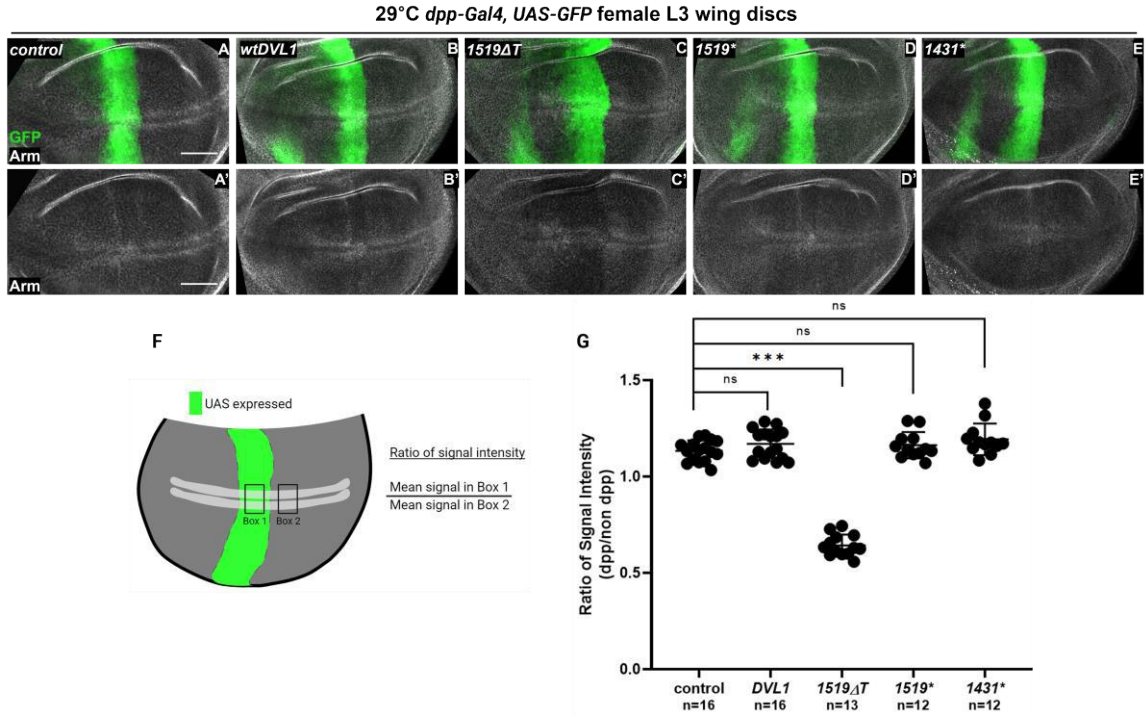

Figure 3.10. C-terminal truncated DVL1 proteins do not disrupt Arm stabilization in wing imaginal discs when expressed in higher levels at 29°C

(**A-E**) Z-stack maximum projections of Arm protein (white) and *dpp>GFP* expression domain (green) staining in control (*dpp>GFP*) (**A**) and *DVL1*-expressing female wing discs (**B**-**E**) with corresponding single channel Arm (white) staining shown in (**A'-E'**). Significant decrease in Arm levels relative to control is indicated with white arrow in **C'**. Scale bar = 50 µm. **(F**) Schematic of an imaginal wing disc pouch with *dpp-Gal4* expression domain (green), position of most stabilized Arm protein (white). Boxes 1 and 2 show the regions where ratio of Arm signal intensity was quantified within and outside of the *dpp* expression domain. (**G**) The Arm signal intensity ratio quantified as described is plotted. Crosses were performed at 29°C and analyses show averages from 12-16 discs per genotype. Error bars show mean with SD. Statistics were performed with ANOVA.

Chapter 4. Discussion and Conclusions

In this project, we investigated one of the mutations in human *DVL1* gene associated with autosomal dominant Robinow Syndrome (RS). Adding onto the previous work done by Katja MacCharles in our lab and the chicken embryo studies done in Richman Lab in UBC, we directly tested how RS-DVL1 variants alter normal development of an organism and lead to RS phenotypes *in vivo*.

Chapter 2 describes the part of the project that is mainly focused on the morphological alterations caused by the expression of $DVL1^{1519\Delta T}$ variant. The neomorphic phenotypes observed when the variant is expressed in *Drosophila* tissues were investigated further via several experiments, primarily in the wing imaginal discs since they are the precursor tissue that forms the adult wings and nota.

Among the 3 DVL1 variants found in autosomal dominant RS patients and studied by our lab, I focused on investigating the alterations caused by $DVL1^{1519\Delta T}$ variant. The phenotypes caused by the expression of all three variants were comparable. The frequencies of these phenotypes were also found to be quite similar (Gignac et al., 2023) . Therefore, I chose to proceed by using the variant that seemed to be more stable with its relatively high protein expression levels at both 25°C and 29°C, which was $DVL1^{1519\Delta T}$.

Chapter 3 describes the part of the project that is mainly focused on the investigation of mutations in *DVL1* gene that cause RS. All *DVL1* mutations associated with autosomal dominant Robinow syndrome are located within the penultimate exon, resulting in a frameshift that leads to the translation of an abnormal peptide (109 aa) at the C-terminus (Hu et al., 2022; White et al., 2015; Zhang et al., 2022). This novel C-terminal peptide is consistent among individuals with the *DVL1* associated autosomal dominant RS. These mutations do not affect the three primary functional domains of DVL1 protein, suggesting that frameshifts in the C-terminus are compatible with life. Our study of RS frameshift mutations in *DVL1* by using the C-terminal truncated DVL1 proteins has provided insights into the pathogenesis of RS and the requirement of C-terminus in development and cell signalling in the fruit fly model.

4.1. Validation of *DVL1* transgenic fly lines

When we initially compared the expression of the wild type *DVL1* and the variants on the transcriptional level, we found that all DVL1 transgenes were expressed comparably with no significant differences in the qRT-PCR results (Fig. 2.1A). However, on the protein level, the products of $DVL1^{1519\Delta T}$ and $DVL1^{1529\Delta G}$ appeared more stable compared to the $DVL1^{1615\Delta A}$ on blots. The expression levels of the $DVL1^{1519\Delta T}$ and $DVL1^{1529\Delta G}$ variant proteins were also higher than the product of wt*DVL1.* In terms of the phenotypes caused by all three variants, it was shown that the higher expression of $DVL1^{1615\Delta A}$ at 29°C resulted in adult wing and thorax phenotypes similar to the other variants (Gignac et al., 2023).

The exact reason for the differences between the stability of the variants is unknown. We think that it could be due to the location of where the frameshift is introduced in the amino acid sequence of the protein product. The $DVL1^{1615\Delta A}$ variant retains more of the reference sequence of the wt*DVL1*, hence the sites that would target the protein for degradation might be present in this variant while the others have lost it, which made them more stable.

It must be noted that the activity of all variants in the molecular level was shown to follow the same trend in our previous work, meaning that if we could increase the levels of the $DVL1^{1615\Delta A}$ variant, it caused the same phenotypes as the more stable variants (Gignac et al., 2023). With this information and the measuring of the expression levels, we were able to choose $DVL1^{1519\Delta T}$ as a representative variant for the work presented in this thesis.

It should also be stated that the stability of the variants compared to the product of wt*DVL1* is also not known exactly. However, as a control, we made sure that all the fly lines were generated in the same way and the transgenes were inserted in the same chromosomal site. The mRNA levels we showed with the qPCR results showed that this control was useful. In our western blots, we found that the expression levels of the products of $DVL1^{1519\Delta T}$ and $DVL1^{1529\Delta G}$ were higher than the wt*DVL1* product at both temperatures. The expression of the variants on the protein level might not be the same as physiological levels but this does not change the fact that the expression of the variants in this *in vivo* developmental context is highly important for the disease study.

4.2. DVL1 variant induce neomorphic phenotypes

Previously it was shown that the expression of *DVL1* variants cause neomorphic phenotypes in the adult wings such as ectopic bristles, thickening of veins and creases in the wing blade which are not induced by the expression of the wt*DVL1* (Gignac et al., 2023). Here we also showed that the expression of the variant in larger expression domains induces neomorphic adult phenotypes in the form of reduced thorax and scutellum, bent or blistered small wings and abnormally segmented legs with altered leg posture (Fig. 2.3, Fig. 2.4, Fig. 2.5, Fig. 2.6).

The signalling pathways governing *Drosophila* development are well established. Most of the adult thorax is developed from the wing disc notum and this development is governed by a balance between Wg and EGFR signalling (S. H. Wang et al., 2000; Tripathi & Irvine, 2022). Development of legs from the embryo to adult is known to be regulated by Dpp, Notch and Hh signalling pathways (Lecuit & Cohen, 1997; Córdoba et al., 2016; Heingård et al., 2019). The patterning of cross veins in the wings is dependent on BMP and Dpp signalling (Montanari et al., 2022). Many signalling pathways are involved in the shaping of bristles, one of which is the Notch signalling (Furman & Bukharina, 2011).

All these information in the literature on top of the neomorphic phenotypes induced by the variant expression strongly suggests that the variants but not the wt*DVL1* are altering other signalling pathways. The specific pathways altered by the expression of the variant requires further investigation.

4.3. DVL1 variant disrupt morphology in wing imaginal discs

After observing the adult phenotypes induced by the expression of $DVL1^{1519\Delta T}$, we also investigated the precursor tissue in larvae, namely the wing imaginal discs. We found that wing disc morphology was highly altered when the variant expression was driven with two different Gal4 drivers (Fig. 2.7, Fig. 2.8, Fig. 2.9, Fig. 2.10). Common abnormalities in the wing disc morphology were the overgrown appearance of the discs and the disrupted fold structure. In the $ap>DVL1^{1519\Delta T}$ discs, the posterior side appeared to be bending the discs basally (Fig. 2.7, Fig. 2.8). Extra folds were observed in both

apicobasal and dorsoventral axes in the *hh>DVL1*$^{1519\Delta T}$ discs in maximum projection and orthogonal views. The expression of the variant resulted in more complex and disorganized morphology of the wing imaginal discs.

As the wing imaginal disc grows, the flat epithelium of the wing disc changes and folds begin to appear at precise locations. The location and formation of these folds are regulated by multiple molecules that depend on various signalling pathways such as Wg and Jak-Stat (Johnstone et al., 2013; Sui et al., 2012; Sui & Dahmann, 2020; Villa-Cuesta et al., 2007; D. Wang et al., 2016). There are also a multitude of cellular mechanism associated with the fold formation such as the apical-basal shortening of cells, redistribution of microtubules from apical to basal side and proper degradations of the ECM locally (Sui et al., 2012; D. Wang et al., 2016). Recently, computational studies also showed that the differential growth between regions of the wing disc is also involved in fold formation (Tozluoğlu et al., 2019).

All these factors governing wing disc morphology are subject to possible alterations that might be caused by the variant expression. The pivotal role of DVL1 in Wg and non canonical/PCP signalling pathways makes it a possible candidate that induces alterations in morphology. We hypothesized that the one strong reason for the abnormal folding and overall morphology is the differential growth between the half of the wing that grows normally and the other half that shows altered growth. We think that this could induce physical tension and result in abnormal fold formation. Therefore, we investigated the cell proliferation and cell death in the wing imaginal discs.

4.4. DVL1 variant induces cell death but not proliferation

When we tested the *DVL1*$^{1519\Delta T}$ expressing wing discs for cell proliferation and cell death, we found that the variant expression significantly increases apoptosis, but no significant difference is induced in cell proliferation levels compared to wt*DVL1* expressing discs and the controls.

Programmed cell death (PCD) is a crucial part of animal development and tissue homeostasis. Abnormalities in this mechanism are associated with many developmental diseases. In *Drosophila*, PCD during development is regulated similarly to vertebrates by various stimuli from within and outside the cell (Kornbluth & White, 2005). Another

mechanism important for tissue homeostasis is the compensatory cell proliferation, which is regulated by a multitude of pathways including Dpp, JNK and Hh signalling pathways (Wells et al., 2006; Xu et al., 2009). It appears that the *DVL1*$^{1519\Delta T}$ variant expression is disrupting the balance between these two mechanisms during development by inducing cell death in higher levels in wing imaginal discs. This disruption of the highly conserved developmental processes causes abnormal tissue development as we have observed. This increased cell death also helps explain the altered mechanical tension between the parts of the wing discs that causes the abnormal basally bent appearance of the proximal side.

We also observed an increase in the curvature of the wing imaginal discs that expresses the *DVL1*$^{1519\Delta T}$ variant in the *hedgehog* domain. Computational studies on wing disc development showed that the basal curvature of the discs could be affected by the induction of growth via different pathways such as insulin signalling, which would lead to the alteration of cellular cytoskeleton and ECM (Kumar et al., 2024). In order to be able to detect the specific mechanisms *DVL1*$^{1519\Delta T}$ variant alters tissue morphology, further investigation focusing on these topics is required.

4.5. DVL1 variant alters dorso-ventral cell adhesion and basement membrane in pupal wings

Previous studies on wing tissue has shown that the overexpression of Matrix metalloproteinase-2 (Mmp2) can induce blisters that would be retained in the adult wings (Sun et al., 2021). The same study hypothesizes that the proper adhesion of the dorsal and ventral layers of the wing requires slow and controlled degradation of the basement membranes. With this logic, when the basement membrane degradation is insufficient or induced to be faster, the adhesion of the two layers will be disrupted and blister formation will be induced (Sun et al., 2021). Since previous work has previously shown Mmp1 induction in wing imaginal discs (Gignac et al., 2023), we also looked at the Mmp1 expression in the blistered wing discs that expresses the *DVL1*$^{1519\Delta T}$ variant. We found that the blisters that appears to be enlarged veins were filled with Mmp1 (Fig. 2.20). *Drosophila* Mmps (Mmp1 and Mmp2) are known to have different roles: Mmp1 mostly cleaves extracellular lateral connections between cells and Mmp2 cleaves cells from the extracellular matrix. However, studies in fruit flies have shown a functional redundancy between these two molecules (Jia et al., 2014).

In this work we showed that the basement membrane degradation is suppressed in the presence of the *DVL1*$^{1519\Delta T}$ variant (Fig. 2.21). We used Vkg-GFP as a proxy for the basement membrane in our studies, since Vkg, *Drosophila* Collagen IV is the most abundant of the four basement membrane components. It was shown that, in earlier stages of pupal wing development, Vkg is present in the distal lumen of the L3 longitudinal veins (Murray et al., 1995). Later in the pupal wing development, some of the basement membrane components including Vkg are eliminated by high levels of Mmp1 activity (De Las Heras et al., 2018). These findings were validated by comparing wing development to the haltere development in *Drosophila* (De Las Heras et al., 2018). In the light of this information and our findings, we think that the altered regulation of canonical and non-canonical Wnt signalling, as well as all the other pathways the variant expression possibly alter, the balance between Vkg and Mmp1 expression is disrupted. Even when Mmp1 expression is induced ectopically, it was not sufficient to cleave the connections together with the high abundance of the basement membrane. It seems that the inability to degrade the basement membrane in the earlier stages of pupal wing development caused an increase in the Mmp1 expression in later stages. In the adult wings, the blister is seemed to be resolved, causing just the crease phenotype when the variant is expressed in the *dpp-Gal4* domain (Gignac et al., 2023). This suggests that the high expression of *Mmp1* eventually becomes sufficient to degrade the basement membrane when the variant expression is limited. However, when the variant expression is induced in a larger domain such as the *apterous*, we found that the adult wings were blistered, and the wing blades were not extended. Further investigation by testing the pupal wings that expresses the variant with different drivers is required to explain this mechanism.

4.6. DVL1 variant causes differential expression of genes involved in various biological processes

In this thesis, I carried out RNA sequencing using the wing imaginal discs to detect differentially expressed genes that are involved in other signalling pathways. The analysis of the sequencing results led us to a large number of DEGs involved in many biological processes including wing disc and appendix morphogenesis. These results were promising with respect to gross morphological changes that we observed in the

flies. However, it was difficult to detect groups of genes involved in signalling pathways that could be associated with the expression and function of the DVL1 variant.

Previous studies have found that expression of the variant in the *apterous* domain just like the discs used for RNA sequencing induced expression of *puc-lacZ* in wing imaginal discs (Gignac et al., 2023). Due to the insertion of a *lacZ* reporter gene into the *puckered* locus, the ectopic *puc-lacZ* expression shows an induction in the *puckered* gene transcription, an established target gene of the Jnk pathway (Martin-Blanco et al., 1998). However, *puckered* was not one of the genes that was found to be significantly differentially expressed in the RNA sequencing results. Induced Mmp1 protein expression was also shown in wing imaginal discs that expresses the $DVL1^{1519\Delta T}$ variant in the *dpp-Gal4* domain (Gignac et al., 2023), but this was also not found in the sequencing analysis. The different expression domain and the fact that the alterations were found on the protein level could be an explanation for these.

We think that the batch effect might be another reason for our RNA sequencing results to be insufficient. As mentioned, the first batch of samples were sent separately from the rest, in order to make sure that our samples matched the quality control requirements. Then the rest of the larvae used for RNA extractions were grown after we obtained the quality control results. Since the crosses were not grown all together, this might have introduced a batch effect as well.

Another reason for these unexpected results we have found might be the extremely high significance levels chosen for the clustering and filtration of the data. In these processes and the many pipelines applied to the raw RNA sequencing results, some genes might have been filtered out, which made it more difficult for us to detect groups of genes that are components of different signalling pathways.

Overall, the RNA sequencing showed us that the expression of the $DVL1^{1519\Delta T}$ variant in the wing imaginal discs causes differential expression of hundreds of genes compared to both control and wt*DVL1* expressing wing discs. The analysis of sequencing results by using different methods could improve the results we obtain in this sequencing.

4.7. Role of the abnormal C-terminus in DVL1 variants

Among the RS-associated mutations in DVL1, DVL2 and DVL3, except for one *de novo* missense variant in *DVL3*, all variants carry frameshift mutations (White et al., 2015; White et al., 2016; Rai et al., 2021; Zhang et al., 2022). An analysis done by our collaborators in Richman Lab at UBC showed that just like the RS-*DVL1* variants, the novel C-terminal peptides of RS-associated *DVL3* variants have identical sequences among patients, despite the variants occurring at different positions in the gene. If the novel C-terminal peptide sequence were responsible for driving the RS phenotypes, we would expect the same sequence in frameshift mutations of both *DVL1* and *DVL3*. However, there is no homology between the C-terminal novel peptides of DVL1 and DVL3. Therefore, the specific sequence of the mutant C-terminus does not seem to be the most crucial factor.

Given the high conservation of the C-terminus across vertebrate Dishevelled proteins (Fig. 1.6C) and its known roles in ubiquitination (Angers et al., 2006), protein interactions (Witte et al., 2010; Bernatík et al., 2014), and autoinhibition (Qi et al., 2017), we investigated whether the loss of the C-terminus could cause signalling abnormalities. We did a literature search and found that, in a study that introduced a stop codon after nucleotide 1519 to remove the DVL1 C-terminus, this truncated DVL1 could still activate the Wnt reporter superTopFlash luciferase, albeit less effectively than wt*DVL1* (Bunn et al., 2015). This suggests that the absence of the C-terminus may partially reduce canonical signalling levels.

Another study showed that the PDZ binding motif (PBM) at the end of the C-terminus is crucial to keep the balance between the canonical and noncanonical Wnt signalling since it keeps DVL in an autoinhibited form which helps the protein to be regulated by other interaction partners. In this study, expression of small PDZ-binding molecules was induced to compete with the C-terminus of Xdsh itself in *Xenopus* embryos and this led to an enhanced non-canonical/PCP signalling activity (Lee et al., 2015). In a later study from the same group, only the C-terminus of Xdsh, the peptide sequence after the DEP domain expressed along with increasing amounts of Xenopus Xdsh itself, causing the forced binding of the PBM to the PDZ domain. This caused a decrease in Wnt/PCP signalling likely due to the closed formation of Xdsh caused by this interaction and this may be negatively affecting the DEP domain's interactions with its

binding partners involved in PCP signalling. On the contrary, they showed that the absence of C-terminus or blocking it's binding to the PDZ domain increased the non-canonical/PCP pathway activity. These results strongly suggested that the C-terminus of Xdsh might be involved in regulating the pathway specificity (Qi et al., 2017).

In addition to the loss of specific functions of the C-terminus, the gain of an abnormal peptide likely has a significant impact on DVL1 function. Our previous work indicated that abnormal DVL1 variants cause an imbalance in two Wnt pathways (Gignac et al., 2023). Other potential effects of the frameshift mutations include abnormal protein folding or protein-protein interactions (Lee et al., 2015; Hu et al., 2022). It should be noted that our earlier work did not show a correlation between specific variants and the severity of phenotypes, as there were only minor differences between variants, with overall trends remaining consistent. The variation in clinical phenotypes, even among patients with the same mutation, is likely due to individual genetic backgrounds (Abu-Ghname et al., 2021; Conlon et al., 2021; Schwartz et al., 2021).

Here, we showed that the lack of original human DVL1 C-terminus, in both *DVL1*^{1519*} and *DVL1*^{1431*} expressing *Drosophila* tissue, caused PCP defects. However, the reporters we used to measure the activity of both canonical and non-canonical pathways only showed alterations with expression of the *DVL1*$^{1519\Delta T}$ variant.

4.8. Role of the abnormal C-terminus in Noncanonical/PCP signalling

The expression of all transgenes, wildtype, variant and C-terminal truncated, produced hair polarity defects in adult wings (Figs. 3.2 and 3.3). This result is not a surprise since both downregulation and overexpression of *Drosophila* Dsh also induces this phenotype. In this case, major functional domains of DVL1 proteins are overexpressed along with the endogenous Dsh. It should also be noted that the *DVL1*$^{1519\Delta T}$ variant expression led to a more pronounced disorganization in the hair alignment compared to the expression of wt*DVL1*, *DVL1*^{1519*} and *DVL1*^{1431*}. Further investigation on noncanonical/Wnt signalling activity in wing imaginal disc showed that the upregulation we have shown with the expression of three RS-DVL1 variants (Gignac et al., 2023) was not induced by the expression of *DVL1*^{1519*} or *DVL1*^{1431*}. This partially fits the earlier findings in *Xenopus* with the *Xenopus* dsh, which has a more similar C-

terminus to human DVL1 than the *Drosophila* Dsh does. In that study, it was suggested that blocking the binding of PBM to PDZ domain increases the noncanonical Wnt pathway activity by making the Xdsh more available to DEP interaction partners (Qi et al., 2017).

This same study also highlights the importance of the C-terminus in keeping Dvl in an autoinhibited state which makes it accessible for regulation by other interaction partners, hence the C-terminal tagged Dishevelled fusion proteins are not ideal for the study of functional studies since it would hinder the conformational changes of the Dvl protein itself and also the interaction partners (Qi et al., 2017). This suggest that the transgene constructs we use in our study are ideal for our purposes.

This explains the induced noncanonical Wnt signalling activity shown with ectopic Mmp1 and *puc-lacZ* expression in the wing imaginal discs due to the expression of the $DVL1^{1519\Delta T}$ variant. The novel peptide sequence on the C-terminus of this variant is highly different than the original C-terminus and the structure of this peptide is not predicted to be forming a loop to bind to the PDZ domain according to AlphaFold2. This makes the PDZ domain less rigid and more available to its interaction partners. It could also be the folding of this peptide sequence that alters the interactions of the DEP domain with its partners hence increasing the noncanonical/Wnt signalling activity. With this logic, one would expect the C-terminal truncated proteins to have similar affects. However, we showed that the signalling activity was not altered even when these proteins were expressed in higher levels at 29°C. This could be due to the lower expression levels of these proteins. The other reason could be more related to the *Drosophila* Dsh itself. Since the endogenous Dsh contain similar DIX, PDZ and DEP domains but a different C-terminus compared to the human DVL1 (Fig. 1.6C), just lack of the C-terminus without the addition of a new peptide sequence in a *Drosophila* model might not be showing the similar affects since the interaction partners already are adapted to a different C-terminus.

4.9. Role of the abnormal C-terminus in Canonical Wnt signalling

In this study, we showed that the canonical/Wnt signalling activity is only altered by the expression of the *DVL1*$^{1519\Delta T}$ variant. The expression of the C-terminal truncated *DVL1*^{1519*} or *DVL1*^{1431*} constructs had the same effects as the expression of wt*DVL1.*

Our earlier work has shown that *DVL1* variants decreased canonical Wnt signalling *in vivo* during development even when the fly *Dsh* was overexpressed. Hence, RS-associated *DVL1* variants had dominant negative activity and interfered with the activity of Dsh in canonical Wnt signalling (Gignac et al., 2023).

In the *Xenopus* study mentioned earlier, researchers made a Xdsh construct that would have PDZ- binding motif that is constantly bound to the PDZ domain. This construct was shown to cause lower activity in canonical Wnt signalling by interrupting the interactions between Xdsh and Wnt coreceptor LRP6 (Qi et al., 2017). In accordance with this study, the lack of C-terminus in DVL1 is not supposed to negatively affect the canonical Wnt signalling since it provides an open conformation which would facilitate easy interactions between DVL1 and the receptors and that is what we observe with the expression of c or *DVL1*^{1431*}. We see a slightly higher ratio in β-catenin levels with the expression of *DVL1*^{1519*} or *DVL1*^{1431*} compared to the wt*DVL1* but the statistical analysis showed no significance. The lower canonical Wnt signalling activity caused by the *DVL1*$^{1519\Delta T}$ variant could be due to the structural conformation of the novel C-terminal peptide that could be causing a hindrance in the DVL1-LRP6 interactions that is similar to the constantly bound PBM and PDZ.

In the light of these results, the novel peptide sequence conformation seems to affect DVL1's function in noncanonical Wnt/PCP pathway positively and canonical Wnt signalling negatively. Further studies on these signalling interactions and the novel peptide sequence conformation are needed.

4.10. Role of the original DVL1 C-terminus in RS and normal development

In this study we found that the lack of both the full C-terminus (peptide after the DEP domain of DVL1) and the sequence missing in the DVL1$^{1519\Delta T}$ variant did not cause

any abnormalities during development. This suggested that the looping back of the PBM to bind the PDZ and autoinhibit the DVL1 protein is not critical for DVL1 function during development.

Our collaborators in Richman Lab had similar findings for *DVL1*^{1519*}. However, when they injected the *DVL1*^{1431*} construct into developing chick embryos, they got more severe craniofacial phenotypes than the RS variants and the *DVL1*^{1519*}. They found that the lack of a full C-terminus profoundly disrupted normal chicken embryo development, potentially through the interference with the endogenous DVL1 gene. It could also be due to the disruption of the nuclear export sequence in the product of the *DVL1*^{1431*} construct. By transfecting triple knockout HEK293 cells that lack all three human *DVL* paralogs, they showed that the localization of DVL1^{1431*} and DVL1$^{1519\Delta T}$ were nuclear in 80% of the cells. It is surprising considering that the 30 amino acid sequence that contains the NES is retained in the variant protein. This data also suggested that the abnormal C-terminus might be influencing the function of the protein and the development of the organism due to the tertiary structure of the novel peptide sequence (Tophkhane, Gignac, et al., 2024).

The different results we get might be due to the genetic background of the animal models and how the endogenous proteins interact with the transgenes expressed. Modelling a human skeletal disorder in an invertebrate model can be challenging in terms of the phenotypes observed hence our collaboration with the Richman is valuable to overcome this obstacle. We need further investigation of the fly Dsh interaction partners and how they can interact with human DVL1 proteins. Deciphering the tertiary structure of the novel peptide sequence of RS-associated DVL1 variants is also necessary for a better understanding of the mechanistic.

4.11. Limitations of the study

In this study, we expressed human genes and alleles on top of the endogenous *Drosophila* genome. We managed to express the transgenes above physiological levels. However, when the expression of the variant was driven ubiquitously like the RS patients, using drivers such as *Act5C-Gal4*, the flies did not survive (data not shown). Hence, we had to proceed by targeting the expression of our transgenes to specific

regions by using specific drivers. Using this method helps us with tightly controlling the levels of transgene overexpression.

It should also be noted that RS is a rare genetic disease that mostly affects the skeleton in humans. *Drosophila* does not have a skeleton that we could investigate, hence we were limited to investigating cellular mechanisms or appendage and wing development. Our collaboration with the Richman Lab that studied the same variant in the chicken embryo helped us overcome this limitation. While we provided a genetic and signalling model for this work, their studies in chicken embryos provided a great model for skeletal development.

4.12. Future directions

As discussed, many aspects of the wing imaginal disc, pupal wing and adult tissue morphology could be further investigated. Some of these that of primary interest could be listed as follows:

- Investigating the possible alterations in the components of cytoskeleton in wing imaginal discs that expresses wt*DVL1* and $DVL1^{1519\Delta T}$
- Investigating the disruption of dorsoventral adhesion and the abnormal degradation of the basement membrane induced by the expression of $DVL1^{1519\Delta T}$ variant in pupal wings at multiple earlier and later pupal stages
- Re-analysis of the RNA sequencing results based on our findings in *Drosophila* tissue
- Validating the expression of differentially expressed genes in the presence of $DVL1^{1519\Delta T}$ variant via qRT-PCR

The C-terminal truncated proteins do not have physiological relevance in terms of the protein structure; however, they can be used as tools for the further investigation of DVL1 C-terminus. Possible future directions for this part of our studies can be listed as follows:

- Investigation of the subcellular localizations of both $DVL1^{1519*}$ or $DVL1^{1431*}$ in *Drosophila* model system in order to learn more information regarding the

function and location of NES and its interactions with the rest of the C-terminus

- Generating a C-terminal truncated DVL1 protein only lacking the PDZ-B motif for the investigation of its function and interaction partners

- Computational investigation of the possible interaction partners of the DVL1 C-terminus with endogenous *Drosophila* proteins

4.13. Conclusions

This research provided insights into the morphological alterations induced by the autosomal dominant RS-associated DVL1 mutations. Our work builds on the previous work that showed the imbalance between canonical and non-canonical Wnt signalling induced by the expression of *DVL1* variant and suggests multiple biological processes affected by the RS-associated mutations in *DVL1* gene (Gignac et al., 2023). We provided further evidence of the neomorphic activity of the *DVL1* variant disrupting normal development of wing imaginal discs, pupal wings and adult tissues. We showed that the expression of $DVL1^{1519\Delta T}$ variant alters the transcriptome of wing disc epithelial cells. Our study provides further insights into the underlying mechanistic of RS by showing the abnormal activity of DVL1 variant in a developmental context *in vivo*.

The part of the study presented in Chapter 3 provided molecular insight into how the novel peptide sequence in RS-DVL1 variants is the cause of the altered morphology and the signalling abnormalities in the fruit fly model. DVL1 is the most mutated gene in autosomal dominant RS cases reported and the abnormal C-terminus is found in all 18 frameshifted DVL1 variants (Zhang et al., 2022). Considering the pathogenicity of these mutations and our findings together, we can conclude that disease-causing alterations are due to the presence of the novel peptide sequence at the C-terminus of DVL1, a key signalling molecule that establishes a balance between canonical and noncanonical Wnt signalling pathways. Our work here provided evidence that the neomorphic activity of DVL1 variants are not caused by the lack of the original C-terminus of human DVL1 that is highly conserved among vertebrates.

Chapter 5. Materials and Methods

5.1. Generation of transgenes DVL1 fly stocks

The transgenes were generated by the Richman Lab at the University of British Columbia. The open reading frame encoding human DVL1 was purchased from Origene (#RC217691). The insert was initially in a pCMV6 vector containing a full coding sequence with two C-terminal tags: myc and DDK (Flag similar). To change pCMV6 vector to an entry clone (pDONR221), gateway cloning with BP clonase II (ThermoFisher #11789020) was performed. Then restriction free cloning was used to insert kozak- N-terminal flag (DYKDDDDK) sequence and 3' C-terminal STOP (added to eliminate commercial tags from company) to this pDONR221 vector. Site-directed mutagenesis was performed in the pDONR221 (Gateway compatible) vector and then recombined into destination vectors (pcDNA3.2 expression vector and RCAS retroviral vector) using LR Clonase II enzyme (ThermoFisher # 11791019) (Bond & Naus, 2012; Loftus et al., 2001). Gateway cloning (ThermoFisher) was used to move human *DVL1* into the pDONR221. Site-directed mutagenesis was used to knock-in the mutations. Autosomal dominant RS *DVL1* frameshift mutation (OMIM: 616331) was knocked in (*DVL1*$^{1519\Delta T}$) (White et al., 2015). Two additional *DVL1* constructs were made for this study - either a STOP codon was placed immediately after amino acid W507* (*DVL1*^{1519*}) or the entire C-terminus was prevented from being expressed by placing a stop codon after the DEP domain at amino acid 477 and before the DVL1 C-terminus to generate *DVL1*$^{1431*.}$ The plasmids were cloned into the *Drosophila* pUASg_attB_Gateway vector. These Flag-tagged wild-type, variant and C-terminal truncated DVL1 constructs were sent to BestGene Inc., California for integration into the attP40 locus on the second chromosome for the generation of stably integrated fly strains.

5.2. *Drosophila* Husbandry

Flies were raised on standard media. Stocks were kept at room temperature (~22°C) and crosses were performed at 25°C or 29°C as indicated. Three Gal4 driver fly lines were used to induce transgene expression: *dpp-Gal4, UAS-GFP* /TM6B (Swarup et al., 2015), *Dll-lacZ/Cyo; Hh-Gal4/TM6B* (Hall et al., 2017)*, apterous (ap)-Gal4* (Bloomington #3041). Additional stocks used were: *;vkg-GFP;* (Flytrap) (Blaquiere et al.,

2018), *puc-LacZ* (Martin-Blanco et al., 1998), w^{1118}, *UAS-GFP*, *UAS-myr-RFP* (Bloomington #7118).

5.3. Dissections

5.3.1. Salivary glands

Salivary glands were dissected out of third instar larvae in cold phosphate-buffered saline (PBS). Larval heads were separated from the body and flipped to expose the internal tissues. Fat tissue and the guts were removed while leaving the salivary glands attached to the cuticle.

5.3.2. Wing imaginal discs

Third instar larval wing imaginal discs were dissected out of larvae in cold PBS. The top half of the larvae were separated and flipped inside out to expose the imaginal discs. Fat tissue and the guts were removed while leaving the imaginal tissue attached to the cuticle.

5.3.3. Pupal wings

Pupal wings were dissected as described by Bolatto and coworkers (Bolatto et al., 2017) with some modifications. 0hr APF pupae were collected and placed ventral side down onto a microscope slide covered with double-sided tape. The microscope slides were placed at 25°C until the desired stage of development. Pupal cases were opened with forceps and naked pupae were transferred onto a new microscope slide with double-sided tape and covered with 4% paraformaldehyde (PFA) in PBS. After a 30-minute incubation, pupal wings were dissected out and placed into a 4% PFA filled well of an HLA plate for an additional 15-minute incubation. All immunofluorescence experiments with pupal wings were performed in Greiner HLA Terasaki multiwell (54-well) plates rather than Eppendorf tubes.

5.3.4. Adult wings

Adult flies of the target genotype were collected in small glass vials filled with 70% ethanol. The wings were dissected using forceps in 95% ethanol in dissection dishes and mounted immediately. Aquatex (EMD Chemicals) was used as mounting media. The slides were baked overnight at 65°C incubator with small weights on them.

5.4. Immunofluorescence staining, microscopy, and image processing

Tissue was dissected in phosphate-buffered saline (PBS) and fixed in 4% PFA at room temperature for 15 minutes. Samples were washed twice for 10 minutes with PBS with 0.1% Triton X-100 (PBS-T). Following a 1-hour block with 5% bovine serum albumin diluted in PBST at room temperature, samples were incubated overnight with primary antibodies at 4°C. The following primary antibodies were used:

Table 5.1. List of primary antibodies used in this study

Antibody	Dilution	Clone	Distributor
Mouse anti-FLAG	1:500	M2	Sigma
Rabbit anti-FLAG	1:500	SIG1-25	Sigma
Rabbit anti-Dcp1	1:500	Asp215	Cell Signaling
Rabbit anti-PH3 Ser10	1:500	D2C8	Cell Signaling
Mouse anti-Armadillo	1:50	N2 7A1	DSHB
Mouse anti-β-Galactosidase	1:50	40-1a	DSHB
Rabbit-anti-GFP	1:500	A-11122	Thermo Fisher
Mouse anti-Mmp1	1:100 (each)	3A6B4 3B8D12 5H7B11	DSHB

Samples were washed twice for 10 minutes with PBS-T (0.5% Triton-X100 in PBS) and incubated with Cy3 and/or Alexa Fluor 647-conjugated secondary antibody (1:500, Jackson ImmunoResearch Laboratories), DAPI (4',6-Diamidino-2-Phenylindole) or Rhodamine Phalloidin (Invitrogen™ R415). for 2 hr at room temperature. After two 10-minute washes, samples were mounted in 70% Glycerol in PBS or VECTASHIELD® Antifade Mounting Medium (Vector Labs) and imaged using a Nikon Air laser-scanning confocal microscope or a Zeiss LSM880 with Airyscan confocal microscope. Images

were processed with ImageJ, FIJI software (Schindelin et al., 2012; Schneider et al., 2012) and are presented as Z-stack maximum intensity projections unless otherwise stated.

5.5. Quantification of cell death and cell proliferation using Dcp1 and PH3 staining

After completing the staining and mounting steps, wing imaginal discs were imaged as described in the previous section. Using FIJI (Schindelin et al., 2012), the *ap-GFP* or *hh-Gal4* domains on wing imaginal discs were marked. PH3 or Dcp1 positive cells were counted within each region automatically using the Analyze → Analyze Particles tool after thresholding. The difference between the number of PH3 or Dcp1 puncta within the *apterous* or *hedgehog* domains were then plotted.

5.6. Quantification of Armadillo protein levels

Imaginal wing discs were subjected to the immunofluorescence protocol described above. Following imaging, maximum projection images were processed with FIJI software (Schindelin et al., 2012). Using a box of identical dimensions, mean Arm signal intensity was quantified inside and outside of the transgene expression domain either on the most stabilized stripes of Arm protein or slightly above them as indicated. The ratio of signal inside/outside Arm signal was used to determine loss or gain or Arm levels within the transgene expression domain.

5.7. Western Blots on *Drosophila* salivary glands

Drosophila salivary glands were used for western blots due to the increased yield of protein compared to imaginal discs. Due to DVL1 protein instability in lysis buffer, salivary glands had to be dissected immediately before western blots were performed. Thus, salivary glands were dissected and lysed by vortexing samples for 30 seconds in 1x SDS sample buffer. Samples were then boiled for 5-10 minutes and then resolved on 10-12% SDS/PAGE gels before being transferred to nitrocellulose membranes. Following the transfer, membranes were blocked in 5% skimmed milk in TBS-T and then incubated with primary and secondary antibodies. The following primary antibodies were used: (1) mouse anti-FLAG (1:1000, Sigma M2), (2) mouse anti-β-tubulin (1:1000,

Abcam G098). Anti-mouse HRP (1:5000, Jackson ImmunoResearch Laboratories) secondary antibody was used. Membranes were visualized using ClarityTM Western enhanced chemiluminescence (ECL) Substrate (BIO-RAD 170-5061), imaged on a GE AI 600 Imager and band density/protein levels were determined with FIJI software (Schindelin et al., 2012).

5.8. Protein lysate preparation from larval heads and Western blotting

Five late L3 developmentally stage-matched larval heads (with attached imaginal discs) were dissected and lysed with a 100 µl solution of 1× Cell Lysis Buffer (Cell Signaling Technology), supplemented with 1× Protease Inhibitors (Roche), 1 mM phenylmethylsulfonyl fluoride (PMSF) and 1 mM sodium fluoride (NaF). The tissues were mechanically homogenized and vortexed for 30 seconds. Lysates obtained after centrifugation for 10 min were mixed with 30 µl of 4X Laemmli buffer and the tubes were kept in boiling water for five minutes. The protein extracts were kept at –20°C until used for western blotting. The blots were run as described in the previous section.

5.9. RNA extraction for qRT-PCR

RNA extractions were performed using the Qiagen RNeasy® Plus Mini Kit (#74134). Larval heads from five female larvae were dissected in PBS before being spot dried on a clean KimWipe and transferred to 350 µl buffer RLT Plus, supplemented with freshly added β-mercaptoethanol to 1%. Larvae were homogenized by vortexing in 1.5 mL tubes before being centrifuged for three min at maximum speed to pellet debris. Supernatant was transferred to a gDNA Eliminator spin column, with the remaining RNA extraction steps following the manufacturer's instructions.

5.10. RNA extraction for RNA-seq

RNA extractions were performed again by using the Qiagen RNeasy® Plus Mini Kit (#74134). Six pairs of wing imaginal discs from six female larvae were dissected in PBS for the extraction. The rest of the extraction was done as described in the previous section. The cDNA synthesis and the library preparation followed by the sequencing

were all done at the School of Biomedical Engineering (SBME) Sequencing Core at the Biomedical Research Center (BRC) at University of British Columbia.

5.11. cDNA synthesis and qRT-PCR

cDNA synthesis was performed using ABM® OneScript® Plus cDNA Synthesis Kit (#G236). For each sample, 100 ng mRNA was used in combination with Oligo (dT) primers to perform first-strand cDNA synthesis of poly-adenylated mRNA following manufacturer's instructions. Resulting cDNA was diluted 1:10 before being used for qPCR.

qPCR for each sample/primer mix was performed in triplicate with 10 µl samples (technical replicates), utilizing Bioline's sensiFAST SYBR Lo-ROX Kit (#BIO-94005) on an Applied Biosystems QuantStudio 3. One microliter of diluted cDNA was used per reaction. Primers targeting *rp49* and *GAPDH2* were used as reference targets. *DVL1* primers used in this study were designed by Richman Lab within exon 7 of the coding sequence: *DVL1* Fwd: 5′-CAGCATAACCGACTCCACC-3′; *DVL1* Rev: 5′-TGATGCCCAGAAAGTGATGTC-3′

5.12. Statistical analyses

Statistical analyses of the plotted data of mRNA and protein expression were done using one-way analysis of variance (ANOVA). For immunofluorescence experiments, paired (Arm stability within 1 wing disc) or unpaired (all other experiments) t-tests were performed to determine p-values. All statistical analyses were performed using GraphPad Prism 9.3.1 (GraphPad Software, San Diego, USA). Analyzed data with $p<0.05$ was considered statistically significant. Significance depicted as *$p < 0.05$, **$p < 0.01$, ***$p < 0.001$, ****$p < 0.0001$, ns = not significant.

References

Abu-Ghname, A., Trost, J., Davis, M. J., Sutton, V. R., Zhang, C., Guillen, D. E., Carvalho, C. M. B., & Maricevich, R. S. (2021). Extremity anomalies associated with Robinow syndrome. *American Journal of Medical Genetics. Part A*, *185*(12), 3584–3592. https://doi.org/10.1002/ajmg.a.61884

Adams, M. D., Celniker, S. E., Holt, R. A., Evans, C. A., Gocayne, J. D., Amanatides, P. G., Scherer, S. E., Li, P. W., Hoskins, R. A., Galle, R. F., George, R. A., Lewis, S. E., Richards, S., Ashburner, M., Henderson, S. N., Sutton, G. G., Wortman, J. R., Yandell, M. D., Zhang, Q., … Venter, J. C. (2000). The Genome Sequence of Drosophila melanogaster. *Science*, *287*(5461), 2185–2195. https://doi.org/10.1126/science.287.5461.2185

Adler, P. N. (2002). Planar signaling and morphogenesis in Drosophila. *Developmental Cell*, *2*(5), 525–535. https://doi.org/10.1016/s1534-5807(02)00176-4

Aldaz, S., & Escudero, L. M. (2010). Imaginal discs. *Current Biology*, *20*(10), Article 10. https://doi.org/10.1016/j.cub.2010.03.010

Aldaz, S., Escudero, L. M., & Freeman, M. (2010). Live imaging of Drosophila imaginal disc development. *Proceedings of the National Academy of Sciences of the United States of America*, *107*(32), 14217–14222. https://doi.org/10.1073/pnas.1008623107

Amin, N., & Vincan, E. (2012). The Wnt signaling pathways and cell adhesion. *Frontiers in Bioscience (Landmark Edition)*, *17*(2), 784–804. https://doi.org/10.2741/3957

Angers, S., Thorpe, C. J., Biechele, T. L., Goldenberg, S. J., Zheng, N., MacCoss, M. J., & Moon, R. T. (2006). The KLHL12–Cullin-3 ubiquitin ligase negatively regulates the Wnt–β-catenin pathway by targeting Dishevelled for degradation. *Nature Cell Biology*, *8*(4), 348–357. https://doi.org/10.1038/ncb1381

Ashburner, M., Ball, C. A., Blake, J. A., Botstein, D., Butler, H., Cherry, J. M., Davis, A. P., Dolinski, K., Dwight, S. S., Eppig, J. T., Harris, M. A., Hill, D. P., Issel-Tarver, L., Kasarskis, A., Lewis, S., Matese, J. C., Richardson, J. E., Ringwald, M., Rubin, G. M., & Sherlock, G. (2000). Gene Ontology: Tool for the unification of biology. *Nature Genetics*, *25*(1), 25–29. https://doi.org/10.1038/75556

Avidor-Reiss, T., Maer, A. M., Koundakjian, E., Polyanovsky, A., Keil, T., Subramaniam, S., & Zuker, C. S. (2004). Decoding Cilia Function: Defining Specialized Genes Required for Compartmentalized Cilia Biogenesis. *Cell*, *117*(4), 527–539. https://doi.org/10.1016/S0092-8674(04)00412-X

Axelrod, J. D., Miller, J. R., Shulman, J. M., Moon, R. T., & Perrimon, N. (1998). Differential recruitment of Dishevelled provides signaling specificity in the planar cell polarity and Wingless signaling pathways. *Genes Dev*, *12*(16), Article 16.

Baker, N. E. (1987). Molecular cloning of sequences from wingless, a segment polarity gene in Drosophila: The spatial distribution of a transcript in embryos. *EMBO J*, *6*(6), Article 6.

Balmer, S., Dussert, A., Collu, G. M., Benitez, E., Iomini, C., & Mlodzik, M. (2015). Components of Intraflagellar Transport complex A (IFT-A) function independently of the cilium to regulate canonical Wnt signaling in Drosophila. *Developmental Cell*, *34*(6), 705–718. https://doi.org/10.1016/j.devcel.2015.07.016

Bate, M., & Arias, A. M. (1991). The embryonic origin of imaginal discs in Drosophila. *Development*, *112*(3), 755–761. https://doi.org/10.1242/dev.112.3.755

Behrens, J., von Kries, J. P., Kühl, M., Bruhn, L., Wedlich, D., Grosschedl, R., & Birchmeier, W. (1996). Functional interaction of beta-catenin with the transcription factor LEF-1. *Nature*, *382*(6592), 638–642. https://doi.org/10.1038/382638a0

Beiraghi, S., Leon-Salazar, V., Larson, B. E., John, M. T., Cunningham, M. L., Petryk, A., & Lohr, J. L. (2011). Craniofacial and intraoral phenotype of Robinow syndrome forms. *Clinical Genetics*, *80*(1), 15–24. https://doi.org/10.1111/j.1399-0004.2011.01683.x

Bellen, H. J., Tong, C., & Tsuda, H. (2010). 100 years of Drosophila research and its impact on vertebrate neuroscience: A history lesson for the future. *Nature Reviews. Neuroscience*, *11*(7), 514–522. https://doi.org/10.1038/nrn2839

Bernatík, O., Šedová, K., Schille, C., Ganji, R. S., Červenka, I., Trantírek, L., Schambony, A., Zdráhal, Z., & Bryja, V. (2014). Functional Analysis of Dishevelled-3 Phosphorylation Identifies Distinct Mechanisms Driven by Casein Kinase 1ϵ and Frizzled5. *The Journal of Biological Chemistry*, *289*(34), 23520–23533. https://doi.org/10.1074/jbc.M114.590638

Bienz, M. (2014). Signalosome assembly by domains undergoing dynamic head-to-tail polymerization. *Trends in Biochemical Sciences*, *39*(10), 487–495. https://doi.org/10.1016/j.tibs.2014.08.006

Bier, E. (2005). Drosophila, the golden bug, emerges as a tool for human genetics. *Nat Rev Genet*, *6*(1), Article 1. https://doi.org/10.1038/nrg1503

Blair, S. S. (2007). Wing vein patterning in Drosophila and the analysis of intercellular signaling. *Annu Rev Cell Dev Biol*, *23*, 293–319.

Blaquiere, J. A., Wong, K. K. L., Kinsey, S. D., Wu, J., & Verheyen, E. M. (2018). Homeodomain-interacting protein kinase promotes tumorigenesis and metastatic cell behavior. *Disease Models & Mechanisms*, *11*(1), dmm031146. https://doi.org/10.1242/dmm.031146

Bolatto, C., Parada, C., & Colmenares, V. (2017). A Rapid and Efficient Method to Dissect Pupal Wings of Drosophila Suitable for Immunodetections or PCR Assays. *Journal of Visualized Experiments : JoVE*, *130*, 55854. https://doi.org/10.3791/55854

Bond, S. R., & Naus, C. C. (2012). RF-Cloning.org: An online tool for the design of restriction-free cloning projects. *Nucleic Acids Research*, *40*(Web Server issue), W209–W213. https://doi.org/10.1093/nar/gks396

Boutros, M., & Mlodzik, M. (1999). Dishevelled: At the crossroads of divergent intracellular signaling pathways. *Mech Dev*, *83*(1–2), Article 1–2.

Boutros, M., Paricio, N., Strutt, D. I., & Mlodzik, M. (1998). Dishevelled activates JNK and discriminates between JNK pathways in planar polarity and wingless signaling. *Cell*, *94*(1), Article 1.

Brand, A. H., & Perrimon, N. (1993). Targeted gene expression as a means of altering cell fates and generating dominant phenotypes. *Development (Cambridge, England)*, *118*(2), 401–415. https://doi.org/10.1242/dev.118.2.401

Brown, M. S., & Goldstein, J. L. (1984). How LDL Receptors Influence Cholesterol and Atherosclerosis. *Scientific American*, *251*(5), 58–66. https://doi.org/10.1038/scientificamerican1184-58

Bunn, K. J., Daniel, P., Rösken, H. S., O'Neill, A. C., Cameron-Christie, S. R., Morgan, T., Brunner, H. G., Lai, A., Kunst, H. P. M., Markie, D. M., & Robertson, S. P. (2015). Mutations in DVL1 Cause an Osteosclerotic Form of Robinow Syndrome. *American Journal of Human Genetics*, *96*(4), 623–630. https://doi.org/10.1016/j.ajhg.2015.02.010

Butler, M. J., Jacobsen, T. L., Cain, D. M., Jarman, M. G., Hubank, M., Whittle, J. R. S., Phillips, R., & Simcox, A. (2003). Discovery of genes with highly restricted expression patterns in the Drosophila wing disc using DNA oligonucleotide microarrays. *Development (Cambridge, England)*, *130*(4), 659–670. https://doi.org/10.1242/dev.00293

Capelluto, D. G. S., Kutateladze, T. G., Habas, R., Finkielstein, C. V., He, X., & Overduin, M. (2002). The DIX domain targets dishevelled to actin stress fibres and vesicular membranes. *Nature*, *419*(6908), 726–729. https://doi.org/10.1038/nature01056

Capelluto, D. G. S., & Overduin, M. (2005). Secondary Structure,1H, 13C and15N Resonance Assignments and Molecular Interactions of the Dishevelled DIX Domain. *Journal of Biochemistry and Molecular Biology*, *38*(2), 243–247.

Chae, J., Kim, M.-J., Goo, J. H., Collier, S., Gubb, D., Charlton, J., Adler, P. N., & Park, W. J. (1999). The Drosophila tissue polarity gene starry night encodes a member of the protocadherin family. *Development*, *126*(23), 5421–5429. https://doi.org/10.1242/dev.126.23.5421

Chanet, S., Sharan, R., Khan, Z., & Martin, A. C. (2017). Myosin 2-Induced Mitotic Rounding Enables Columnar Epithelial Cells to Interpret Cortical Spindle Positioning Cues. *Current Biology: CB*, *27*(21), 3350-3358.e3. https://doi.org/10.1016/j.cub.2017.09.039

Chien, S., Reiter, L. T., Bier, E., & Gribskov, M. (2002). Homophila: Human disease gene cognates in Drosophila. *Nucleic Acids Research*, *30*(1), 149–151. https://doi.org/10.1093/nar/30.1.149

Classen, A.-K., Anderson, K. I., Marois, E., & Eaton, S. (2005). Hexagonal Packing of Drosophila Wing Epithelial Cells by the Planar Cell Polarity Pathway. *Developmental Cell*, *9*(6), 805–817. https://doi.org/10.1016/j.devcel.2005.10.016

Cohen, B., Simcox, A. A., & Cohen, S. M. (1993). Allocation of the thoracic imaginal primordia in the Drosophila embryo. *Development*, *117*(2), 597–608. https://doi.org/10.1242/dev.117.2.597

Conlon, C. J., Abu-Ghname, A., Raghuram, A. C., Davis, M. J., Guillen, D. E., Sutton, V. R., Carvalho, C. M. B., & Maricevich, R. S. (2021). Craniofacial phenotypes associated with Robinow syndrome. *American Journal of Medical Genetics Part A*, *185*(12), 3606–3612. https://doi.org/10.1002/ajmg.a.61986

Cooper, G. M. (2000). Signaling Molecules and Their Receptors. In *The Cell: A Molecular Approach. 2nd edition*. Sinauer Associates. https://www.ncbi.nlm.nih.gov/books/NBK9924/

Córdoba, S., Requena, D., Jory, A., Saiz, A., & Estella, C. (2016). The evolutionarily conserved transcription factor Sp1 controls appendage growth through Notch signaling. *Development*, *143*(19), 3623–3631. https://doi.org/10.1242/dev.138735

Dai, J., Estrada, B., Jacobs, S., Sánchez-Sánchez, B. J., Tang, J., Ma, M., Magadán-Corpas, P., Pastor-Pareja, J. C., & Martín-Bermudo, M. D. (2018). Dissection of Nidogen function in Drosophila reveals tissue-specific mechanisms of basement membrane assembly. *PLOS Genetics*, *14*(9), e1007483. https://doi.org/10.1371/journal.pgen.1007483

De Las Heras, J. M., García-Cortés, C., Foronda, D., Pastor-Pareja, J. C., Shashidhara, L. S., & Sánchez-Herrero, E. (2018). The Drosophila Hox gene Ultrabithorax controls appendage shape by regulating extracellular matrix dynamics. *Development (Cambridge, England)*, *145*(13), dev161844. https://doi.org/10.1242/dev.161844

Diaz de la Loza, M. C., & Thompson, B. J. (2017). Forces shaping the *Drosophila* wing. *Mechanisms of Development*, *144*, 23–32. https://doi.org/10.1016/j.mod.2016.10.003

Diaz-de-la-Loza, M.-D.-C., Ray, R. P., Ganguly, P. S., Alt, S., Davis, J. R., Hoppe, A., Tapon, N., Salbreux, G., & Thompson, B. J. (2018). Apical and Basal Matrix Remodeling Control Epithelial Morphogenesis. *Developmental Cell*, *46*(1), 23-39.e5. https://doi.org/10.1016/j.devcel.2018.06.006

Duffy, J. B. (2002). GAL4 system in Drosophila: A fly geneticist's Swiss army knife. *Genesis*, *34*(1–2), Article 1–2. https://doi.org/10.1002/gene.10150

Dugger, S. A., Platt, A., & Goldstein, D. B. (2018). Drug development in the era of precision medicine. *Nature Reviews Drug Discovery*, *17*(3), 183–196. https://doi.org/10.1038/nrd.2017.226

Eaton, S., Wepf, R., & Simons, K. (1996). Roles for Rac1 and Cdc42 in planar polarization and hair outgrowth in the wing of Drosophila. *Journal of Cell Biology*, *135*(5), 1277–1289. https://doi.org/10.1083/jcb.135.5.1277

Ehebauer, M. T., & Arias, A. M. (2009). The structural and functional determinants of the Axin and Dishevelled DIX domains. *BMC Structural Biology*, *9*, 70. https://doi.org/10.1186/1472-6807-9-70

Etheridge, S. L., Ray, S., Li, S., Hamblet, N. S., Lijam, N., Tsang, M., Greer, J., Kardos, N., Wang, J., Sussman, D. J., Chen, P., & Wynshaw-Boris, A. (2008). Murine dishevelled 3 functions in redundant pathways with dishevelled 1 and 2 in normal cardiac outflow tract, cochlea, and neural tube development. *PLoS Genetics*, *4*(11), e1000259. https://doi.org/10.1371/journal.pgen.1000259

Fahmy, O. G., & Fahmy, M. J. (1959a). Complementation Among the Sub-Genic Mutants in the r-Locus of Drosophila Melanogaster. *Nature*, *184*(4703), 1927–1929. https://doi.org/10.1038/1841927a0

Fahmy, O. G., & Fahmy, M. J. (1959b). Differential Gene Response to Mutagens in Drosophila Melanogaster. *Genetics*, *44*(6), 1149–1171.

Farrell, R. E. (2017). Chapter 6—Quality Control for RNA Preparations. In R. E. Farrell (Ed.), *RNA Methodologies (Fifth Edition)* (pp. 167–185). Academic Press. https://doi.org/10.1016/B978-0-12-804678-4.00006-3

Feiguin, F., Hannus, M., Mlodzik, M., & Eaton, S. (2001). The ankyrin repeat protein Diego mediates Frizzled-dependent planar polarization. *Developmental Cell*, *1*(1), 93–101. https://doi.org/10.1016/s1534-5807(01)00010-7

Fristrom, D., Wilcox, M., & Fristrom, J. (1993). The distribution of PS integrins, laminin A and F-actin during key stages in Drosophila wing development. *Development*, *117*(2), Article 2.

Furman, D. P., & Bukharina, T. A. (2011). Drosophila mechanoreceptors as a model for studying asymmetric cell division. *The International Journal of Developmental Biology*, *55*(2), Article 2. https://doi.org/10.1387/ijdb.103129df

Gajos-Michniewicz, A., & Czyz, M. (2020). WNT Signaling in Melanoma. *International Journal of Molecular Sciences*, *21*(14), Article 14. https://doi.org/10.3390/ijms21144852

Gammons, M. V., Renko, M., Johnson, C. M., Rutherford, T. J., & Bienz, M. (2016). Wnt Signalosome Assembly by DEP Domain Swapping of Dishevelled. *Molecular Cell*, *64*(1), 92–104. https://doi.org/10.1016/j.molcel.2016.08.026

Gan, X., Wang, J., Xi, Y., Wu, Z., Li, Y., & Li, L. (2008). Nuclear Dvl, c-Jun, β-catenin, and TCF form a complex leading to stabiLization of β-catenin–TCF interaction. *The Journal of Cell Biology*, *180*(6), 1087–1100. https://doi.org/10.1083/jcb.200710050

Gao, C., & Chen, Y.-G. (2010). Dishevelled: The hub of Wnt signaling. *Cellular Signalling*, *22*(5), 717–727. https://doi.org/10.1016/j.cellsig.2009.11.021

Gautam, N. (1999). Defects in Signal Transduction Proteins Leading to Disease. In A. Sitaramayya (Ed.), *Introduction to Cellular Signal Transduction* (pp. 267–285). Birkhäuser. https://doi.org/10.1007/978-1-4612-1990-3_11

Gignac, S. J., MacCharles, K. R., Fu, K., Bonaparte, K., Akarsu, G., Barrett, T. W., Verheyen, E. M., & Richman, J. M. (2023). Mechanistic studies in Drosophila and chicken give new insights into functions of DVL1 in dominant Robinow syndrome. *Disease Models & Mechanisms*, *16*(4), dmm049844. https://doi.org/10.1242/dmm.049844

Goold, R. G., Owen, R., & Gordon-Weeks, P. R. (1999). Glycogen synthase kinase 3beta phosphorylation of microtubule-associated protein 1B regulates the stability of microtubules in growth cones. *Journal of Cell Science*, *112 (Pt 19)*, 3373–3384. https://doi.org/10.1242/jcs.112.19.3373

Grandy, D., Shan, J., Zhang, X., Rao, S., Akunuru, S., Li, H., Zhang, Y., Alpatov, I., Zhang, X. A., Lang, R. A., Shi, D.-L., & Zheng, J. J. (2009). Discovery and Characterization of a Small Molecule Inhibitor of the PDZ Domain of Dishevelled. *The Journal of Biological Chemistry*, *284*(24), 16256–16263. https://doi.org/10.1074/jbc.M109.009647

Grumolato, L., Liu, G., Mong, P., Mudbhary, R., Biswas, R., Arroyave, R., Vijayakumar, S., Economides, A. N., & Aaronson, S. A. (2010). Canonical and noncanonical Wnts use a common mechanism to activate completely unrelated coreceptors. *Genes & Development*, *24*(22), 2517–2530. https://doi.org/10.1101/gad.1957710

Gubb, D., & García-Bellido, A. (1982). A genetic analysis of the determination of cuticular polarity during development in Drosophila melanogaster. *Development*, *68*(1), 37–57. https://doi.org/10.1242/dev.68.1.37

Gui, J., Huang, Y., Montanari, M., Toddie-Moore, D., Kikushima, K., Nix, S., Ishimoto, Y., & Shimmi, O. (2019). Coupling between dynamic 3D tissue architecture and BMP morphogen signaling during Drosophila wing morphogenesis. *Proceedings of the National Academy of Sciences*, *116*(10), 4352–4361. https://doi.org/10.1073/pnas.1815427116

Habas, R., & Dawid, I. B. (2005). Dishevelled and Wnt signaling: Is the nucleus the final frontier? *Journal of Biology*, *4*(1), 2. https://doi.org/10.1186/jbiol22

Habas, R., Dawid, I. B., & He, X. (2003). Coactivation of Rac and Rho by Wnt/Frizzled signaling is required for vertebrate gastrulation. *Genes & Development*, *17*(2), 295–309. https://doi.org/10.1101/gad.1022203

Habas, R., Kato, Y., & He, X. (2001). Wnt/Frizzled activation of Rho regulates vertebrate gastrulation and requires a novel Formin homology protein Daam1. *Cell*, *107*(7), 843–854. https://doi.org/10.1016/s0092-8674(01)00614-6

Hall, E. T., Pradhan-Sundd, T., Samnani, F., & Verheyen, E. M. (2017). The protein phosphatase 4 complex promotes the Notch pathway and wingless transcription. *Biology Open*, *6*(8), 1165–1173. https://doi.org/10.1242/bio.025221

Hariharan, I. K., & Serras, F. (2017). Imaginal disc regeneration takes flight. *Current Opinion in Cell Biology*, *48*, 10–16. https://doi.org/10.1016/j.ceb.2017.03.005

Harnoš, J., Cañizal, M. C. A., Jurásek, M., Kumar, J., Holler, C., Schambony, A., Hanáková, K., Bernatík, O., Zdráhal, Z., Gömöryová, K., Gybeľ, T., Radaszkiewicz, T. W., Kravec, M., Trantírek, L., Ryneš, J., Dave, Z., Fernández-Llamazares, A. I., Vácha, R., Tripsianes, K., … Bryja, V. (2019). Dishevelled-3 conformation dynamics analyzed by FRET-based biosensors reveals a key role of casein kinase 1. *Nature Communications*, *10*(1), 1804. https://doi.org/10.1038/s41467-019-09651-7

Hayat, R., Manzoor, M., & Hussain, A. (2022). Wnt signaling pathway: A comprehensive review. *Cell Biology International*, *46*(6), 863–877. https://doi.org/10.1002/cbin.11797

Heingård, M., Turetzek, N., Prpic, N.-M., & Janssen, R. (2019). FoxB, a new and highly conserved key factor in arthropod dorsal–ventral (DV) limb patterning. *EvoDevo*, *10*(1), 28. https://doi.org/10.1186/s13227-019-0141-6

Honeyman, A. L., Cote, C. K., & Curtiss, R. (2002). Construction of transcriptional and translational lacZ gene reporter plasmids for use in Streptococcus mutans. *Journal of Microbiological Methods*, *49*(2), 163–171. https://doi.org/10.1016/s0167-7012(01)00368-2

Hu, R., Qiu, Y., Li, Y., & Li, J. (2022). A novel frameshift mutation of DVL1 -induced Robinow syndrome: A case report and literature review. *Molecular Genetics & Genomic Medicine*, *10*(3), e1886. https://doi.org/10.1002/mgg3.1886

Huber, O., Korn, R., McLaughlin, J., Ohsugi, M., Herrmann, B. G., & Kemler, R. (1996). Nuclear localization of beta-catenin by interaction with transcription factor LEF-1. *Mechanisms of Development*, *59*(1), 3–10. https://doi.org/10.1016/0925-4773(96)00597-7

Hynes, R. O., & Zhao, Q. (2000). The Evolution of Cell Adhesion. *Journal of Cell Biology*, *150*(2), F89–F96. https://doi.org/10.1083/jcb.150.2.F89

Igaki, T. (2009). Correcting developmental errors by apoptosis: Lessons from Drosophila JNK signaling. *Apoptosis: An International Journal on Programmed Cell Death*, *14*(8), 1021–1028. https://doi.org/10.1007/s10495-009-0361-7

Iioka, H., Iemura, S., Natsume, T., & Kinoshita, N. (2007). Wnt signalling regulates paxillin ubiquitination essential for mesodermal cell motility. *Nature Cell Biology*, *9*(7), 813–821. https://doi.org/10.1038/ncb1607

Itoh, K., Brott, B. K., Bae, G.-U., Ratcliffe, M. J., & Sokol, S. Y. (2005). Nuclear localization is required for Dishevelled function in Wnt/β-catenin signaling. *Journal of Biology*, *4*(1), 3. https://doi.org/10.1186/jbiol20

Jenny, A., Darken, R. S., Wilson, P. A., & Mlodzik, M. (2003). Prickle and Strabismus form a functional complex to generate a correct axis during planar cell polarity signaling. *The EMBO Journal*, *22*(17), 4409–4420. https://doi.org/10.1093/emboj/cdg424

Jenny, A., Reynolds-Kenneally, J., Das, G., Burnett, M., & Mlodzik, M. (2005). Diego and Prickle regulate Frizzled planar cell polarity signalling by competing for Dishevelled binding. *Nature Cell Biology*, *7*(7), 691–697. https://doi.org/10.1038/ncb1271

Jia, Q., Liu, Y., Liu, H., & Li, S. (2014). Mmp1 and Mmp2 cooperatively induce Drosophila fat body cell dissociation with distinct roles. *Scientific Reports*, *4*(1), 7535. https://doi.org/10.1038/srep07535

Johnstone, K., Wells, R. E., Strutt, D., & Zeidler, M. P. (2013). Localised JAK/STAT Pathway Activation Is Required for Drosophila Wing Hinge Development. *PLoS ONE*, *8*(5), e65076. https://doi.org/10.1371/journal.pone.0065076

Jursnich, V. A., Fraser, S. E., Held, L. I., Ryerse, J., & Bryant, P. J. (1990). Defective gap-junctional communication associated with imaginal disc overgrowth and degeneration caused by mutations of the dco gene in Drosophila. *Developmental Biology*, *140*(2), 413–429. https://doi.org/10.1016/0012-1606(90)90090-6

Kaissi, A. A., Kenis, V., Shboul, M., Grill, F., Ganger, R., & Kircher, S. G. (2020). Tomographic Study of the Malformation Complex in Correlation With the Genotype in Patients With Robinow Syndrome: Review Article. *Journal of Investigative Medicine High Impact Case Reports*, *8*, 2324709620911771. https://doi.org/10.1177/2324709620911771

Katja Maccharles author. (2022). *Characterizing pathogenic Robinow Syndrome-associated Dishevelled1 variants in Drosophila / by Katja Maccharles.* [Simon Fraser University]. https://summit.sfu.ca/identifier/etd22286

Kennedy, M. B. (1995). Origin of PDZ (DHR, GLGF) domains. *Trends in Biochemical Sciences*, *20*(9), 350. https://doi.org/10.1016/S0968-0004(00)89074-X

Kishida, S., Yamamoto, H., Hino, S., Ikeda, S., Kishida, M., & Kikuchi, A. (1999). DIX Domains of Dvl and Axin Are Necessary for Protein Interactions and Their Ability To Regulate β-Catenin Stability. *Molecular and Cellular Biology*, *19*(6), 4414–4422.

Klein, T. J., & Mlodzik, M. (2005). Planar cell polarization: An emerging model points in the right direction. *Annual Review of Cell and Developmental Biology*, *21*, 155–176. https://doi.org/10.1146/annurev.cellbio.21.012704.132806

Klingensmith, J., Yang, Y., Axelrod, J. D., Beier, D. R., Perrimon, N., & Sussman, D. J. (1996). Conservation of dishevelled structure and function between flies and mice: Isolation and characterization of Dvl2. *Mechanisms of Development*, *58*(1–2), 15–26. https://doi.org/10.1016/s0925-4773(96)00549-7

Koch, C. M., Chiu, S. F., Akbarpour, M., Bharat, A., Ridge, K. M., Bartom, E. T., & Winter, D. R. (2018). A Beginner's Guide to Analysis of RNA Sequencing Data. *American Journal of Respiratory Cell and Molecular Biology*, *59*(2), 145–157. https://doi.org/10.1165/rcmb.2017-0430TR

Komiya, Y., & Habas, R. (2008). Wnt signal transduction pathways. *Organogenesis*, *4*(2), 68–75. https://doi.org/10.4161/org.4.2.5851

Kornbluth, S., & White, K. (2005). Apoptosis in Drosophila: Neither fish nor fowl (nor man, nor worm). *Journal of Cell Science*, *118*(9), 1779–1787. https://doi.org/10.1242/jcs.02377

Krasnow, R. E., & Adler, P. N. (1994). A single frizzled protein has a dual function in tissue polarity. *Development*, *120*(7), Article 7.

Kumar, N., Rangel Ambriz, J., Tsai, K., Mim, M. S., Flores-Flores, M., Chen, W., Zartman, J. J., & Alber, M. (2024). Balancing competing effects of tissue growth and cytoskeletal regulation during Drosophila wing disc development. *Nature Communications*, *15*(1), 2477. https://doi.org/10.1038/s41467-024-46698-7

La Marca, J. E., & Richardson, H. E. (2020). Two-Faced: Roles of JNK Signalling During Tumourigenesis in the Drosophila Model. *Frontiers in Cell and Developmental Biology*, *8*, 42. https://doi.org/10.3389/fcell.2020.00042

Lecuit, T., & Cohen, S. M. (1997). Proximal-distal axis formation in the Drosophila leg. *Nature*, *388*(6638), Article 6638.

Lee, H.-J., Shi, D.-L., & Zheng, J. J. (2015). Conformational change of Dishevelled plays a key regulatory role in the Wnt signaling pathways. *eLife*, *4*, e08142. https://doi.org/10.7554/eLife.08142

Lee, I., Choi, S., Yun, J.-H., Seo, S. hwa, Choi, S., Choi, K.-Y., & Lee, W. (2017). Crystal structure of the PDZ domain of mouse Dishevelled 1 and its interaction with CXXC5. *Biochemical and Biophysical Research Communications*, *485*(3), 584–590. https://doi.org/10.1016/j.bbrc.2016.12.023

Lee, J.-Y., Marston, D. J., Walston, T., Hardin, J., Halberstadt, A., & Goldstein, B. (2006). Wnt/Frizzled signaling controls C. elegans gastrulation by activating actomyosin contractility. *Current Biology: CB*, *16*(20), 1986–1997. https://doi.org/10.1016/j.cub.2006.08.090

Lijam, N., Paylor, R., McDonald, M. P., Crawley, J. N., Deng, C. X., Herrup, K., Stevens, K. E., Maccaferri, G., McBain, C. J., Sussman, D. J., & Wynshaw-Boris, A. (1997). Social interaction and sensorimotor gating abnormalities in mice lacking Dvl1. *Cell*, *90*(5), 895–905. https://doi.org/10.1016/s0092-8674(00)80354-2

Lodish, H. F. (2000). *Molecular Cell Biology*. W.H. Freeman.

Loftus, S. K., Larson, D. M., Watkins-Chow, D., Church, D. M., & Pavan, W. J. (2001). Generation of RCAS Vectors Useful for Functional Genomic Analyses. *DNA Research*, *8*(5), 221–226. https://doi.org/10.1093/dnares/8.5.221

Louie, S. H., Yang, X. Y., Conrad, W. H., Muster, J., Angers, S., Moon, R. T., & Cheyette, B. N. (2009). Modulation of the beta-catenin signaling pathway by the dishevelled-associated protein Hipk1. *PLoS One*, *4*(2), Article 2.

Lu, W., Yamamoto, V., Ortega, B., & Baltimore, D. (2004). Mammalian Ryk is a Wnt coreceptor required for stimulation of neurite outgrowth. *Cell*, *119*(1), 97–108. https://doi.org/10.1016/j.cell.2004.09.019

Lucas, F. R., Goold, R. G., Gordon-Weeks, P. R., & Salinas, P. C. (1998). Inhibition of GSK-3beta leading to the loss of phosphorylated MAP-1B is an early event in axonal remodelling induced by WNT-7a or lithium. *Journal of Cell Science*, *111 (Pt 10)*, 1351–1361. https://doi.org/10.1242/jcs.111.10.1351

Lykke-Andersen, S., & Jensen, T. H. (2015). Nonsense-mediated mRNA decay: An intricate machinery that shapes transcriptomes. *Nature Reviews Molecular Cell Biology*, *16*(11), 665–677. https://doi.org/10.1038/nrm4063

Mahindroo, N., Punchihewa, C., Bail, A. M., & Fujii, N. (2008). Indole-2-amide based biochemical antagonist of Dishevelled PDZ domain interaction down-regulates Dishevelled-driven Tcf transcriptional activity. *Bioorganic & Medicinal Chemistry Letters*, *18*(3), 946–949. https://doi.org/10.1016/j.bmcl.2007.12.039

Mansour, T. A., Lucot, K., Konopelski, S. E., Dickinson, P. J., Sturges, B. K., Vernau, K. L., Choi, S., Stern, J. A., Thomasy, S. M., Döring, S., Verstraete, F. J. M., Johnson, E. G., York, D., Rebhun, R. B., Ho, H.-Y. H., Brown, C. T., & Bannasch, D. L. (2018). Whole genome variant association across 100 dogs identifies a frame shift mutation in DISHEVELLED 2 which contributes to Robinow-like syndrome in Bulldogs and related screw tail dog breeds. *PLoS Genetics*, *14*(12), e1007850. https://doi.org/10.1371/journal.pgen.1007850

Martin-Blanco, E., Gampel, A., Ring, J., Virdee, K., Kirov, N., Tolkovsky, A. M., & Martinez-Arias, A. (1998). Puckered encodes a phosphatase that mediates a feedback loop regulating JNK activity during dorsal closure in Drosophila. *Genes Dev*, *12*(4), Article 4.

Matamoro-Vidal, A., Salazar-Ciudad, I., & Houle, D. (2015). Making quantitative morphological variation from basic developmental processes: Where are we? The case of the Drosophila wing. *Developmental Dynamics: An Official Publication of the American Association of Anatomists*, *244*(9), 1058–1073. https://doi.org/10.1002/dvdy.24255

Maung, S. M. T. W., & Jenny, A. (2011). Planar cell polarity in Drosophila. *Organogenesis*, *7*(3), 165–179. https://doi.org/10.4161/org.7.3.18143

Mazzeu, J. F., Pardono, E., Vianna-Morgante, A. M., Richieri-Costa, A., Ae Kim, C., Brunoni, D., Martelli, L., de Andrade, C. E. F., Colin, G., & Otto, P. A. (2007). Clinical characterization of autosomal dominant and recessive variants of Robinow syndrome. *American Journal of Medical Genetics. Part A*, *143*(4), 320–325. https://doi.org/10.1002/ajmg.a.31592

McClure, K. D., & Schubiger, G. (2005). Developmental analysis and squamous morphogenesis of the peripodial epithelium in Drosophila imaginal discs. *Development (Cambridge, England)*, *132*(22), 5033–5042. https://doi.org/10.1242/dev.02092

Meyer, E. J., Ikmi, A., & Gibson, M. C. (2011). Interkinetic nuclear migration is a broadly conserved feature of cell division in pseudostratified epithelia. *Current Biology: CB*, *21*(6), 485–491. https://doi.org/10.1016/j.cub.2011.02.002

Might, M., & Crouse, A. B. (2022). Why rare disease needs precision medicine—And precision medicine needs rare disease. *Cell Reports Medicine*, *3*(2), 100530. https://doi.org/10.1016/j.xcrm.2022.100530

Mirnezami, R., Nicholson, J., & Darzi, A. (2012). Preparing for Precision Medicine. *New England Journal of Medicine*, *366*(6), 489–491. https://doi.org/10.1056/NEJMp1114866

Mirzoyan, Z., Sollazzo, M., Allocca, M., Valenza, A. M., Grifoni, D., & Bellosta, P. (2019). Drosophila melanogaster: A Model Organism to Study Cancer. *Frontiers in Genetics*, *10*. https://doi.org/10.3389/fgene.2019.00051

Miyakoshi, A., Ueno, N., & Kinoshita, N. (2004). Rho guanine nucleotide exchange factor xNET1 implicated in gastrulation movements during Xenopus development. *Differentiation; Research in Biological Diversity*, *72*(1), 48–55. https://doi.org/10.1111/j.1432-0436.2004.07201004.x

Montanari, M. P., Tran, N. V., & Shimmi, O. (2022). Regulation of spatial distribution of BMP ligands for pattern formation. *Developmental Dynamics*, *251*(1), 178–192. https://doi.org/10.1002/dvdy.397

Moon, R. T., & Shah, K. (2002). Developmental biology: Signalling polarity. *Nature*, *417*(6886), 239–240. https://doi.org/10.1038/417239a

Morgan, T. H. (1910). Sex Limited Inheritance in Drosophila. *Science*, *32*(812), 120–122. https://doi.org/10.1126/science.32.812.120

Mukherjee, P., Roy, S., Ghosh, D., & Nandi, S. K. (2022). Role of animal models in biomedical research: A review. *Laboratory Animal Research*, *38*, 18. https://doi.org/10.1186/s42826-022-00128-1

Murray, M. A., Fessler, L. I., & Palka, J. (1995). Changing Distributions of Extracellular Matrix Components during Early Wing Morphogenesis in *Drosophila*. *Developmental Biology*, *168*(1), 150–165. https://doi.org/10.1006/dbio.1995.1068

Nagasaki, K., Nishimura, G., Kikuchi, T., Nyuzuki, H., Sasaki, S., Ogawa, Y., & Saitoh, A. (2018). Nonsense mutations in FZD2 cause autosomal-dominant omodysplasia: Robinow syndrome-like phenotypes. *American Journal of Medical Genetics Part A*, *176*(3), 739–742. https://doi.org/10.1002/ajmg.a.38623

Nishita, M., Itsukushima, S., Nomachi, A., Endo, M., Wang, Z., Inaba, D., Qiao, S., Takada, S., Kikuchi, A., & Minami, Y. (2010). Ror2/Frizzled Complex Mediates Wnt5a-Induced AP-1 Activation by Regulating Dishevelled Polymerization. *Molecular and Cellular Biology*, *30*(14), 3610–3619. https://doi.org/10.1128/MCB.00177-10

Nussinov, R., Jang, H., Nir, G., Tsai, C.-J., & Cheng, F. (2021). A new precision medicine initiative at the dawn of exascale computing. *Signal Transduction and Targeted Therapy*, *6*(1), 1–8. https://doi.org/10.1038/s41392-020-00420-3

Nüsslein-Volhard, C., & Wieschaus, E. (1980). Mutations affecting segment number and polarity in Drosophila. *Nature*, *287*(5785), 795–801. https://doi.org/10.1038/287795a0

Nüsslein-Volhard, C., Wieschaus, E., & Kluding, H. (1984). Mutations affecting the pattern of the larval cuticle inDrosophila melanogaster. *Wilhelm Roux's Archives of Developmental Biology*, *193*(5), 267–282. https://doi.org/10.1007/BF00848156

Oparin, A. I. (1957). *The Origin of Life on the Earth*. Academic Press.

Orphanet: Robinow syndrome. (n.d.). Retrieved July 9, 2024, from https://www.orpha.net/en/disease/detail/97360

Pan, W. J., Pang, S. Z., Huang, T., Guo, H. Y., Wu, D., & Li, L. (2004). Characterization of function of three domains in dishevelled-1: DEP domain is responsible for membrane translocation of dishevelled-1. *Cell Research*, *14*(4), 324–330. https://doi.org/10.1038/sj.cr.7290232

Park, T. J., Gray, R. S., Sato, A., Habas, R., & Wallingford, J. B. (2005). Subcellular localization and signaling properties of dishevelled in developing vertebrate embryos. *Current Biology: CB*, *15*(11), 1039–1044. https://doi.org/10.1016/j.cub.2005.04.062

Pastor-Pareja, J. C., Grawe, F., Martin-Blanco, E., & Garcia-Bellido, A. (2004). Invasive cell behavior during Drosophila imaginal disc eversion is mediated by the JNK signaling cascade. *Dev Cell*, *7*(3), Article 3.

Peifer, M., Sweeton, D., Casey, M., & Wieschaus, E. (1994). Wingless signal and Zeste-white 3 kinase trigger opposing changes in the intracellular distribution of Armadillo. *Development*, *120*(2), Article 2.

Peifer, M., & Wieschaus, E. (1990). The segment polarity gene armadillo encodes a functionally modular protein that is the Drosophila homolog of human plakoglobin. *Cell*, *63*(6), 1167–1176. https://doi.org/10.1016/0092-8674(90)90413-9

Perrimon, N., Engstrom, L., & Mahowald, A. (1989). Zygotic lethals with specific maternal effect phenotypes in Drosophilamelanogaster I Loci on the X Chromosome. *Genetics*, *121*, 333–352.

Perrimon, N., & Mahowald, A. P. (1987). Multiple functions of segment polarity genes in Drosophila. *Dev Biol*, *119*(2), Article 2.

Person, A. D., Beiraghi, S., Sieben, C. M., Hermanson, S., Neumann, A. N., Robu, M. E., Schleiffarth, J. R., Billington Jr, C. J., van Bokhoven, H., Hoogeboom, J. M., Mazzeu, J. F., Petryk, A., Schimmenti, L. A., Brunner, H. G., Ekker, S. C., & Lohr, J. L. (2010). WNT5A mutations in patients with autosomal dominant Robinow syndrome. *Developmental Dynamics*, *239*(1), 327–337. https://doi.org/10.1002/dvdy.22156

Pinal, N., Calleja, M., & Morata, G. (2019). Pro-apoptotic and pro-proliferation functions of the JNK pathway of drosophila: Roles in cell competition, tumorigenesis and regeneration. *Open Biology*. https://doi.org/10.1098/rsob.180256

Pizzuti, A., Amati, F., Calabrese, G., Mari, A., Colosimo, A., Silani, V., Giardino, L., Ratti, A., Penso, D., Calzà, L., Palka, G., Scarlato, G., Novelli, G., & Dallapiccola, B. (1996). cDNA characterization and chromosomal mapping of two human homologues of the Drosophila dishevelled polarity gene. *Human Molecular Genetics*, *5*(7), 953–958. https://doi.org/10.1093/hmg/5.7.953

Qi, J., Lee, H.-J., Saquet, A., Cheng, X.-N., Shao, M., Zheng, J. J., & Shi, D.-L. (2017). Autoinhibition of Dishevelled protein regulated by its extreme C terminus plays a distinct role in Wnt/β-catenin and Wnt/planar cell polarity (PCP) signaling pathways. *Journal of Biological Chemistry*, *292*(14), 5898–5908. https://doi.org/10.1074/jbc.M116.772509

Rai, A., Patil, S. J., Srivastava, P., Gaurishankar, K., & Phadke, S. R. (2021). Clinical and molecular characterization of four patients with Robinow syndrome from different families. *American Journal of Medical Genetics Part A*, *185*(4), 1105–1112. https://doi.org/10.1002/ajmg.a.62082

Requena, D., Álvarez, J. A., Gabilondo, H., Loker, R., Mann, R. S., & Estella, C. (2017). Origins and Specification of the Drosophila Wing. *Current Biology*, *27*(24), 3826-3836.e5. https://doi.org/10.1016/j.cub.2017.11.023

Robinow, M., Silverman, F. N., & Smith, H. D. (1969). A newly recognized dwarfing syndrome. *American Journal of Diseases of Children (1960)*, *117*(6), 645–651. https://doi.org/10.1001/archpedi.1969.02100030647005

Saal, H. M., Prows, C. A., Guerreiro, I., Donlin, M., Knudson, L., Sund, K. L., Chang, C.-F., Brugmann, S. A., & Stottmann, R. W. (2015). A mutation in FRIZZLED2 impairs Wnt signaling and causes autosomal dominant omodysplasia. *Human Molecular Genetics*, *24*(12), 3399–3409. https://doi.org/10.1093/hmg/ddv088

Sakamoto, K., Senda, D., von Däniken, S., Boztepe, B., Komuro, Y., & Shimoji, K. (2021). Robinow syndrome in a newborn presenting with hydrocephalus and craniosynostosis. *Child's Nervous System: ChNS: Official Journal of the International Society for Pediatric Neurosurgery*, *37*(10), 3235–3239. https://doi.org/10.1007/s00381-021-05087-x

Schindelin, J., Arganda-Carreras, I., Frise, E., Kaynig, V., Longair, M., Pietzsch, T., Preibisch, S., Rueden, C., Saalfeld, S., Schmid, B., Tinevez, J.-Y., White, D. J., Hartenstein, V., Eliceiri, K., Tomancak, P., & Cardona, A. (2012). Fiji: An open-source platform for biological-image analysis. *Nature Methods*, *9*(7), 676–682. https://doi.org/10.1038/nmeth.2019

Schneider, C. A., Rasband, W. S., & Eliceiri, K. W. (2012). NIH Image to ImageJ: 25 years of Image Analysis. *Nature Methods*, *9*(7), 671–675.

Schwartz, D. D., Fein, R. H., Carvalho, C. M. B., Sutton, V. R., Mazzeu, J. F., & Axelrad, M. E. (2021). Neurocognitive, adaptive, and psychosocial functioning in individuals with Robinow syndrome. *American Journal of Medical Genetics Part A*, *185*(12), 3576–3583. https://doi.org/10.1002/ajmg.a.61854

Schwarz-Romond, T., Fiedler, M., Shibata, N., Butler, P. J., Kikuchi, A., Higuchi, Y., & Bienz, M. (2007). The DIX domain of Dishevelled confers Wnt signaling by dynamic polymerization. *Nat Struct Mol Biol*, *14*(6), Article 6.

Sebastian-Leon, P., Vidal, E., Minguez, P., Conesa, A., Tarazona, S., Amadoz, A., Armero, C., Salavert, F., Vidal-Puig, A., Montaner, D., & Dopazo, J. (2014). Understanding disease mechanisms with models of signaling pathway activities. *BMC Systems Biology*, *8*, 121. https://doi.org/10.1186/s12918-014-0121-3

Seifert, J. R. K., & Mlodzik, M. (2007). Frizzled/PCP signalling: A conserved mechanism regulating cell polarity and directed motility. *Nature Reviews Genetics*, *8*(2), 126–138. https://doi.org/10.1038/nrg2042

Semënov, M. V., & Snyder, M. (1997). Human dishevelled genes constitute a DHR-containing multigene family. *Genomics*, *42*(2), 302–310. https://doi.org/10.1006/geno.1997.4713

Sharma, M., Castro-Piedras, I., Simmons, G. E., & Pruitt, K. (2018). Dishevelled: A masterful conductor of complex Wnt signals. *Cellular Signalling*, *47*, 52–64. https://doi.org/10.1016/j.cellsig.2018.03.004

Sharma, R. P., & Chopra, V. L. (1976). Effect of the Wingless (wg1) mutation on wing and haltere development in Drosophila melanogaster. *Dev Biol*, *48*(2), Article 2.

Sheldahl, L. C., Slusarski, D. C., Pandur, P., Miller, J. R., Kühl, M., & Moon, R. T. (2003). Dishevelled activates Ca2+ flux, PKC, and CamKII in vertebrate embryos. *The Journal of Cell Biology*, *161*(4), 769–777. https://doi.org/10.1083/jcb.200211094

Shiomi, K., Uchida, H., Keino-Masu, K., & Masu, M. (2003). Ccd1, a novel protein with a DIX domain, is a positive regulator in the Wnt signaling during zebrafish neural patterning. *Current Biology: CB*, *13*(1), 73–77. https://doi.org/10.1016/s0960-9822(02)01398-2

Siegfried, E., Perkins, L. A., Capaci, T. M., & Perrimon, N. (1990). Putative protein kinase product of the Drosophila segment-polarity gene zeste-white3. *Nature*, *345*(6278), Article 6278.

Simons, M., & Mlodzik, M. (2008). Planar Cell Polarity Signaling: From Fly Development to Human Disease. *Annual Review of Genetics*, *42*(Volume 42, 2008), 517–540. https://doi.org/10.1146/annurev.genet.42.110807.091432

Slusarski, D. C., & Pelegri, F. (2007). Calcium signaling in vertebrate embryonic patterning and morphogenesis. *Developmental Biology*, *307*(1), 1–13. https://doi.org/10.1016/j.ydbio.2007.04.043

Sobala, L. F., & Adler, P. N. (2016). The Gene Expression Program for the Formation of Wing Cuticle in Drosophila. *PLOS Genetics*, *12*(5), e1006100. https://doi.org/10.1371/journal.pgen.1006100

Sokol, S. Y., Klingensmith, J., Perrimon, N., & Itoh, K. (1995). Dorsalizing and neuralizing properties of Xdsh, a maternally expressed Xenopus homolog of dishevelled. *Development (Cambridge, England)*, *121*(6), 1637–1647. https://doi.org/10.1242/dev.121.6.1637

Song, Z., McCall, K., & Steller, H. (1997). DCP-1, a Drosophila cell death protease essential for development. *Science (New York, N.Y.)*, *275*(5299), 536–540. https://doi.org/10.1126/science.275.5299.536

Sui, L., & Dahmann, C. (2020). Wingless counteracts epithelial folding by increasing mechanical tension at basal cell edges in Drosophila. *Development (Cambridge, England)*, *147*(5), dev184713. https://doi.org/10.1242/dev.184713

Sui, L., Pflugfelder, G. O., & Shen, J. (2012). The Dorsocross T-box transcription factors promote tissue morphogenesis in the Drosophila wing imaginal disc. *Development*, *139*(15), 2773–2782. https://doi.org/10.1242/dev.079384

Sun, T., Song, Y., Teng, D., Chen, Y., Dai, J., Ma, M., Zhang, W., & Pastor-Pareja, J. C. (2021). Atypical laminin spots and pull-generated microtubule-actin projections mediate Drosophila wing adhesion. *Cell Reports*, *36*(10). https://doi.org/10.1016/j.celrep.2021.109667

Sussman, D. J., Klingensmith, J., Salinas, P., Adams, P. S., Nusse, R., & Perrimon, N. (1994). Isolation and characterization of a mouse homolog of the Drosophila segment polarity gene dishevelled. *Developmental Biology*, *166*(1), 73–86. https://doi.org/10.1006/dbio.1994.1297

Swarup, S., Pradhan-Sundd, T., & Verheyen, E. M. (2015). Genome-wide identification of phospho-regulators of Wnt signaling in Drosophila. *Development (Cambridge, England)*, *142*(8), Article 8. https://doi.org/10.1242/dev.116715

Swarup, S., & Verheyen, E. M. (2012). Wnt/Wingless signaling in Drosophila. *Cold Spring Harb Perspect Biol*, *4*(6), Article 6. https://doi.org/10.1101/cshperspect.a007930

Tabor, H. K., & Goldenberg, A. (2018). What Precision Medicine Can Learn from Rare Genetic Disease Research and Translation. *AMA Journal of Ethics*, *20*(9), E834-840. https://doi.org/10.1001/amajethics.2018.834

Tanegashima, K., Zhao, H., & Dawid, I. B. (2008). WGEF activates Rho in the Wnt–PCP pathway and controls convergent extension in Xenopus gastrulation. *The EMBO Journal*, *27*(4), 606–617. https://doi.org/10.1038/emboj.2008.9

Taylor, J., Abramova, N., Charlton, J., & Adler, P. N. (1998). Van Gogh: A New Drosophila Tissue Polarity Gene. *Genetics*, *150*(1), 199–210. https://doi.org/10.1093/genetics/150.1.199

Teufel, S., & Hartmann, C. (2019). Wnt-signaling in skeletal development. *Current Topics in Developmental Biology*, *133*, 235–279. https://doi.org/10.1016/bs.ctdb.2018.11.010

The Gene Ontology Consortium, Aleksander, S. A., Balhoff, J., Carbon, S., Cherry, J. M., Drabkin, H. J., Ebert, D., Feuermann, M., Gaudet, P., Harris, N. L., Hill, D. P., Lee, R., Mi, H., Moxon, S., Mungall, C. J., Muruganugan, A., Mushayahama, T., Sternberg, P. W., Thomas, P. D., … Westerfield, M. (2023). The Gene Ontology knowledgebase in 2023. *Genetics*, *224*(1), iyad031. https://doi.org/10.1093/genetics/iyad031

The Nobel Prize in Physiology or Medicine 1985. (n.d.). NobelPrize.Org. Retrieved July 5, 2024, from https://www.nobelprize.org/prizes/medicine/1985/press-release/

Thomas, P. D., Ebert, D., Muruganujan, A., Mushayahama, T., Albou, L.-P., & Mi, H. (2022). PANTHER: Making genome-scale phylogenetics accessible to all. *Protein Science*, *31*(1), 8–22. https://doi.org/10.1002/pro.4218

Thompson, B. J. (2021). From genes to shape during metamorphosis: A history. *Current Opinion in Insect Science*, *43*, 1–10. https://doi.org/10.1016/j.cois.2020.08.008

Tolwinski, N. S. (2017). Introduction: Drosophila—A Model System for Developmental Biology. *Journal of Developmental Biology*, *5*(3). https://doi.org/10.3390/jdb5030009

Tophkhane, S. S., Fu, K., Verheyen, E. M., & Richman, J. M. (2024). Craniofacial studies in chicken embryos confirm the pathogenicity of human FZD2 variants associated with Robinow syndrome. *Disease Models & Mechanisms*, *17*(6), dmm050584. https://doi.org/10.1242/dmm.050584

Tophkhane, S. S., Gignac, S. J., Fu, K., Verheyen, E. M., & Richman, J. M. (2024). *DVL1 variants and C-terminal deletions have differential effects on craniofacial development and WNT signaling* (p. 2024.02.28.582602). bioRxiv. https://doi.org/10.1101/2024.02.28.582602

Tozluoğlu, M., Duda, M., Kirkland, N. J., Barrientos, R., Burden, J. J., Muñoz, J. J., & Mao, Y. (2019). Planar Differential Growth Rates Initiate Precise Fold Positions in Complex Epithelia. *Developmental Cell*, *51*(3), 299-312.e4. https://doi.org/10.1016/j.devcel.2019.09.009

Tran, F. H., & Zheng, J. J. (2017). Modulating the wnt signaling pathway with small molecules. *Protein Science : A Publication of the Protein Society*, *26*(4), 650–661. https://doi.org/10.1002/pro.3122

Tree, D. R. P., Shulman, J. M., Rousset, R., Scott, M. P., Gubb, D., & Axelrod, J. D. (2002). Prickle mediates feedback amplification to generate asymmetric planar cell polarity signaling. *Cell*, *109*(3), 371–381. https://doi.org/10.1016/s0092-8674(02)00715-8

Treisman, J. E., Ito, N., & Rubin, G. M. (1997). Misshapen encodes a protein kinase involved in cell shape control in Drosophila. *Gene*, *186*(1), 119–125. https://doi.org/10.1016/s0378-1119(96)00694-4

Tripathi, B. K., & Irvine, K. D. (2022). The wing imaginal disc. *Genetics*, *220*(4), iyac020. https://doi.org/10.1093/genetics/iyac020

Tsang, M., Lijam, N., Yang, Y., Beier, D. R., Wynshaw-Boris, A., & Sussman, D. J. (1996). Isolation and characterization of mouse dishevelled-3. *Developmental Dynamics: An Official Publication of the American Association of Anatomists*, *207*(3), 253–262. https://doi.org/10.1002/(SICI)1097-0177(199611)207:3<253::AID-AJA2>3.0.CO;2-G

Ugur, B., Chen, K., & Bellen, H. J. (2016). Drosophila tools and assays for the study of human diseases. *Disease Models & Mechanisms*, *9*(3), Article 3. https://doi.org/10.1242/dmm.023762

Usui, T., Shima, Y., Shimada, Y., Hirano, S., Burgess, R. W., Schwarz, T. L., Takeichi, M., & Uemura, T. (1999). Flamingo, a seven-pass transmembrane cadherin, regulates planar cell polarity under the control of Frizzled. *Cell*, *98*(5), Article 5.

van de Stolpe, A., Holtzer, L., van Ooijen, H., Inda, M. A. de, & Verhaegh, W. (2019). Enabling precision medicine by unravelling disease pathophysiology: Quantifying signal transduction pathway activity across cell and tissue types. *Scientific Reports*, *9*(1), 1603. https://doi.org/10.1038/s41598-018-38179-x

van de Wetering, M., Cavallo, R., Dooijes, D., van Beest, M., van Es, J., Loureiro, J., Ypma, A., Hursh, D., Jones, T., Bejsovec, A., Peifer, M., Mortin, M., & Clevers, H. (1997). Armadillo coactivates transcription driven by the product of the Drosophila segment polarity gene dTCF. *Cell*, *88*(6), Article 6.

Veeman, M. T., Axelrod, J. D., & Moon, R. T. (2003). A second canon. Functions and mechanisms of beta-catenin-independent Wnt signaling. *Developmental Cell*, *5*(3), 367–377. https://doi.org/10.1016/s1534-5807(03)00266-1

Venken, K. J. T., & Bellen, H. J. (2007). Transgenesis upgrades for Drosophila melanogaster. *Development*, *134*(20), 3571–3584. https://doi.org/10.1242/dev.005686

Villa-Cuesta, E., González-Pérez, E., & Modolell, J. (2007). Apposition of iroquois expressing and non-expressing cells leads to cell sorting and fold formation in the Drosophila imaginal wing disc. *BMC Developmental Biology*, *7*, 106. https://doi.org/10.1186/1471-213X-7-106

Vinson, C. R., & Adler, P. N. (1987). Directional non-cell autonomy and the transmission of polarity information by the frizzled gene of Drosophila. *Nature*, *329*(6139), 549–551. https://doi.org/10.1038/329549a0

Waddington, C. H. (1940). The genetic control of wing development inDrosophila. *Journal of Genetics*, *41*(1), 75–113. https://doi.org/10.1007/BF02982977

Wadlington, W. B., Tucker, V. L., & Schimke, R. N. (1973). Mesomelic Dwarfism With Hemivertebrae and Small Genitalia (the Robinow Syndrome). *American Journal of Diseases of Children*, *126*(2), 202–205. https://doi.org/10.1001/archpedi.1973.02110190176013

Wallingford, J. B., Fraser, S. E., & Harland, R. M. (2002). Convergent extension: The molecular control of polarized cell movement during embryonic development. *Developmental Cell*, *2*(6), 695–706. https://doi.org/10.1016/s1534-5807(02)00197-1

Wallingford, J. B., & Habas, R. (2005). The developmental biology of Dishevelled: An enigmatic protein governing cell fate and cell polarity. *Development*, *132*(20), Article 20.

Wang, D., Li, L., Lu, J., Liu, S., & Shen, J. (2016). Complementary expression of optomotor-blind and the Iroquois complex promotes fold formation to separate wing notum and hinge territories. *Developmental Biology*, *416*(1), 225–234. https://doi.org/10.1016/j.ydbio.2016.05.020

Wang, S. H., Simcox, A., & Campbell, G. (2000). Dual role for Drosophila epidermal growth factor receptor signaling in early wing disc development. *Genes Dev*, *14*(18), Article 18.

Wang, W., Li, X., Lee, M., Jun, S., Aziz, K. E., Feng, L., Tran, M. K., Li, N., McCrea, P. D., Park, J.-I., & Chen, J. (2015). FOXKs promote Wnt/β-catenin signaling by translocating DVL into the nucleus. *Developmental Cell*, *32*(6), 707–718. https://doi.org/10.1016/j.devcel.2015.01.031

Wang, Y., & Nathans, J. (2007). Tissue/planar cell polarity in vertebrates: New insights and new questions. *Development*, *134*(4), 647–658. https://doi.org/10.1242/dev.02772

Weigmann, K., Cohen, S. M., & Lehner, C. F. (1997). Cell cycle progression, growth and patterning in imaginal discs despite inhibition of cell division after inactivation of Drosophila Cdc2 kinase. *Development*, *124*(18), 3555–3563. https://doi.org/10.1242/dev.124.18.3555

Wells, B. S., Yoshida, E., & Johnston*, L. A. (2006). Compensatory Proliferation in Drosophila Imaginal Discs Requires Dronc-Dependent p53 Activity. *Current Biology : CB*, *16*(16), 1606–1615. https://doi.org/10.1016/j.cub2006.07.046

Weston, C. R., & Davis, R. J. (2001). Signal transduction: Signaling specificity- a complex affair. *Science (New York, N.Y.)*, *292*(5526), 2439–2440. https://doi.org/10.1126/science.1063279

White, J. J., Mazzeu, J. F., Coban-Akdemir, Z., Bayram, Y., Bahrambeigi, V., Hoischen, A., Bon, B. W. M. van, Gezdirici, A., Gulec, E. Y., Ramond, F., Touraine, R., Thevenon, J., Shinawi, M., Beaver, E., Heeley, J., Hoover-Fong, J., Durmaz, C. D., Karabulut, H. G., Marzioglu-Ozdemir, E., … Carvalho, C. M. B. (2018). WNT Signaling Perturbations Underlie the Genetic Heterogeneity of Robinow Syndrome. *The American Journal of Human Genetics*, *102*(1), 27–43. https://doi.org/10.1016/j.ajhg.2017.10.002

White, J. J., Mazzeu, J. F., Hoischen, A., Bayram, Y., Withers, M., Gezdirici, A., Kimonis, V., Steehouwer, M., Jhangiani, S. N., Muzny, D. M., Gibbs, R. A., van Bon, B. W. M., Sutton, V. R., Lupski, J. R., Brunner, H. G., & Carvalho, C. M. B. (2016). DVL3 Alleles Resulting in a −1 Frameshift of the Last Exon Mediate Autosomal-Dominant Robinow Syndrome. *The American Journal of Human Genetics*, *98*(3), 553–561. https://doi.org/10.1016/j.ajhg.2016.01.005

White, J., Mazzeu, J. F., Hoischen, A., Jhangiani, S. N., Gambin, T., Alcino, M. C., Penney, S., Saraiva, J. M., Hove, H., Skovby, F., Kayserili, H., Estrella, E., Vulto-van Silfhout, A. T., Steehouwer, M., Muzny, D. M., Sutton, V. R., Gibbs, R. A., Baylor-Hopkins Center for Mendelian Genomics, Lupski, J. R., … Carvalho, C. M. B. (2015). DVL1 frameshift mutations clustering in the penultimate exon cause autosomal-dominant Robinow syndrome. *American Journal of Human Genetics*, *96*(4), 612–622. https://doi.org/10.1016/j.ajhg.2015.02.015

Witte, F., Bernatik, O., Kirchner, K., Masek, J., Mahl, A., Krejci, P., Mundlos, S., Schambony, A., Bryja, V., & Stricker, S. (2010). Negative regulation of Wnt signaling mediated by CK1-phosphorylated Dishevelled via Ror2. *FASEB Journal: Official Publication of the Federation of American Societies for Experimental Biology*, *24*(7), 2417–2426. https://doi.org/10.1096/fj.09-150615

Wolff, T., & Rubin, G. M. (1998). Strabismus, a novel gene that regulates tissue polarity and cell fate decisions in Drosophila. *Development*, *125*(6), Article 6.

Wolfstetter, G., Dahlitz, I., Pfeifer, K., Töpfer, U., Alt, J. A., Pfeifer, D. C., Lakes-Harlan, R., Baumgartner, S., Palmer, R. H., & Holz, A. (2019). Characterization of Drosophila Nidogen/entactin reveals roles in basement membrane stability, barrier function and nervous system patterning. *Development*, *146*(2), dev168948. https://doi.org/10.1242/dev.168948

Wong, H. C., Mao, J., Nguyen, J. T., Srinivas, S., Zhang, W., Liu, B., Li, L., Wu, D., & Zheng, J. (2000). Structural basis of the recognition of the Dishevelled DEP domain in the Wnt signaling pathway. *Nature Structural Biology*, *7*(12), 1178–1184. https://doi.org/10.1038/82047

Wong, H.-C., Bourdelas, A., Krauss, A., Lee, H.-J., Shao, Y., Wu, D., Mlodzik, M., Shi, D.-L., & Zheng, J. (2003). Direct Binding of the PDZ Domain of Dishevelled to a Conserved Internal Sequence in the C-Terminal Region of Frizzled. *Molecular Cell*, *12*(5), 1251–1260.

Wong, L. L., & Adler, P. N. (1993). Tissue polarity genes of Drosophila regulate the subcellular location for prehair initiation in pupal wing cells. *Journal of Cell Biology*, *123*(1), 209–221. https://doi.org/10.1083/jcb.123.1.209

Wynshaw-Boris, A. (2012). Dishevelled: In vivo roles of a multifunctional gene family during development. *Current Topics in Developmental Biology*, *101*, 213–235. https://doi.org/10.1016/B978-0-12-394592-1.00007-7

Xu, D., Woodfield, S. E., Lee, T. V., Fan, Y., Antonio, C., & Bergmann, A. (2009). Genetic control of programmed cell death (apoptosis) in Drosophila. *Fly*, *3*(1), 78–90.

Yamaguchi, T. P., Bradley, A., McMahon, A. P., & Jones, S. (1999). A Wnt5a pathway underlies outgrowth of multiple structures in the vertebrate embryo. *Development (Cambridge, England)*, *126*(6), 1211–1223. https://doi.org/10.1242/dev.126.6.1211

Yamamoto, S., Jaiswal, M., Charng, W.-L., Gambin, T., Karaca, E., Mirzaa, G., Wiszniewski, W., Sandoval, H., Haelterman, N. A., Xiong, B., Zhang, K., Bayat, V., David, G., Li, T., Chen, K., Gala, U., Harel, T., Pehlivan, D., Penney, S., … Bellen, H. J. (2014). A Drosophila Genetic Resource of Mutants to Study Mechanisms Underlying Human Genetic Diseases. *Cell*, *159*(1), 200–214. https://doi.org/10.1016/j.cell.2014.09.002

Yamamoto, S., Kanca, O., Wangler, M. F., & Bellen, H. J. (2024). Integrating non-mammalian model organisms in the diagnosis of rare genetic diseases in humans. *Nature Reviews Genetics*, *25*(1), 46–60. https://doi.org/10.1038/s41576-023-00633-6

Yanagawa, S., Lee, J.-S., Haruna, T., Oda, H., Uemura, T., Takeichi, M., & Ishimoto, A. (1997). Accumulation of Armadillo Induced by Wingless, Dishevelled, and Dominant-negative Zeste-white 3 Leads to Elevated DE-cadherin in*Drosophila* Clone 8 Wing Disc Cells*. *Journal of Biological Chemistry*, *272*(40), 25243–25251. https://doi.org/10.1074/jbc.272.40.25243

Yanagawa, S., Matsuda, Y., Lee, J. S., Matsubayashi, H., Sese, S., Kadowaki, T., & Ishimoto, A. (2002). Casein kinase I phosphorylates the Armadillo protein and induces its degradation in Drosophila. *EMBO J*, *21*(7), Article 7.

Yu, H., Smallwood, P. M., Wang, Y., Vidaltamayo, R., Reed, R., & Nathans, J. (2010). Frizzled 1 and frizzled 2 genes function in palate, ventricular septum and neural tube closure: General implications for tissue fusion processes. *Development (Cambridge, England)*, *137*(21), 3707–3717. https://doi.org/10.1242/dev.052001

Yu, J. J. S., Maugarny-Calès, A., Pelletier, S., Alexandre, C., Bellaiche, Y., Vincent, J.-P., & McGough, I. J. (2020). Frizzled-Dependent Planar Cell Polarity without Secreted Wnt Ligands. *Developmental Cell*, *54*(5), 583-592.e5. https://doi.org/10.1016/j.devcel.2020.08.004

Zhang, C., Jolly, A., Shayota, B. J., Mazzeu, J. F., Du, H., Dawood, M., Soper, P. C., Lima, A. R. de, Ferreira, B. M., Coban-Akdemir, Z., White, J., Shears, D., Thomson, F. R., Douglas, S. L., Wainwright, A., Bailey, K., Wordsworth, P., Oldridge, M., Lester, T., … Carvalho, C. M. B. (2022). Novel pathogenic variants and quantitative phenotypic analyses of Robinow syndrome: WNT signaling perturbation and phenotypic variability. *Human Genetics and Genomics Advances*, *3*(1). https://doi.org/10.1016/j.xhgg.2021.100074

Zhang, X., Zhu, J., Yang, G.-Y., Wang, Q.-J., Qian, L., Chen, Y.-M., Chen, F., Tao, Y., Hu, H.-S., Wang, T., & Luo, Z.-G. (2007). Dishevelled promotes axon differentiation by regulating atypical protein kinase C. *Nature Cell Biology*, *9*(7), 743–754. https://doi.org/10.1038/ncb1603

Zhang, Y., Appleton, B. A., Wiesmann, C., Lau, T., Costa, M., Hannoush, R. N., & Sidhu, S. S. (2009). Inhibition of Wnt signaling by Dishevelled PDZ peptides. *Nature Chemical Biology*, *5*(4), 217–219. https://doi.org/10.1038/nchembio.152

Zilian, O., Frei, E., Burke, R., Brentrup, D., Gutjahr, T., Bryant, P. J., & Noll, M. (1999). Double-time is identical to discs overgrown, which is required for cell survival, proliferation and growth arrest in Drosophila imaginal discs. *Development*, *126*(23), 5409–5420. https://doi.org/10.1242/dev.126.23.5409